

Experimental investigation under laser-driven shocks of the dynamic behavior of materials for beam-intercepting devices in particle accelerators

Original

Experimental investigation under laser-driven shocks of the dynamic behavior of materials for beam-intercepting devices in particle accelerators / Baudin, Lucie; Accettura, Carlotta; Morena, Alberto; Wegert, Leonard; Martynenko, Artem S.; Neumayeur, Paul; Tomut, Marilena; Bertarelli, Alessandro; Carra, Federico; Peroni, Lorenzo; Scapin, Martina; C, Christian Brabetz. - ELETTRONICO. - 3rd International Conference on Impact Loading of Structures and Materials ICILSM 2022:(2022), pp. 48-49. (Intervento presentato al convegno ICILSM 2022 tenutosi a Throndeim nel 13-17 June 2022)

Availability:

This version is available at: 11583/2968417 since: 2022-06-21T15:49:44Z

Publisher:

NTNU

Published

DOI:

Terms of use:

This article is made available under terms and conditions as specified in the corresponding bibliographic description in the repository

Publisher copyright

(Article begins on next page)



ICILSM ▶ 2022

Proceedings

3rd International Conference on
IMPACT LOADING OF STRUCTURES
AND MATERIALS

ISBN 978-82-998249-5-8

Organized by:

International Society of Impact Engineering

Local committee:

Professor Magnus Langseth

Professor Odd Sture Hopperstad

Professor Tore Børvik

Professor Arild Clausen

Associate Prof. David Morin

Associate Prof. Vegard Aune

Associate Prof. Miguel Costas

Adviser Peter Karlsaune

Sponsored by:

SFI CASA - Centre for Advanced Structural Analysis

NTNU - Norwegian University of Science and Technology



TABLE OF CONTENTS

WELCOME TO TRONDHEIM	5
PROGRAMME	7
INVITED LECTURES - BIOS AND ABSTRACTS	15
Marcilio Alves.....	17
James D. Walker.....	19
Tore Børvik.....	22
Vikram Desphande	25
Genevieve Langdon.....	27
Dirk Mohr.....	30
Guoxing Lu	32
Eric Markiewicz	34
Patricia Verleysen.....	37
Timon Rabczuk	40
François Moussy	43
ABSTRACTS	45
Session 1	47-54
Session 2.....	55-62
Session 3.....	63-75
Session 4.....	76-90
Session 5.....	91-93
Session 6.....	94-96
Session 7	97-112
Session 8.....	113-124
Session 9.....	125-130
Session 10.....	131-140

WELCOME TO TRONDHEIM

The 3rd ICILSM conference was planned to be held in June 2020. Unfortunately, the corona pandemic forced us to postpone it. However, after two years of waiting, it is a pleasure to welcome you to Trondheim and the 3rd International Conference on Impact Loading of Structures and Materials 2022.

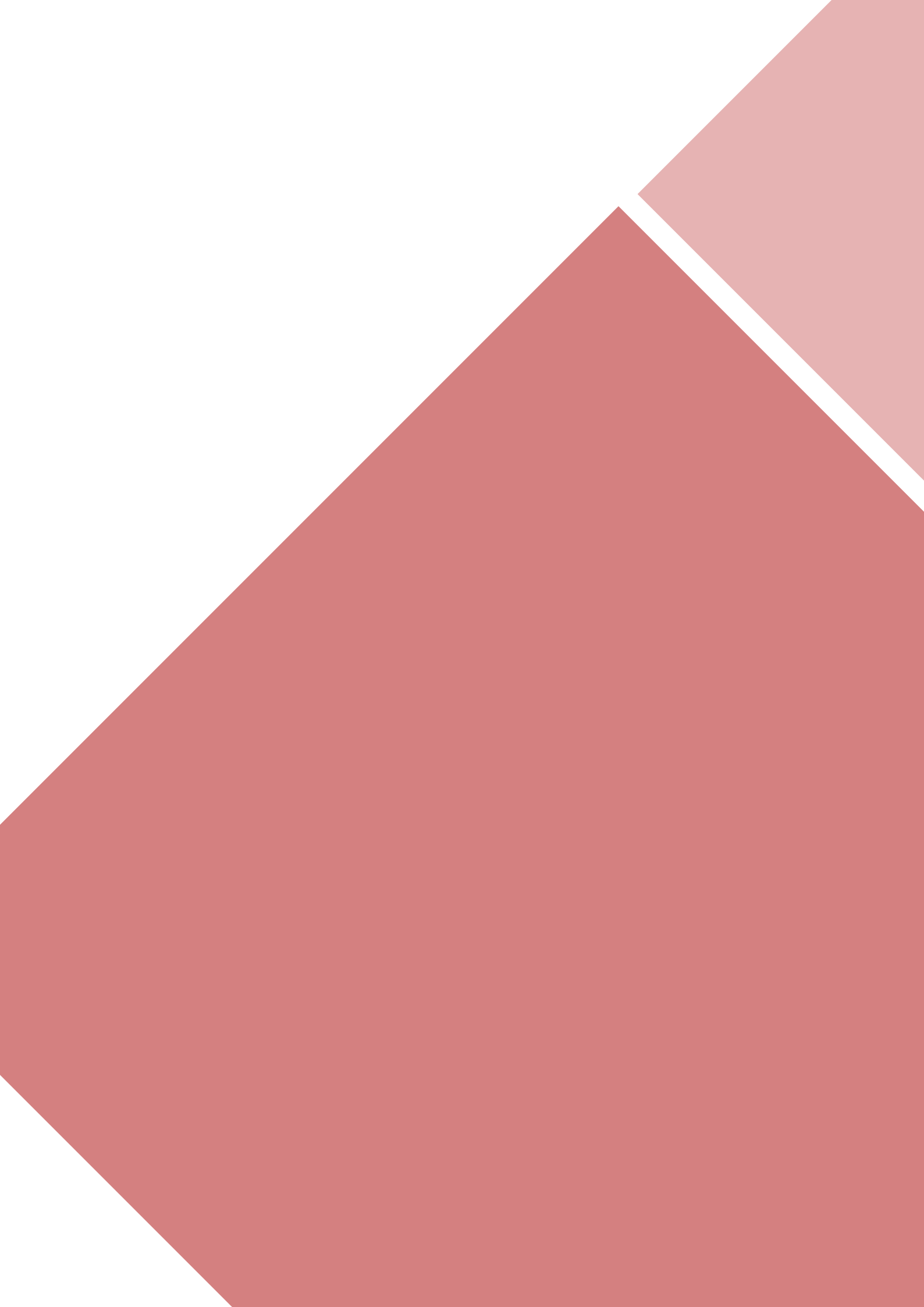
This conference series started in Liverpool, UK, in 1983, followed by Boston, US, in 1993, and again in Liverpool, UK, in 1998. Four conferences named ICILLS were held in Florianópolis, Brazil, in 2005, Trondheim, Norway, in 2008, Valenciennes, France, in 2011, and Cape Town, South Africa, in 2014. The conference name was then changed to ICILSM and held in Torino, Italy, in 2016 and Xi'an, China, in 2018.

We are happy to present the conference program on behalf of the organizing committee. We have 11 invited lectures by reputable experts in our domain of engineering. In all, 59 presentations cover all sub-domains of our community of impact engineering. Hopefully, this conference will become an excellent arena for exchanging ideas and experiences.

We hope that you will enjoy your stay in Trondheim.

Sincerely yours,
The organizing committee

Magnus Langseth
Tore Børvik
Odd Sture Hopperstad
Arild Holm Clausen
David Morin
Vegard Aune
Miguel Costas



PROGRAMME

The background of the page features a series of overlapping geometric shapes in various shades of red and pink. These shapes, including diamonds and triangles, are arranged in a way that creates a sense of depth and movement. The colors range from a deep, vibrant red to a soft, pale pink. The shapes are oriented diagonally, adding to the dynamic feel of the design.

MONDAY 13 JUNE 2022

18.00-21.00	Icebreaking get-together
-------------	--------------------------

TUESDAY 14 JUNE 2022

Plenum - Invited lectures Place: Trondhemssalen 1 - Chair: M. Langseth	
08.30-08.50	Welcome - Olav Bolland , Dean at the Faculty of Engineering, NTNU
08.50-09.20	<i>Impact Loading of Components and Structures</i> M. Alves (University of São Paulo)
09.20-09.50	<i>Modelling of Failure in Aluminium Structures</i> O.S. Hopperstad (NTNU)
09.50-10.20	BREAK
Session 1 - Failure of structures and materials under impact and blast loading - Chair: T. Børvik	
10.20-10.40	<i>Modeling the Interaction of a Generic Hollow Projectile with Different Types of Masonry</i> A. Heine , C. Sauer, W. Riedel (Fraunhofer EMI)
10.40-11.00	<i>Experimental investigation under laser-driven shocks of the dynamic behavior of materials for beam-intercepting devices in particle accelerators</i> L. Baudin (CERN), C. Accettura (CERN), A. Morena (Politecnico di Torino), L. Wegert (GSI), A.S. Martynenko (GSI), P. Neumayeur (GSI), M. Tomut (GSI/University of Münster), A. Bertarelli (CERN), F. Carra (CERN), L. Peroni (Politecnico di Torino), M. Scapin Politecnico di Torino), C. Brabetz (GSI)
11.00-11.20	<i>New insights into the role of porous microstructure on dynamic shear localization</i> A. R. Vishnu, M. Marvi-Mashhadi, J. C. Nieto-Fuentes, J. A. Rodríguez-Martínez (University Carlos III Madrid)
11.20-11.40	BREAK
11.40-12.00	<i>The behavior of ceramics and geomaterials during impact events</i> K.T. Ramesh (Johns Hopkins University)
12.00-12.20	<i>Sensitivity analysis of analysis program to crash analysis results of the aircraft engine for the spent fuel transport cask</i> J.S. Kim (Sejong University), M.S. Cha (Graduate School, Sejong University)
12.20-12.40	<i>Performance of a Welded Steel Component Under Shock Loading</i> M. Cotton , A. Whorton (AWE Aldermaston)
12.40-13.00	<i>Studying Dynamic Fragmentation of Metallic Rings Using a Single-stage Gas Gun: A Novel Experimental Approach</i> J.C. Nieto Fuentes (UC3M) N. Jacques (ENSTA), J.A. Rodríguez-Martínez (UC3M)
13.00-14.00	LUNCH
Session 2 - Failure of structures and materials under impact and blast loading - Chair: M. Alves	
14.00-14.20	<i>A distribution model for low-velocity impact tests on Kevlar-epoxy composites reinforced by nanoparticles</i> D. Ma (Politecnico di Milano), S.C. Amico (Federal University of Rio Grande do Sul), M. Giglio (Politecnico di Milano), A. Manes (Politecnico di Milano)
14.20-14.40	<i>Deformation and energy absorption characteristics of 3D-printed polymeric lattices under static and impact compression</i> Z.P. Sun (National University of Singapore), Y.B. Guo (National University of Singapore), V.P.W. Shim (Ningbo University/National University of Singapore)
14.40-15.00	<i>Data-driven approach to account for fluid-structure interaction effects on blast loaded steel plates</i> L. Lomazzi (Politecnico di Milano), A. Manes (Politecnico di Milano), F. Cadini (Politecnico di Milano), D. Morin (NTNU), V. Aune (NTNU)
15.00-15.20	<i>Adiabatic Shear Failure of Lightweight Materials: From Titanium Alloys to PA66-GF30 Composite</i> L. Zhang , D. Townsend (University of Oxford)
15.20-15.40	<i>Snow Avalanche Impact Loads: Work-Energy Methods to Calculate Impulsive Pile-Up and Deflection Forces with Shear Traction</i> P. Bartelt, J. Borner , A. Caviezel (WSL Institute for Snow and Avalanche Research SLF)

15.40-16.00	BREAK
Plenum - Invited lectures - Chair: M. Langseth	
16.00-16.30	<i>Additively Manufactured Protective Structures</i> T. Børvik (NTNU), M. Costas (NTNU), M. Edwards-Mowforth (The University of Edinburgh), M. Kristoffersen (NTNU)
16.30-17.00	<i>Post-Failure Momentum Transfer in Momentum Enhancement, Size Scaling, and Comments on the DART Impact in September</i> J. Walker , S. Chocron (Southwest Research Institute)
18.00-20.00	Concert and Welcome Reception at Nidaros Cathedral

WEDNESDAY 15 JUNE 2022

Plenum - Invited lectures - Chair: M. Langseth		
08.30-09.00	<i>Transient response of structures subjected to blast loading: the chase for better experimental measurements</i> G.S Langdon (The University of Sheffield/BISRU), R.J. Curry (The University of Sheffield), S.E. Rigby (The University of Sheffield), S.D. Clarke (The University of Sheffield), A. Tyas (The University of Sheffield/Blastech Inc.)	
09.00-09.30	<i>Crash Response of Li-ion Battery cells: From multi-scale analysis to engineering models</i> T. Tancogne-Dejean (ETH Zurich), J. Zhu (MIT), D. Mohr (ETH Zurich/MIT)	
09.30-10.00	BREAK	
Parallel sessions 10.00-15.00		
	Session 3 - Failure of structures and materials under impact and blast loading Place: Trondhemssalen 1 - Chair: G.S. Langdon	Session 4 - Dynamic material behaviour and failure Place: Trondhemssalen 2 - Chair: P. Verleysen
10.00-10.20	<i>Comparison of drone collision and bird strike on aircraft radome using experimental and simulation methods</i> S. Heimbs , J. Hansen, M. Woidt (TU Braunschweig)	<i>Mechanical behavior of Ultra High Molecular Weight PolyEthylene for blast and ballistic protection</i> M. Arrigoni , M. Castres, A. El Malki Alaoui (IRD/L/ENSTA Bretagne)
10.20-10.40	<i>Behaviour of multi-layered plates impacted by high-velocity projectiles</i> M. Orlov , V.P. Glazyrin, T.V. Fazylov (Tomsk State University) <i>Optimization of the electromechanical behavior of a piezoresistive polyurethane based foam during quasi-static and dynamic solicitations</i> A. Poirot (ESTACALAB/ENSTA Bretagne), M. Arrigoni (ENSTA Bretagne), N. Bedrici (ESTACALAB), Jean-Christophe Walrick (ESTACALAB)	<i>The challenge of accurate strain measurement during dynamic testing of fibrous composites in the split Hopkinson bar technique</i> A. Gilat , J. Seidt, M. Konieczny (The Ohio State University)
10.40-11.00	<i>Carbon fibre composite exposed to blast loading: A preliminary study</i> R. del Cuvallo (UC3M), M. Costas (NTNU) V. Aune (NTNU), T. Børvik (NTNU) J. A. Artero-Guerrero (UC3M), J. Pernas-Sánchez (UC3M), J. López-Puente (UC3M)	<i>Failure characterization for polymers at different strain rates and temperatures</i> V. Dorléans (FAURECIA), R. Delille (UPHF), F. Lauro (UPHF), D. Notta-Cuvier (UPHF), G. Haugou (UPHF), E. Michau (FAURECIA)
11.00-11.20	<i>Effects of Ship Collision on Offshore Wind Turbines</i> N. Mehreganian (University of Massachusetts Dartmouth), G.K. Boiger (ZHAW), Y. Safa (ZHAW), A.S. Fallah (Oslo Metropolitan University)	<i>Mechanical response of an armour steel alloy under combined condition of elevated temperature, high strain rate and triaxiality</i> E. Cadoni , M. Dotta, D. Forni (University of Applied Sciences and Arts of Southern Switzerland) <i>Experimental study on the response of sacrificial add-on armor</i> L. Blanc , D. Eckenfels, J.F. Legendre (ISL)

10

11.20-11.40	BREAK	BREAK
	Chair: O.S. Hopperstad	Chair: D. Mohr
11.40-12.00	<i>Experimental and Numerical Investigation of High Density Polyurethane Foam for Impact Against Metallic Target Plates</i> D. Narayan , M. Singh, N. Bhatnagar (Indian Institute of Technology Delhi)	<i>A simplified approach in the design of energy absorbing cellular structures by means of the efficiency curves</i> M. Avalle (University of Genoa)
12.00-12.20	<i>A state of the art review of numerical models for Hyper Velocity Impacts in Space</i> T. Cardone (Delft University of Technology/ESTEC ESA), C. Bisagni (Delft University of Technology)	<i>Blast Attenuation in Cohesive Soils</i> A. van Lerberghe (University of Sheffield), S. Clarke (University of Sheffield), A.D. Barr (University of Sheffield), S.L. Kerr (DSTL)
12.20-12.40	<i>Low-velocity impact on aluminium plates with geometric defects. An experimental and numerical study</i> V. Espeseth , T. Børvik, O.S. Hopperstad (NTNU)	<i>Polymer testing with a pre-tensioned steel split-Hopkinson bar</i> E. Schwenke , D. Morin, A.H. Clausen (NTNU)
12.40-13.00	<i>Blast resistance of pre-damaged steel plates</i> B.S. Elveli , T. Berstad, T. Børvik, V. Aune (NTNU)	<i>Impact of Full-field Measurement Biases on Identification of Anisotropic Material Behavior Model</i> J.D. Thoby (ONERA/UPHF/LAMIH), T. Fourest (ONERA), D. Notta-Cuvier (ONERA/LAMIH), E. Markiewicz (UPHF/LAMIH), B. Langrand (ONERA/LAMIH)
13.00-14.00	LUNCH	LUNCH
	Session 5 - Terminal ballistics Chair: O.S. Hopperstad	Session 6 - Dynamic material behaviour and failure Chair: D. Mohr
14.00-14.20	<i>A numerical modelling and generative deep learning approach to the ballistic impact resistance of additive manufactured maraging steel plates</i> M. Edwards-Mowforth (The University of Edinburgh), S. Thompson (The University of Edinburgh), M. Costas (NTNU), M. Kristoffersen (NTNU), T. Børvik (NTNU), F. Teixeira-Dias (The University of Edinburgh)	<i>Characterization with LASer Shock Adhesion Test of the interface strength of a HDPE composite coated with ceramic</i> R. Ben Saada (ENSTA Bretagne), A. El Malki Alaoui (ENSTA Bretagne), G. Darut (Université Bourgogne Franche-Comté), J. Le Blanche (ENSTA Bretagne), M. Arrigoni (ENSTA Bretagne)
14.20-14.40	<i>Modelling of concrete subjected to projectile impact</i> S. Dey (Norwegian Defence Estates Agency), M. Kristoffersen (NTNU), O. Toreskås (Norwegian Defence Estates Agency), T. Børvik (NTNU)	<i>Static and dynamic characterization of UHMWPE with nanoparticles</i> A.R. Aziz, H. Alabdouli, A. Alshehhi, M. Gutierrez, R. Santiago, Z. Guan (Advanced Materials Research Center)
14.40-15.00	BREAK	BREAK
	Plenum - Invited lectures Place: Trondhemssalen 1 - Chair: M. Langseth	
15.00-15.30	<i>Some studies of the mechanics of origami structures and materials</i> G. Lu (Swinburne University of Technology)	
17.00-21.00	Boat trip to Munkhomen (Monk's islet)	

THURSDAY 16 JUNE 2022

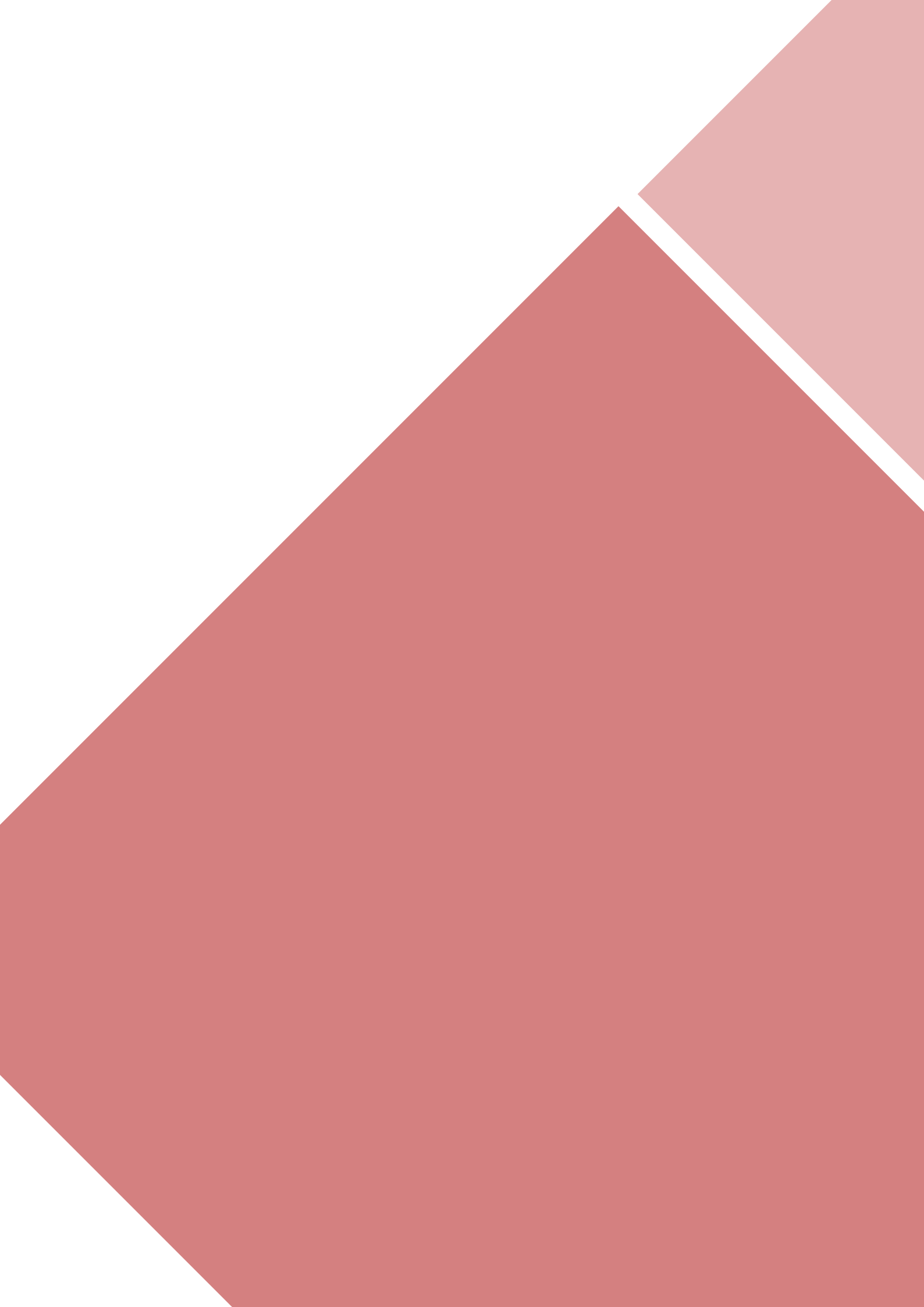
Plenum: Invited lectures - Chair: M. Langseth		
08.30-09.00	<i>Heterogeneous field based tests for identification of materials constitutive models at high rate of strains</i> E. Markiewicz (UPHF), B. Langrand (UPHF/ONERA), D. Notta-cuvier (INSA/UPHF)	
09.00-09.30	<i>Revealing the strain rate dependent behaviour of a dual phase automotive steel by in-depth analysis of test data</i> P. Verleysen , S. Chandran (Ghent University)	

09.30-10.00	BREAK	
Parallel sessions 10.00-16.00		
	Session 7 - Structural crashworthiness Place: Trondhemssalen 1 Chair: E. Markiewicz	Session 8 - Impact, blast and high-rate loading/ measurement techniques and their applications Place: Trondhemssalen 2 - Chair: G. Lu
10.00-10.20	<i>Determination of mechanical property profiles for improved crash performance of a dual phase automotive steel</i> S. Chandran , P. Verleysen (Ghent University)	<i>The Virtual Fields Method for Reconstruction of Impact and Blast Loading</i> R. Kaufmann , S.N. Olufsen, E. Fagerholt, V. Aune (NTNU)
10.20-10.40	<i>Experimental study for water impact of composite panels</i> Y. Tu (Delft University of Technology), M. Zanella (Politecnico di Milano), P. Astori (Politecnico di Milano), C. Bisagni (Delft University of Technology)	<i>Suppression of Extra Oscillations on Impact Force Wave in Instrumented Taylor Impact Test by Pulse-shaping Technique</i> C. Gao (Hiroshima University), T. Iwamoto (Hiroshima University), Y. Tanaka (Hiroshima University), T. Kusaka (Ritsumeikan University)
10.40-11.00	<i>Using machine learning to analyze and design low-density foam for impact energy absorption</i> F. Zhu (Johns Hopkins University), R. Zhou (Johns Hopkins University), Z. Yang (Suffolk University)	<i>A Measurement of Impact Force by PVDF for Instrumented Taylor Impact Test</i> N. Sakata , G. Chong, T. Iwamoto, Y. Tanaka (Hiroshima University)
11.00-11.20	<i>The effective width and fold size of thick square tubes under axial loading</i> N. Jafarzadeh Aghdam , K.U. Schroeder (RWTH-Aachen University)	<i>Impact of PU Foam Projectiles to Assess the Performance of Aluminum Panels Against Blast Loading</i> D. Narayan , N. Bhatnagar (Indian Institute of Technology Delhi)
11.20-11.40	BREAK	BREAK
	Chair: A.H. Clausen	Chair: B. Langrand
11.40-12.00	<i>Characterization and modelling of the fast dynamics strength of a Pa66/Aluminum SPR assembly</i> N. Leconte, B. Bourel, F. Lauro , E. Markiewicz (UPHF)	<i>Optimization of the electromechanical behavior of a piezoresistive polyurethane based foam during quasi-static and dynamic solicitations</i> A. Poirot (ESTACALAB/ENSTA Bretagne), M. Arrighoni (ENSTA Bretagne), N. Bedrici (ESTACALAB), Jean-Christophe Walrick (ESTACALAB)
12.00-12.20	<i>Development of a numerical model of a motorcycle helmet for the investigation of road traffic accidents</i> H. Ramos (University of São Paulo/Technology Innovation Institute), R. Santiago (University of São Paulo/Technology Innovation Institute), M. Alves (University of São Paulo)	<i>Design of a high strain rate in-plane torsion test</i> V. Grolleau (ETH Zürich/IRDL), C.C. Roth (ETH Zürich), B. Galpin (IRDL/CREC), D. Mohr (ETH Zürich)
12.20-12.40	<i>Simulation of a 1000 MPa Front Side Frame</i> S.H. Lee (University of Waterloo), M. Tummers (University of Waterloo), Michael Worswick (University of Waterloo), S. Malcolm (Honda Development and Manufacturing). Presented by C. Tolton (University of Waterloo)	<i>High strain-rate tests at high temperature in controlled atmosphere</i> A. Morena , M. Scapin, L. Peroni (Politecnico di Torino)
12.40-13.00	<i>Novel test for characterizing resistance spot weld group assemblies under shear loading</i> C. Tolton (University of Waterloo), J. Imbert-Boyd (University of Waterloo), M. Worswick (University of Waterloo), S. Malcolm (Honda Development and Manufacturing)	<i>A simple methodology to perform dynamic triaxial tests using split-Hopkinson bars</i> D. Kumar (Indian Institute of Technology Hyderabad/Swinburne University of Technology), S.N. Khaderi (Indian Institute of Technology Hyderabad/Swinburne University of Technology), D. Ruan (Swinburne University of Technology)

13.00-14.00	LUNCH	LUNCH
Session 9 - Structural crashworthiness, Impact/blast/measurement techniques, Stress waves, High-rate mechanical and forming processes, and Systems for protection Place: Trondhjemssalen 1 - Chair: A. Benallal		
14.00-14.20	Testing and modelling of aluminium rims under quasi-static and dynamic loadings D. Morin, O.S. Hopperstad, M. Langseth (NTNU)	
14.20-14.40	Effect of Diaphragm on Pressure Profiles Generated in Shocktube L. Gaur, R. Singh, T. Chakraborty (Indian Institute of Technology (IIT) Delhi)	
14.40-15.00	Theoretical predictions of dynamic necking formability of ductile metallic sheets with evolving plastic anisotropy and tension-compression asymmetry M. Anil Kumar (UC3M) , K. E. N'souglo (UC3M), N. Hosseini (UC3M), N. Jacques (ENSTA) , J.A.Rodríguez Martinez (UC3M)	
15.00-15.20	A simple and computationally efficient stress integration scheme based on numerical approximation of the yield function gradients: Application to advanced yield criteria N. Hosseini, J.A. Rodríguez-Martínez (UC3M)	
15.20-15.40	Impact of Power Transmission Lines by Powder Avalanches O. Gorynina, P. Bartelt (WSL Institute for Snow and Avalanche Research SLF)	
15.40-16.00	BREAK	
	Plenum: Invited lectures - Chair: M. Langseth	
16.00-16.30	An explicit phase field method for dynamic fracture H. Ren (Leibniz University), X. Zhuang (Leibniz University), C. Anitescu (Bauhaus University Weimar), T. Rabczuk (Bauhaus University Weimar)	
16.30-17.00	Dynamical Behaviour of Champagne Bubbles: from initiation to explosion F. Moussy (Renault)	
19.00-22.00	Banquet - Rockheim Museum	

FRIDAY 17 JUNE 2022

Session 10 - Structural crashworthiness, Impact/blast/measurement techniques, Stress waves, High-rate mechanical and forming processes, and Systems for protection Place: Trondhjemssalen 1 - Chair: D. Morin		
09.00-09.20	<i>Identification of armour technological solutions following experiment-simulation correlation</i> Y. Cosquer (ISAE-SUPAERO), P. Longère (ISAE-SUPAERO), O. Pantalé (LGP), C. Gailhac (CNIM Systèmes Industriels)	
09.20-09.40	<i>On the Mechanical Properties of Tungsten Heavy Alloy at Low, Intermediate and High Strain Rates</i> C. Roth (ETH Zürich) Teresa Fras (ETH Zürich/ISL), D. Mohr (ETH Zürich)	
09.40-10.00	<i>Experimental study on the response of sacrificial add-on armor</i> L. Blanc , D. Eckenfels, J.F. Legendre (ISL)	
10.00-10.20	<i>The Treatment of Contact/Impact Problems in Rockfall Dynamics</i> A. Caviezel (WSL Institute for Snow and Avalanche Research SLF/CERC), J. Borner (WSL Institute for Snow and Avalanche Research SLF/CERC), A. Lanter (Geogrugg), P. Bartelt (WSL Institute for Snow and Avalanche Research SLF/CERC)	
10.20-10.40	BREAK	
10.40-11.00	<i>"Numerical simulation of a climber fall: comparison of different models"</i> M. Avalle (University of Genoa), A. Scattina (Politecnico di Torino)	
11.00-11.20	<i>"High strain-rate behavior of 316L architected materials manufactured by LMD-P and SLM"</i> C. Buros (University of Bordeaux), P.Viot (Arts et Métiers), J.Lartigau (University of Bordeaux)	
11.20-12.00	LUNCH	





INVITED LECTURES

**Marcilio Alves**

University Of São Paulo

Marcilio Alves graduated in Mechanical Engineering in 1983 and obtained the Doctoral Degree at The University of Liverpool in 1996. He is a Professor at the University of São Paulo, where he established the Group of Solid Mechanics and Structural Impact. He obtained various grants which supports his research activities in the areas of structural impact, material characterisation and non-linear finite elements. He has published many international articles in scientific journals with authors from Brazil, UK, Germany, Bulgaria, China, Iran and Norway, covering theoretical, experimental and numerical aspects of impact engineering. He edited 4 books on Structural Impact and Solid Mechanics and is the Editor-in-Chief and founder of the Latin American Journal of Solids and Structures. He was president of the International Society of Impact Engineering and author of the book Impact Engineering: Fundamentals, Experiments and Nonlinear Finite Elements.

3rd International Conference on Impact Loading of Structures and Materials
ICILSM 2022

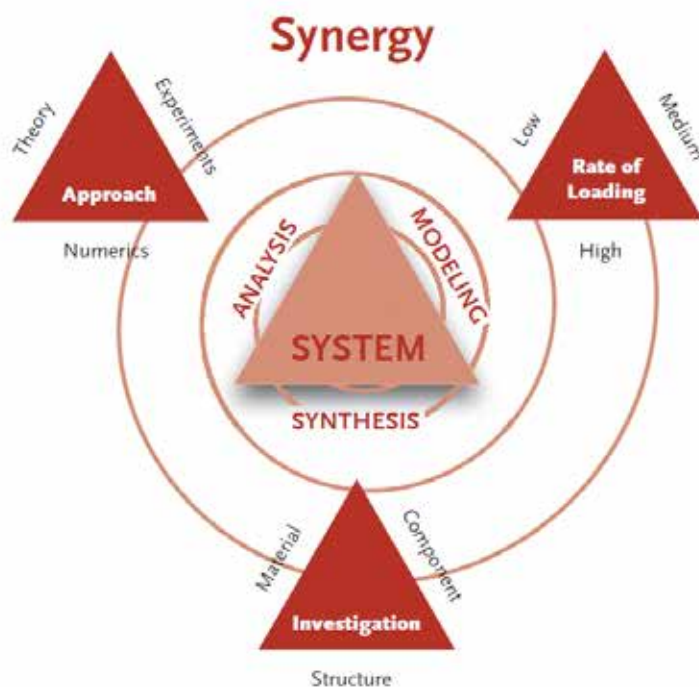
Impact loading of components and structures

Marcilio Alves

*Group of Solid Mechanics and Structural Impact
Department of Mechatronics and Mechanical Systems Engineering, University of São Paulo*

Abstract

Components and structures present a complex response when subjected to high intense dynamic loading. This is due to effects like inertia and material nonlinear response. To understand their behaviour it is necessary an integrated approach comprising experimental and numerical analysis and a firm theoretical background. Some of these aspects of impact engineering are therefore presented here. They are based on various studies developed by the author along the years. This includes human body response to crash accidents, impact on plates, measurement of material strength, scaling of structures, 3D printed components behaviour, etc. A broad overview of the presentation is depicted in the figure [1].



An overview of an integrative approach to building knowledge in the area of impact engineering.

Reference

1-M. Alves, Impact Engineering: Fundamentals, Experiments and Nonlinear Finite Elements, 2020 DOI 978-85-455210-0-6



James D. Walker

Southwest Research
Institute

James D. Walker is Director of the Engineering Dynamics Department and an Institute Scientist at Southwest Research Institute (SwRI), where he oversees a multi-disciplinary effort investigating the dynamic response of materials and structures. His work includes and combines large scale numerical simulations, analytical techniques, and experiments. He authored *Modern Impact and Penetration Mechanics* published by Cambridge University Press (2021). Dr. Walker is the recipient of three NASA Group Achievement Awards. In 2004 he was included in *Popular Science*'s third annual list of "Brilliant 10" scientists. He was awarded the 2005 ASME Holley Medal and the 2014 TAMEST O'Donnell Award in Technology Innovation. He is a Ballistics Science Fellow of the International Ballistics Society (IBS) and is a fellow AIAA and ASME. He is a past president of the Hypervelocity Impact Society and is the current president of the IBS. He lives with his wife and daughters in San Antonio, Texas.

3rd International Conference on Impact Loading of Structures and Materials
ICILSM 2020

Post-Failure Momentum Transfer in Momentum Enhancement, Size Scaling, and Comments on the DART Impact in September

James D. Walker* and Sidney Chocron

Southwest Research Institute, 6220 Culebra Rd., San Antonio, Texas 78238, USA

Abstract

When a hypervelocity impact occurs, a crater forms. The crater ejecta moves in the opposite direction of the impactor and increases the momentum transferred to the impacted body. This effect is called momentum enhancement and is quantified by $\beta - 1$, the extra momentum transferred above that of the projectile normalized by the impactor momentum. There are a number of very interesting behaviors in momentum enhancement, including a strong dependence on the impactor size. Quantifying the size scale behavior is hampered by the actual sizes of projectiles that can be launched with existing two-stage light gas guns. Thus, it is necessary to extrapolate experimental data or to perform computations if we are interested in large (decimeter scale or larger) impacts. Unfortunately, we are hampered in using computations because, at present, computations do not match the existing data. It appears the lack of agreement is due to the fact that momentum enhancement occurs from post-failed debris interacting with the target, where ejecta material impacts and slides along the crater walls of the target as it exits. Thus, not only do we have the traditional complications encountered in impact and penetration mechanics of large deformation and then failure, but to quantitatively compute the momentum enhancement it is necessary to accurately compute the post-failed behavior and interactions.

As a specific example, we examine the amount of material liberated in hypervelocity impacts from aluminum targets (1100-O and 2024-T351). Experiments have been performed for impact speeds up to 8 km/s, with work being done at NASA Ames and SwRI. The range of size scales is 19, from 0.16 cm to 3 cm diameter aluminum sphere impactors. We show that a sophisticated damage model that includes a failure distance for a sliding slip band can reproduce the amount of ejecta material (i.e., the amount of material liberated from the crater). These computations were performed with high fidelity Eulerian computations using CTH. However, the momentum enhancement is not correctly computed, which we believe is due to the post-failed behavior of material and interactions not occurring correctly. We look at possible ways to address these problems, including performing computations in a Lagrangian framework using EPIC with its transformation of elements to particles after a given criterion is met.

Finally, we will make a few comments related to the impact of the DART (Double Asteroid Redirection Test) spacecraft into the asteroid Didymos' moon scheduled for September 2022. The issue of size scaling is paramount. A big challenge for a prediction, though, is the unknown surface material and condition at the impact site.

Understanding the physics of the post-failure interactions so that we can produce believable computational results is of considerable interest. If the experimentally-observed size scaling continues to meter size scales, then we obtain β s of greater than 10 for spacecraft scale impacts into asteroids. If the size scaling saturates at a small impactor diameter, then β s will be

* Corresponding author. Tel.: 210-522-2051; fax: 210-522-6290.
E-mail address: james.walker@swri.org

relatively small for spacecraft impacts. Large values of β would make the hypervelocity impactor a method of interest for deflecting potentially dangerous asteroids and comet nuclei.

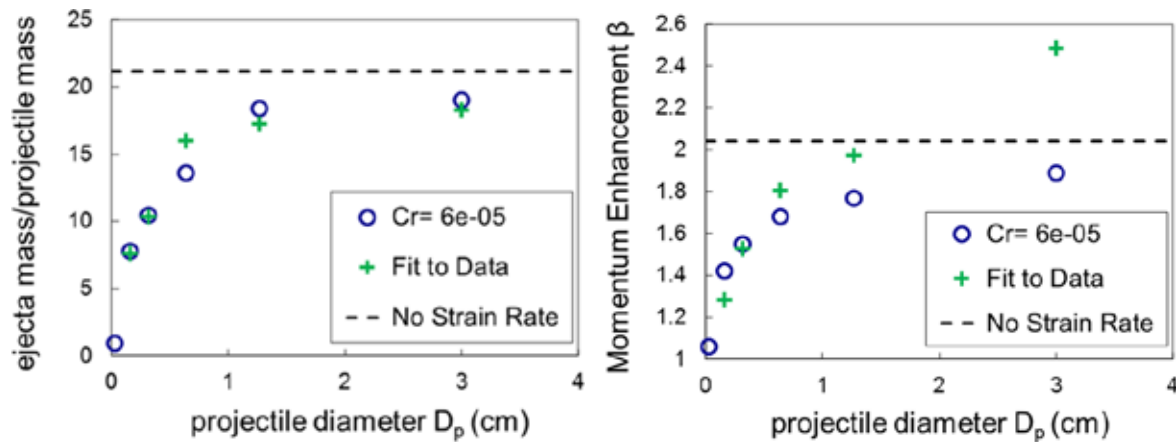


Figure 1. Experimental results for 5.77 km/s impacts for a range of aluminum projectile sizes striking Al 2024-T4 and T351 targets, performed at NASA Ames and SwRI (green crosses). Corresponding CTH computations with a sophisticated failure model are shown (blue circles; dashed lines correspond to computation of extremely large size impactor saturation case) [1].

1. "Size Scaling of Hypervelocity-impact Ejecta Mass and Momentum Enhancement: Experiments and a Nonlocal-shear-band-motivated Strain-rate-dependent Failure Model," J. D. Walker, S. Chocron, D. J. Grosch, *Int. J. Impact Engng* **135** (2020) 103388:1-14 DOI: 10.1016/j.ijimpeng.2019.103388.
2. *Modern Impact and Penetration Mechanics*, J. D. Walker, Cambridge University Press, Cambridge (2021).
3. "The Double Asteroid Redirection Test (DART): Planetary Defense Investigations and Requirements," Rivkin, A. S., Chabot, N. L., Stickle1, A. M., Thomas, C. A., Richardson, D. C., Barnouin, O., Fahnestock, E. G., Ernst, C. M., Cheng, A. F., Chesley, S., Naidu, S., Statler, T. S., Barbee, B., Agrusa, H., Moskovitz, N., Daly, R. T., Pravec, P., Scheirich, P., Dotto, E., Corte, V., D., Michel, P., Küppers, M., Atchison, J., & Hirabayashi1, M. *PSJ* **2**, 17 (2021).
4. "Momentum enhancement from a 3-cm-diameter aluminum sphere striking a small boulder assembly at 5.4 km/s," J. D. Walker, S. Chocron, D. J. Grosch, S. Marchi, A. M. Alexander, *PSJ*, submitted (2022).



Tore Børvik
NTNU

Dr. Børvik is currently a professor (100% position) at Department of Structural Engineering, NTNU, and a senior advisor (20% position) for the Norwegian Defence Estates Agency. He has an expertise and research interest in modelling, simulation and testing of materials and structures exposed to extreme loadings, such as ballistic impact, blast loading, dropped objects and crashworthiness. He was the programme head of the research programme Optimal Energy Absorption and Protection in SFI SIMLab at NTNU from 2007-2014, and he is the vice director and a programme head of the research programme Structures in SFI CASA at NTNU from 2015-2023. Currently he is the group leader of SIMLab, NTNU. From 2016-2021 he was a core team member of the FRIPRO Toppforsk-project FractAl. He has authored 200 articles in peer-reviewed journals, and a corresponding number of papers at international conferences. At present, he serves as an Associate Editor in the International Journal of Impact Engineering and on the Editorial Board of Strain.

3rd International Conference on Impact Loading of Structures and Materials
ICILSM 2022

Additively Manufactured Protective Structures

Tore Børvik^{a,*}, Miguel Costas^a, Maisie Edwards-Mowforth^b, Martin Kristoffersen^a

^a*SFI CASA and SIMLab, Department of Structural Engineering, NTNU – Norwegian University of Science and Technology, NO-7491 Trondheim, Norway*

^b*School of Engineering, The University of Edinburgh, Edinburgh EH9 3FG, UK*

^c*SINTEF Manufacturing AS, NO-7465 Trondheim, Norway*

Abstract

Additive manufacturing (AM) is presumed to have a transformational effect in many industries, especially where low weight combined with high performance is in demand. Metal AM, in particular, possesses a large and unrealised potential regarding protective structures for ballistic impact, crashworthiness, and spacecraft. In a recent study by some of the authors [1], the ballistic perforation resistance of AM AlSi10Mg aluminium plates was investigated and compared to plates from a traditionally die-cast block of the same material. The important conclusion from that study was that an AM material may have similar or even better ballistic properties than a traditionally manufactured material with the same chemical composition. Additionally, a standard and widely used material model for ballistic impact simulations was calibrated based on material tests using inverse modelling. 3D finite element models of the ballistic impact problems were established in ABAQUS/Explicit, and the predicted results were compared to the experimental data. The agreement between numerical and experimental results was in general good (see Figure 1), even though no special measures were undertaken concerning the fact that the target material was produced by additive manufacturing.



Figure 1: Comparison of experimental test and numerical simulation of a 7.62 mm AP bullet perforating a 5 mm thick AM AlSi10Mg plate [1].

In a subsequent study [2], the ballistic properties of AM maraging steel, a material known for its extreme strength after heat treating, were investigated. First, monolithic plates with dimensions 100 mm × 100 mm × 5 mm and 100 mm × 100 mm × 10 mm were fabricated by powder bed fusion. In addition to the plates, profile panels with the same areal density as the thickest plates were printed. Post AM, half of the samples were heat-treated at 490°C for 6 hours, while the rest were left as built. From these samples, material specimens were extracted in different directions with respect to the build direction for material characterisation. The mechanical response was then revealed based on quasi-static tensile tests at room and elevated temperatures, and dynamic tensile tests in a Split-Hopkinson bar at room temperature. Metallurgical investigations were also conducted to study the microstructure of the material both before and after testing. The ballistic perforation resistance of the AM maraging steel samples was finally investigated in a ballistic range by firing 7.62 mm APM2 bullets towards the different targets. In the

* Corresponding author. Tel.: + 47 93 05 94 62
E-mail address: tore.borvik@ntnu.no

tests, a high-speed camera was used to measure initial and residual velocities of the bullet, and to capture high-resolution videos of the impact process. From these results, ballistic limit curves and velocities were obtained. It was found that especially the thickest maraging plate after heat treatment has a great potential in ballistic protection. The hard core of the AP bullet broke in all tests, and in some of the tests it was completely shattered (see Figure 2). However, due to the severe brittleness of the material, the targets showed significant fragmentation in some cases.

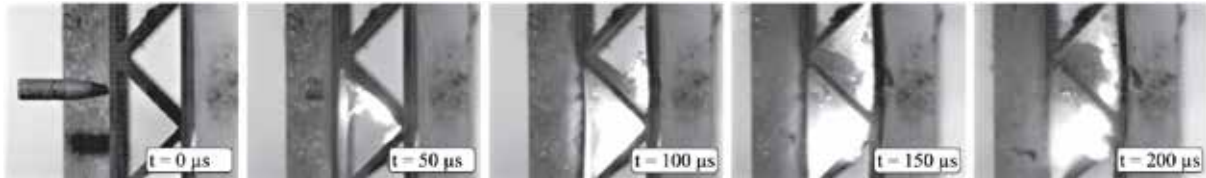


Figure 2: High-speed video pictures showing complete shattering of the 7.62 mm AP bullet during impact of an AM maraging steel profile panel [2].

In a similar manner to [1], a standard material model for ballistic impact simulations was calibrated based on the material tests; 3D finite element models of the ballistic impact problems were established in ABAQUS/Explicit, and the predicted results were compared to the experimental data. As was the case for the AM AlSi10Mg aluminium target plates in [1], the agreement between numerical and experimental results was satisfactory again despite that no special measures were undertaken to account for the AM production of the maraging target material.

From these studies, some preliminary conclusions can be drawn: 1) AM materials seem to have similar ballistic properties as traditionally manufactured materials with the same chemical composition, 2) standard material models seem to give good agreement between numerical predictions and experimental results in ballistic impact without accounting for the fact that the material is additively manufactured, 3) the potential of AM materials as a protective structure seems large. The next step in this ongoing research is to combine numerical optimization, additive manufacture, and materials design in an attempt to establish better protective solutions.

References

- [1] Kristoffersen M, Costas M, Koenis T, Brøtan V, Paulsen C, Børvik T. On the ballistic perforation resistance of additively manufactured AlSi10Mg aluminium plates. *International Journal of Impact Engineering* 2020;137:103476.
- [2] Costas M, Edwards-Mowforth M, Kristoffersen M, Teixeira-Dias F, Brøtan V, Paulsen CO, Børvik T. Ballistic impact resistance of additive manufactured high-strength maraging steel: An experimental study. *International Journal of Protective Structures* 2021;12:577-603.



Vikram Deshpande
Cambridge University

Prof. Vikram Deshpande joined the faculty of Engineering at the University of Cambridge as a lecturer in 2001 and was promoted to a professorship in Materials Engineering in 2010. He has written more than 270 journal articles in experimental and theoretical solid mechanics. He serves on the editorial boards of several journals in mechanics and biomechanics including Journal of the Mechanics and Physics of Solids, Modelling and Simulation in Materials Science and Engineering and the Proceedings of the Royal Society, London. He has been awarded recognitions that include the 2020 Rodney Hill Prize in Solid Mechanics, the 2022 William Prager medal, the 2022 ASME Koiter Medal and elected Fellow of the Royal Society, London

3rd International Conference on Impact Loading of Structures and Materials
ICILSM 2022

Micro-mechanics of ultra-high molecular weight polyethylene fibre composites

V.S. Deshpande

Cambridge University Engineering Department, Cambridge CB2 1PZ, UK

Abstract

Fibre composites comprising Ultra High Molecular Weight Polyethylene (UHMWPE) fibres in a polyurethane or polyethylene matrix are now extensively used for ballistic protection applications. This interest arises from a recognition that the ballistic limit of fibre composites scales linearly with the so-

called Cunniff velocity c^* given by $c^* = \left(\frac{\sigma_f \epsilon_f}{2\rho_f} \sqrt{\frac{E_f}{\rho_f}} \right)^{1/3}$ where σ_f and ϵ_f are tensile failure

strength and strain of the fibres, respectively while E_f is the tensile modulus of the fibres and ρ_f is the density of the fibres. Based on this parameter the UHMWPE fibres outperform most known materials as the UHMWPE fibres have a tensile strength exceeding 3.5 GPa at a density less than water. However, a detailed experimental investigation reveals that the Cunniff model fails to rationalise two key observations: (i) the ballistic performance of fibre based composites is strongly dependent on the shear strength of matrix and (ii) penetration of the UHMWPE composites does not occur in a membrane mode but rather in progressive manner, such that the number of failed plies increases with increasing impact velocity.

A comprehensive experimental and numerical investigation of the mechanics of these composites under both static and dynamic loading conditions will be reported. The understanding of the range of deformation/failure mechanisms gained from this combined numerical/experimental investigation will be used to motivate a discussion on a new class of UHMWPE composites that have the potential to further enhance performance.

**Genevieve Langdon**

Department of Civil and
Structural Engineering,
University of Sheffield

Genevieve Langdon is Professor of Blast and Impact Engineering at the University of Sheffield. She trained as a mechanical engineer, completing her undergraduate and doctoral studies at the University of Liverpool. She is a chartered engineer, member of the British Society for Strain Measurement, member of the Academy of Sciences of South Africa and is the secretary of the International Society of Impact Engineering. She gained first-hand experience in explosion testing after spending fifteen years working in Cape Town as an academic, including serving as Director of the Blast Impact and Survivability Research Unit for five years. She is currently an Honorary Professor at the University of Cape Town. She has been involved in developing and evaluating blast resistant materials and structures for use in transportation, defence and structural applications. She seeks to make the world a safer place through improved understanding of structural and material response under explosion loading. Her work has focused on understanding the mechanisms involved in the response of lightweight materials, composites, aerospace metals and armour steels, to improve their design and to inform the materials selection process. She is involved in extensive international collaborative research because of her expertise in structural blast response and blast experimentation.

3rd International Conference on Impact Loading of Structures and Materials
ICILSM 2022

Transient response of structures subjected to blast loading: the chase for better experimental measurements

G.S. Langdon^{a,b*}, R.J. Curry^a, S.E. Rigby^a, S.D. Clarke^a, A. Tyas^{a,c}

^a*Department of Civil and Structural Engineering, University of Sheffield, Mappin Street, Sheffield, S1 3JD, UK.*

^b*Blast Impact and Survivability Research Unit (BISRU), Department of Mechanical Engineering, University of Cape Town, Rondebosch 7700, Cape Town, South Africa.*

^c*Blastech Ltd., The Innovation Centre, 217 Portobello, Sheffield, S1 4DP, UK.*

Abstract

Providing adequate blast protection systems for infrastructure, equipment and people requires a detailed understanding of the likely threats that each of these faces. The most appropriate blast protection paradigm can be identified by understanding what constitutes “failure” in that context. In some cases, “failure” is simply plastic deformation that exceeds some specified amount, such as the plastic hinge rotation angles specified in some design codes (for example, see reference [1]). In other cases, the transient response and material rupture points are of greater importance, and in mine resistant ambush protected vehicles, the impulse transfer is also a factor [2-3].

What is common in each system is the need to understand the magnitude and distribution of the imparted explosion loading as well as its subsequent effects on the structure of interest. Simple tools exist for rapid evaluation of blast events that can be idealized as far-field explosions, in open spaces, impinging upon simple target geometries, when the structures do not shear or tear. These have been shown to provide good estimates [4] for simple loading, but unfortunately, “real-life” explosive events are complex. Examples of complexity include explosive detonations in confined spaces (urban settings like subways, inside buildings, or in city streets) or in the near-field (small stand-off distance). Transient response, complex failure modes and early-time rupture of the structure compound the difficulties. There is a pressing need for approaches which combine fundamental understanding of complex explosion loading and structural response with the ability to quantitatively predict these effects.

Carefully controlled, systematic, blast experimentation is vital in supporting the efforts of blast engineers and researchers in understanding and predicting blast loading and its effects on structures and materials. There are considerable challenges in measuring and recording data, including the extreme nature of the loading (high pressure, high temperature), the short duration of the loading and response (from microsecond to millisecond range), electromagnetic interference from the detonation, the bright explosive flash and challenges in reliably triggering multiple instruments at the same time. In recent years, general improvements in instrumentation and novel experimental approaches have provided renewed impetus to the chase for better experimental measurements from laboratory scale explosion tests [5-7].

Firstly, this paper briefly evaluates different experimental techniques and presents some recent experimental results from joint experimental work [8] at the explosion laboratories hosted by the Universities of Sheffield and Cape Town. Impulse distributions measured from near-field tests obtained from Sheffield’s Characterisation of Blast Loading (COBL) test facility

* Corresponding author. Tel.: +44 114 222 5737.

E-mail address: Genevieve.langdon@sheffield.ac.uk

(shown in Figure 1) are compared to equivalent scaled single-blind tests performed at BISRU, where the transient response is measured using a high-speed stereo video system (shown in Figure 2).

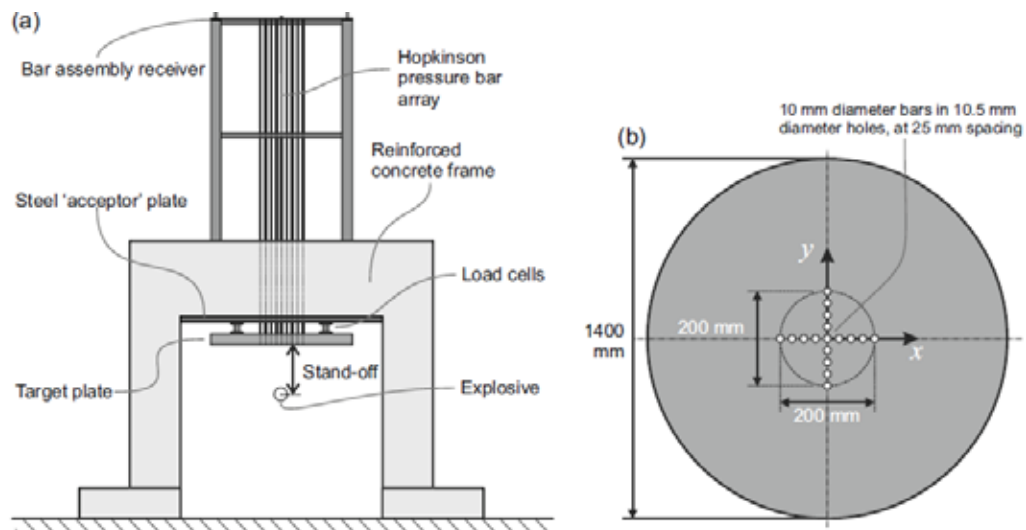


Figure 1: Schematics of the University of Sheffield COBL test facility

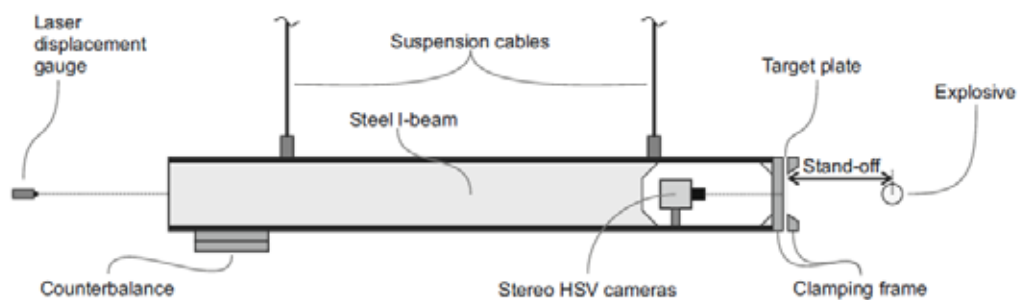


Figure 2: Schematic (side view) of the transient response blast pendulum at BISRU, University of Cape Town

The results are used to validate some numerical approaches commonly employed in LS-Dyna [9]. A new energy equivalent impulse approach is used to demonstrate an improved linear correlation between response and impulse, which better accounts for the spatial distribution of the loading. The inferred impulse method seems to be sensitive enough to detect spatial variations in loading caused by surface instabilities in the expanding detonation product cloud from cylindrical charge detonations. The findings show significant progress in the chase for better experimental measurements that characterize the loading and transient response of structures subjected to near-field explosions.

Secondly, the paper describes some of the continued developments since the success of those early trials, resulting in a new optical diagnostics system for blast capability at the University of Sheffield. This includes an upgraded stereo-imaging system with enhanced capabilities and provides some preliminary results on how it can provide additional insights. It then shows some recent advances in our capability to visualise detonation using ultra-high speed imaging, showing it to be a useful tool for visualizing detonation fronts in explosive charges and the expanding fireball.

References

1. C.E.N, Design of Steel Structures, Part 1–3 Eurocode 3, ENV 1993-1-3, 2006.
2. G.S. Langdon, A. Curry, A. Siddiqui. Thin-walled Struct, 148:106609, 2020.
3. G.S. Langdon, V.R. Shekhar. Int J of Protective Structures, 11(1):69-89, 2020.
4. S.E. Rigby, A. Tyas, T. Bennett. Eng Struct 45:396–404, 2012.
5. S.D. Clarke, S.E. Rigby, S. Fay, A. Barr, A. Tyas, M. Gant, I. Elgy. Proc. R. Soc. A, 476(2236):20190791, 2020.
6. R.J. Curry, G.S. Langdon. Int J Impact Eng, 102:102-116, 2017.
7. S.D. Clarke, S.D. Fay, J.A. Warren, A. Tyas, S.E. Rigby, I. Elgy. Meas Sci Technol 26:015001. 2015.
8. S.E. Rigby, A. Tyas, R.J. Curry, G.S. Langdon, Expt Mechanics, 59:163–178, 2019.
9. S.E. Rigby, O.I. Akintaro, B.J. Fuller, A. Tyas, R.J. Curry, G.S. Langdon, D.J. Pope, Int J Impact Eng, 128:24-36, 2019.



Dirk Mohr
ETH Zürich

Professor Dirk Mohr currently holds the Chair of Artificial Intelligence in Mechanics and Manufacturing at ETH's Department of Mechanical and Process Engineering (MAVT). He joined the faculty of ETH in 2015 after conducting research at the Experimental Dynamics Group at the Solid Mechanics Laboratory at Ecole Polytechnique (France) and MIT's Impact and Crashworthiness Lab. He received his undergraduate education from the University of Karlsruhe (Germany) and the Ecole Nationale des Ponts et Chaussées (France). He continued his graduate studies at the Massachusetts Institute of Technology (USA) where he received his PhD in Applied Mechanics in 2003. Professor Mohr's research activities include the crash response of Li-ion batteries, thermo-mechanical behavior of materials at high strain rates and the mechanics of mechanical metamaterials. He is the recipient of the Hetenyi Award (2007) from the Society of Experimental Mechanics and the IJP Young Investigator Award (2016) for his outstanding contributions to the field of plasticity. He is Associate Editor of the International Journal of Impact Engineering and the International Journal of Solids and Structures. He also serves on the editorial board of the journal Strain and the International Journal of Plasticity.

3rd International Conference on Impact Loading of Structures and Materials
ICILSM 2022

Crash Response of Li-ion Battery cells: From multi-scale analysis to engineering models

Thomas Tancogne-Dejean^a, Juner Zhu^b, Dirk Mohr^{a,b}

^a*Chair of Artificial Intelligence in Mechanics and Manufacturing, ETH Zurich, Switzerland*

^b*Impact and Crashworthiness Lab, MIT Cambridge, USA*

Abstract

The accidental impact loading of battery cell brings the risk of short circuit and thermal runaway. For the engineering of safe transportation vehicles, it is thus essential to have reliable computational models that can predict the large deformation response of batteries. Starting from experimental results on the constituent materials of Li-ion battery cells, a detailed micromechanical model is built to predict the macroscopic response of battery cells. To attain the computational efficiency required for large-scale crash simulations, a homogeneous-equivalent model of a battery cell is also developed based on the Deshpande-Fleck plasticity model. Furthermore, to attain even higher prediction accuracy, a machine-learning based plasticity model is also presented using a recurrent neural network approach. The results from Hopkinson bar impact experiments on battery cells are also shown for both in-plane and out-of-plane loading conditions. The comparison with the corresponding static experiments reveals a pronounced strain rate effects which is taken into account by the proposed macroscopic constitutive model.



Guoxing Lu

Swinburne University
of Technology

Professor Guoxing Lu obtained his PhD in 1989 from the University of Cambridge, supervised by Professor CR Calladine (FRS, FREng). After one year post-doctoral research at Cambridge, he worked as a faculty member at Nanyang Technological University, Singapore, and presently is Professor of Impact Engineering at Swinburne University of Technology, Melbourne, Australia. His research interests are energy absorption of structures and materials, mechanical properties of materials at high strain rates, impact mechanics and most recently origami structures. He has over 260 publications in international journals and one monograph co-authored with Professor Tongxi (TX) Yu, *Energy Absorption of Structures and Materials*, Elsevier, 2003. He has 11300 citations with an H-index of 56. He is an Associate Editor of *International Journal of Impact Engineering* and a member of editorial board of *International Journal of Mechanical Sciences*, *Thin-Walled Structures*, *Composites B* and others. He is President of International Society of Impact Engineering.

3rd International Conference on Impact Loading of Structures and Materials
ICILSM 2022

Some Recent Studies on Impact and Energy Absorption of Origami Structures and Metamaterials

Guoxing Lu*

School of Engineering, Swinburne University of Technology, Hawthorn Vic 3122, Australia

Abstract

This presentation introduces energy absorption and impact response of origami inspired structures and metamaterial, which we have recently studied. Several examples of incorporating the concepts of origami will be presented. They include thin-walled structures under axial loading, Miura metamaterials (Fig 1) and its variations under quasi-static and dynamic compression and origami sandwich panels under quasi-static loading and ballistic impact.

Responses of such materials and structures involve large plastic deformation as well as dynamic effects. For metamaterials, analytical models have been developed to describe the strength and energy absorption capacity. It is assumed that the base material is ductile and can be approximated as a perfectly-plastic material. The analytical model is verified by the numerical simulations as well as quasi-static compression test of a four-sheet origami specimen. Response of such material under impact loading is also investigated and a shock model is proposed for high velocity impact.

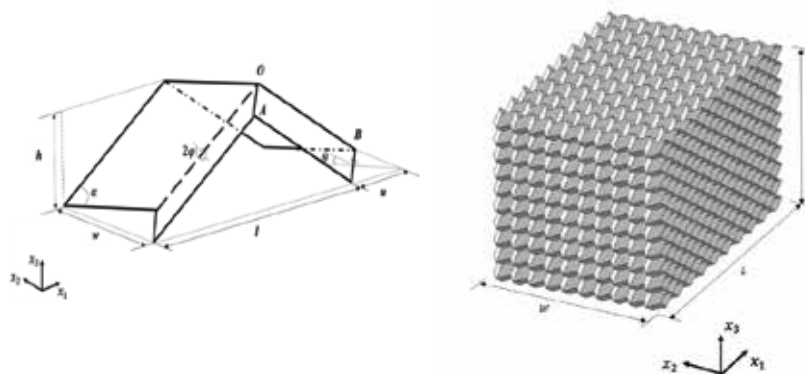


Fig 1 A Miura unit (left) and metamaterial made of Miura units (right)

* Corresponding author. Tel.: +61-3-92148669; fax: +61-3-9214 8264.
E-mail address: glul@swin.edu.au



Eric Markiewicz

Univ. Polytechnique
Hauts-de-France

Eric Markiewicz is Professor of Mechanical Engineering at University Polytechnique Hauts-de-France (UPHF). At the same time he is Vice-president for Research at UPHF and Head of the CNRS Research Federation "Ground Transports and Mobility". Previously he was Head of the Laboratory LAMIH UMR CNRS. He has published 3 book chapters, around 90 journal papers and 130 international conference papers. Prof. Markiewicz was Chairman of the 3rd ICILLS conference, held in 2011 in Valenciennes, France. He was former board member of the International Society of Impact Engineering and of DYMAT association (2012-2021). The research interests of Prof. Markiewicz deal with the behavior and failure of materials and structures submitted to complex loadings paths on a large range of plastic strains and strain rates. This includes the development of new testing and measurement methods, coupled with FE modelling, to understand the physics at various scales from micro to macro and to implement material parameters identification procedures.

3rd International Conference on Impact Loading of Structures and Materials
ICILSM 2022

Heterogeneous Fields Based Tests for Identification of Materials Constitutive Models at High Rate of Strains

Eric MARKIEWICZ^{a,*}, Bertrand LANGRAND^{b,a} and Delphine NOTTA-CUVIER^{c,a}

^aUniv. Polytechnique Hauts-de-France, CNRS, UMR 8201 – LAMIH, F-59313 Valenciennes, France

^bDMAS, ONERA, F-59014 Lille - France

^cINSA, Hauts-de-France, F-59313 Valenciennes, France

Abstract

The lecture aims at providing to the scientific community a synthesis of the research activities performed at the authors laboratories in the field of the characterisation of materials constitutive behaviour and damage under dynamic loadings [1-6].

The characterisation of material properties is very challenging, especially when the number of material parameters governing the constitutive equations is significant. This is particularly true when considering anisotropic materials and/or strongly nonlinear constitutive models, for example, in viscoplasticity or damage theories. Different normalized tests are necessary to calculate the parameters of the material models. Tests are generally exploited based on statically determined approach, i.e. by assuming that the mechanical fields are homogeneous over the specimen gauge length. A first limitation is that several tests are needed to characterize material behaviour dependency to strain-rate, e.g., as each test must be performed at a constant (over time) and uniform (over gauge length) strain rate. Moreover, material parameters are obtained with those tests in one loading direction while constitutive equations involve all strain and stress tensors components. Consequently, a large number of tests are required when complex behaviours at high rate of strains have to be characterised. The limitations of this statically determined approach can be overcome with the statically undetermined approach that considers no hypothesis on homogeneity of mechanical fields and therefore no constraint on loading conditions and test exploitation.

The most widespread statically undetermined approach is the Finite Element Model Updating (FEMU) method. FE simulations are iterated until constitutive parameters leading to the best match between numerical computations and experimental measurements is found. However, the main drawback of this approach is that it requires building a validated numerical model of the test, including the boundary conditions that can be often complex.

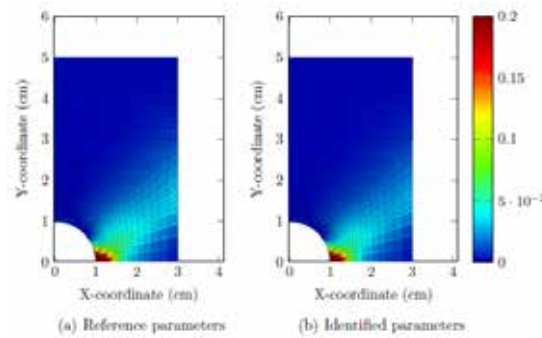
The Virtual Field Method (VFM) is another statically undetermined approach. Based on the principle of virtual work (PVW) the method expresses the global equilibrium of a solid of any shape. The VFM enables to take the full advantages of full-field measurement techniques, such the Digital Image Correlation (DIC) method. One of the main advantages of the VFM compared to FEMU methods is that it does not require building a numerical model of the test.

When virtual work of acceleration can be neglected, the VFM can be applied to identify material parameters with the only knowledge of strain fields and resultant of loading [1,2]. In a more original way, when high strain rates are concerned, some assumptions lead to an expression of the PVW allowing the identification of material parameters with the sole knowledge of strain and acceleration fields (Equation 1) [4]. In particular, the VFM does not require in that case the knowledge of any external loads, thus avoiding the use of an intrusive sensor (e.g. load cell). As optical devices are continuously being improved (notably in terms of spatial/temporal resolution), their combination with a full-field measurement technique is more and more suitable for high strain-rate testing and the identification of material parameters using the VFM.

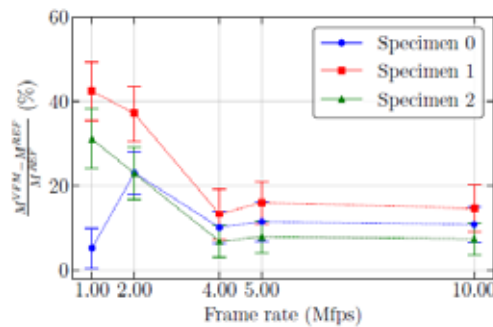
$$\int_V \sigma : \varepsilon^* dV + \rho \int_V \gamma : u^* dV = 0 \quad (1)$$

Several applications for different materials at various loading configurations and models are next given to support the presentation.

As a first example, the VFM is developed for the characterisation of a fully coupled elastoplastic-damage behaviour model, using one uniaxial tensile test only. The process of identification is assessed using two kinds of thin-specimen geometries (simulated strain fields by the FEA). Results demonstrate the efficiency of the VFM for the simultaneous identification of plastic and damage parameters (Figure 1) from a unique uniaxial tensile test, but also highlight that the definition of a suitable specimen geometry is a key factor for result accuracy.



As a second example, non standard Image-Based Inertial Impact (IBII) tests performed on titanium alloy Ti6Al4V specimens are presented. The IBII test uses an impact on one edge of the specimen to generate a short pressure pulse that loads the specimen. Three specimen geometries have been tested: a rectangular specimen, and two specimen geometries with stress concentrators (i.e. a hole and notches) to enhance high levels of plastic strain [4,5]. However, most of the test parameters (e.g. projectile velocity, specimen geometry) are not constrained. Therefore, in a first step a FE-based approach is addressed to optimize the test protocol over a wide range of strain and strain-rate, according to two design criteria: (1) the characterized viscoplastic spectra, (2) the identifiability of the parameters. Whereas the first criterion is assessed by processing the FEA simulations, the second is rated extracting material parameters using synthetic images to input the VFM. Finally, uncertainties regarding the identification of material constants are quantified for each test configuration and different high speed camera performances (Figure 2). In a second step, full-field measurement of the acceleration and strain are successfully used in combination with the VFM to identify the strain rate sensitivity parameter of the Johnson-Cook model. The strain/strain rate spectra covered by each specimen are analysed and compared to the predictions. Finally, the influence of the Virtual Field used in the identification process is discussed as well as the simultaneous identification of the JC viscoplastic model, here both the strain rate sensitivity parameter and the strain rate threshold parameter [4].



A last example deals with the robustness of specimens designed for identification of anisotropic material behavior model in terms of criteria that quantify heterogeneity of stress field on one hand and error in the identification procedure due to measurement biases on the other hand [6].

References

- [1] D. Notta, B. Langrand, E. Markiewicz, F. Lauro, G. Portemont, *Strain*, **49**, 22-45 (2013)
- [2] D. Notta-Cuvier, B. Langrand, F. Lauro, E. Markiewicz, *Int J. Solids and Structures*, **69–70**, 415-427 (2010)
- [3] E. Markiewicz, B. Langrand, D. Notta, *Int. J. of Impact Engineering*, **110**, 371-381 (2017)
- [4] P. Bouda, B. Langrand, D. Notta-Cuvier, E. Markiewicz, F. Pierron, *Comput. Mech.*, **64**, 1639-1654 (2019)
- [5] T. Fourest, P. Bouda, L.C. Fletcher, D. Notta-Cuvier, et al, *Experimental Mechanics*, **60**(2), 235-248 (2020)
- [6] J-D. Thoby, T. Fourest, B. Langrand, D. Notta-Cuvier, E. Markiewicz, *Computational Materials Science*, **207**, (2022)



Patricia Verleysen
Ghent University

Patricia Verleysen is full professor at Ghent University (Belgium) in the research group Materials Science and Technology. She is head of DyMaLab which focusses on the impact-dynamic behaviour of materials and structures. A key expertise of the DyMaLab group is the development of dedicated experimental methodologies to identify the strain rate dependent properties of materials. Over the years, a wide range of advanced high strength steels used by the automotive industry, and lightweight alloys, polymer composites, nanocomposites, etc. for the aeronautical applications have been studied.

Patricia Verleysen is also involved in modelling activities, again with a strong focus on strain rate and temperature dependent deformation and damage of materials. Research outcomes have been published in more than 120 Web of Science, peer reviewed papers and 200+ conference proceedings. Patricia Verleysen is active in several international scientific organisations. She is elected board member of DYMAT (European association for the promotion of research into the dynamic behaviour of materials and its applications) and chair of the EURASEM Technical Committee 'Strain rate dependent behavior and dynamics'.

Patricia Verleysen is teaching courses on fundamental Materials Science, Mechanics of Structures and Mechanical Material Modeling.

3rd International Conference on Impact Loading of Structures and Materials
ICILSM 2022

Revealing the strain rate dependent behaviour of a dual phase automotive steel by in-depth analysis of test data

Patricia Verleysen^{a*}, Sarath Chandran^a

^a*MST-DyMaLab, Department of Electromechanical, Systems and Metal Engineering, Ghent University, Technologiepark 46, 9052, Zwijnaarde, Belgium*

Abstract

Although developed in the 1970's, DP steels still provide solutions for the challenges the automotive industry faces today. Indeed, by combining high levels of strength with an excellent ductility, DP steels allow to reduce the weight of cars while maintaining or even improving their crashworthiness. At the origin of the exceptional combination of properties lies a microstructure consisting of a soft ferritic matrix with hard martensitic islands, in some cases supplemented by minor fractions of other phases. The possibility of obtaining DP steels with different phase fractions, distributions, and morphologies, including grain sizes, ensures that a very wide range of properties can be obtained and, thus, that DP steels can be tailored to specific applications. Since the first DP steels, an evolution towards higher strengths has been evident. The DP1000 steel proposed in present study has a tensile strength well-above 1000 MPa. The material is a commercial advanced high-strength automotive steel with initial thickness of 1.5 mm and fine-grained microstructure consisting of 55 vol% ferrite and 45 vol% martensite.

When advanced high strength steels are used in components designed to absorb crash-energy, such as crash boxes, the material might be subjected to wide ranges of strain rates and stress states at varying temperatures. Although DP steels are by far the most widely used steels for automotive structural and safety parts, their behaviour under different combinations of stress states, strain rates and temperature has not yet been fully explored, let alone understood. Therefore, to identify the deformation, damage and fracture behavior of the DP1000 steel, an extensive test campaign was designed aiming at test conditions relevant for the automotive industry. Temperatures ranging from of -40 to 400°C and strain rates covering seven orders of magnitude from 0.0001 to 1000s⁻¹ were considered. Based on an in-house-developed optimization routine relying on finite element simulations, eight sample geometries were designed aiming at different proportional and non-proportional stress states. The geometries include a smooth dogbone, a shear, a central hole, two plane strain and various notched samples. All test conditions together resulted in 1008 tests. For the static and intermediate strain rate tests a conventional test bench was used, for the dynamic tests a split Hopkinson tensile bar setup. Imaging of a speckle pattern applied on the sample surface combined with digital image correlation processing was used to obtain reliable local strain fields. Additionally, an algorithm was developed to fully reconstruct the evolution of the sample shape during static and dynamic tests. During well-selected tests, additional temperature measurements were performed. Testing was followed by an extensive analysis of the fracture surfaces and damage features close to the fracture.

High yield strengths, significant strain hardening and excellent deformation levels are observed in all tests. These features are mainly attributed to the ultra-fine microstructure. However, the test results indicate some atypical relations between the external loading conditions and mechanical properties. Indeed, non-monotonic relationships are observed between strength and ductility properties, on the one hand, and temperature and strain rate, at the other. For specific combinations of strain rate and temperature, a negative strain rate sensitivity (NSRS), thermal hardening and sharp drops in ductility occur. These observations are linked with the occurrence of dynamic strain aging (DSA), which is further confirmed by the appearance of

* Corresponding author.

E-mail address: Patricia.Verleysen@UGent.be

serrations in the flow curves for specific test conditions. Interstitial dissolved solute atoms, such as carbon, segregating into dislocation cores lie at the origin of DSA. At first instance, the solute atoms hinder the movement of dislocations and result in higher yield strength levels. Consecutive pinning and unpinning of dislocations give rise to serrations in stress-deformation curves, known as the Portevin-Le Chatelier effect. The associated increased strain heterogeneity at the microstructural level leads to deterioration of the material performance in the form of increased surface localization defects, and a lower ductility and crack propagation resistance. Indeed, in the DSA regime additional void nucleation sites are created which accelerate damage and result in premature fracture, the so-called blue brittleness. Generally, higher temperatures and low strain rates promote DSA through their respective influence on solute diffusion and dislocations velocity. Stress states characterised by low stress triaxialities and Lode angle parameters, and stress path changes further amplify DSA effects.

Serration are observed in the flow curves at the lowest strain rates and temperatures of 200 and 300°C in the lowest stress triaxiality samples. At room temperature, a positive effect of the strain rate on the flow stress is observed for all stress states. The most pronounced increase in strength is observed at the transition from intermediate to dynamic strain rates, and for the higher stress triaxiality samples. However, at temperatures from 100 to 300°C DSA results in a negative strain rate sensitivity. While at 100°C, a NSRS is only obtained at the lowest deformation rates, a higher test temperature generally broadens the NSRS range to higher deformation rates. Lower stress triaxialities favour this DSA effect resulting in an extended temperature and strain rate range in which NSRS is observed.

For all considered stress states, the highest ductility is observed at intermediate strain rates, the lowest at dynamic strain rates. The non-monotonic dependence of both the elongation at the maximum force and at fracture is again attributed to DSA. For the tensile dominated samples, the blue brittleness is most severe at 200 °C and intermediate strain rates, while the ductility of the shear samples is most affected at 300 °C under dynamic loading. Increasing strain rates bring about a shift in blue brittleness temperatures to higher values. The occurrence of a low stress triaxiality and/or low Lode angle parameter makes the material more prone to blue brittleness.

Analysis of the fracture surfaces reveals a ductile damage process consisting of void initiation, growth and coalescence for all samples. The DSA-induced embrittlement is reflected in finer and shallower dimples along with flat facets. The mechanisms of damage vary with both stress state and strain rate. Ferrite-martensite interface debonding, active at higher stress triaxialities, is effectively replaced by martensite cracking at low stress triaxialities. Interface debonding, martensite cracking and ferrite-ferrite grain boundary debonding co-exist at intermediate strain rate and hence, delay the fracture. Martensite cracking is activated under low Lode angle parameter and dynamic strain rates.

Keywords: Dual Phase steels, deformation, damage, fracture, strain rate, dynamic strain aging

Acknowledgement: The authors gratefully acknowledge the European Commission Research Fund for Coal and Steel (RFCS) for the financial funding for the project ‘Toolkit for the design of damage tolerant microstructures’ (grant number : 709711) which supported the investigations. The authors also express their gratitude towards ThyssenKrupp Steel for supplying the steel sheets for the study.



Timon Rabczuk

Bauhaus Universität
Weimar

Timon Rabczuk obtained his PhD from the University of Karlsruhe in January 2002. He worked at the Fraunhofer-Institute (Ernst Mach) in Freiburg before joining the Computational Mechanics Group of Prof. Ted Belytschko at Northwestern University in Evanston, USA, where he was working for 4 years as Post-Doctoral Fellow. For 1.5 years, Prof. Rabczuk was a member of the Computational Mechanics group of Prof. W.A. Wall at the Technical University of Munich. In February 2007, he was appointed Senior Lecturer at the Department of Mechanical Engineering at Canterbury University, Christchurch, New Zealand. In 2009, Prof. Rabczuk joined the Bauhaus University Weimar as Full Professor. His key research is Computational Mechanics with focus on developing new methods for the solution of PDEs and applications to moving boundary problems such as fracture or fluid-structure interaction. Post doc Cosmin Anitescu will present the work on Professor Rabczuk's behalf.

3rd International Conference on Impact Loading of Structures and Materials
ICILSM 2022

An explicit phase field method for dynamic fracture

Huilong Ren^a, Xiaoying Zhuang^a, Cosmin Anitescu^b, Timon Rabczuk^{b1}

^a Department of Mathematics and Physics, Leibniz Universität Hannover, Appelstr. 11, 30167 Hannover, Germany

^b Institute of Structural Mechanics, Bauhaus-Universität Weimar, Marienstr. 15, 99423 Weimar, Germany

Abstract

In this lecture, we present an explicit phase field model for dynamic brittle fracture with applications to impact loading. In the phase field method, the cracks are represented by an additional coupled variable which describes the amount of damage in the material. This allows us to model crack nucleation and growth and complex crack patterns in a thermodynamically consistent framework.

In particular, the full potential energy functional is of the form:

$$\Pi_l(\mathbf{u}, s) = \int_{\Omega} \psi_e(\boldsymbol{\epsilon}(\mathbf{u}), s) dV - \int_{\partial\Omega} \mathbf{t}^* \cdot \mathbf{u} dA - \int_{\Omega} \mathbf{b} \cdot \mathbf{u} dV + \int_{\Omega} g_c \left(\frac{s^2}{2l} - \frac{l}{2} \nabla s \cdot \nabla s \right) dV, \quad (1)$$

where \mathbf{u} is the displacement field, $s \in [0,1]$ is the phase field. Here $s = 1$ denotes full damage of the material, while $s = 0$ represents zero damage. Moreover, ψ_e represents the strain energy density, $\boldsymbol{\epsilon}$ is the strain, \mathbf{t}^* is the boundary traction, \mathbf{b} is the body force, g_c is the critical energy release rate, and l is a phase field length scale parameter. When $l \rightarrow 0$, the crack approaches the sharp discontinuous configuration. The strain energy density is decomposed into a tensile part ψ_e^+ , which is affected by the phase field and a compressive part and is written as follows:

$$\psi_e(\boldsymbol{\epsilon}(\mathbf{u}), s) = (1 - s)^2 \psi_e^+(\boldsymbol{\epsilon}(\mathbf{u})) + \psi_e^-(\boldsymbol{\epsilon}(\mathbf{u})). \quad (2)$$

The kinetic energy functional is

$$K(\dot{\mathbf{u}}) = \int_{\Omega} \frac{1}{2} \rho \dot{\mathbf{u}} \cdot \dot{\mathbf{u}} dV, \quad (3)$$

where ρ is the density, and $\dot{\mathbf{u}}$ is the velocity. The Lagrangian of the solid and phase fields is

$$L(\dot{\mathbf{u}}, \mathbf{u}, s) = K(\dot{\mathbf{u}}) - \Pi_l(\mathbf{u}, s). \quad (4)$$

Applying the principle of least action on $S = \int_{t_1}^{t_2} L(\dot{\mathbf{u}}, \mathbf{u}, s) dt$, the variation $\delta S = 0$ leads to mechanical and phase field equations

$$\nabla \cdot \boldsymbol{\sigma}^s + \mathbf{b} = \rho \ddot{\mathbf{u}} \quad \text{and} \quad (5)$$

$$g_c(s - l^2 \nabla^2 s) = 2l(1 - s)H, \quad (6)$$

¹ Corresponding author. Tel.: +49-3643-584511; fax: +49-3643-584514.
E-mail address: timon.rabczuk@uni-weimar.de

where $H(x, T) := \max_{t \in (0, T]} \psi^+(\epsilon(x, t))$ is the local history field of the maximum reference energy and $\sigma^s = \frac{\partial \psi_e(\epsilon, s)}{\partial \epsilon}$ is the Cauchy stress. For more details we refer to [1,2].

While an implicit integration scheme could be used, explicit schemes are easier to implement and are more robust, particularly for impact simulations, since only the first derivative of the energy functional is required. It is also convenient to update the phase and mechanical fields separately in a staggered minimization instead of using a monolithic solver. The phase field is incremented with substeps at each time increment, with the aim of minimizing the residual of (6). In particular, we write:

$$\beta = l^2 \nabla^2 s - s + 2l(1-s) \frac{\psi^+}{g_c} \text{ and} \quad (7)$$

$$\Delta s = \frac{1}{s} \langle \beta \rangle_+, \quad (8)$$

where β is the residual, with $\langle \beta \rangle_+ = (\beta + |\beta|)/2$, n_s is a parameter which controls the number of substeps, and Δs is the phase field increment at each substep. In practice, $n_s = 4$ or 5 , is sufficient to ensure convergence. The mechanical field is integrated with a velocity Verlet scheme [3], and the explicit algorithm is based on linear tetrahedral elements with nodal strain average [4]. This allows for easier mesh generation and overcomes the over-stiffness of conventional tetrahedra elements in dynamic analysis. More detailed derivations can be found in [5].

The proposed scheme shows good performance when compared to conventional implicit or explicit dynamic schemes. For a numerical example, we consider a $0.6\text{m} \times 0.6\text{m} \times 0.3\text{m}$ block which is impacted at the center by a cylinder of radius 0.1m (see Figure 1a). The simulation was conducted on a domain discretized by 548,564 nodes and 3,189,672 tetrahedra. The length scale $l = 0.005$ was used, and the material parameters are $E = 190\text{GPa}$, $\nu = 0.3$, $g_c = 2.213 \times 10^4 \text{J/m}^2$. The computational time for 2500 time steps was 6 hours on a desktop computer with an i7-6700 CPU and the RAM used was 2.5 GB of memory. The crack patterns at different velocities are shown in Figure 1b.

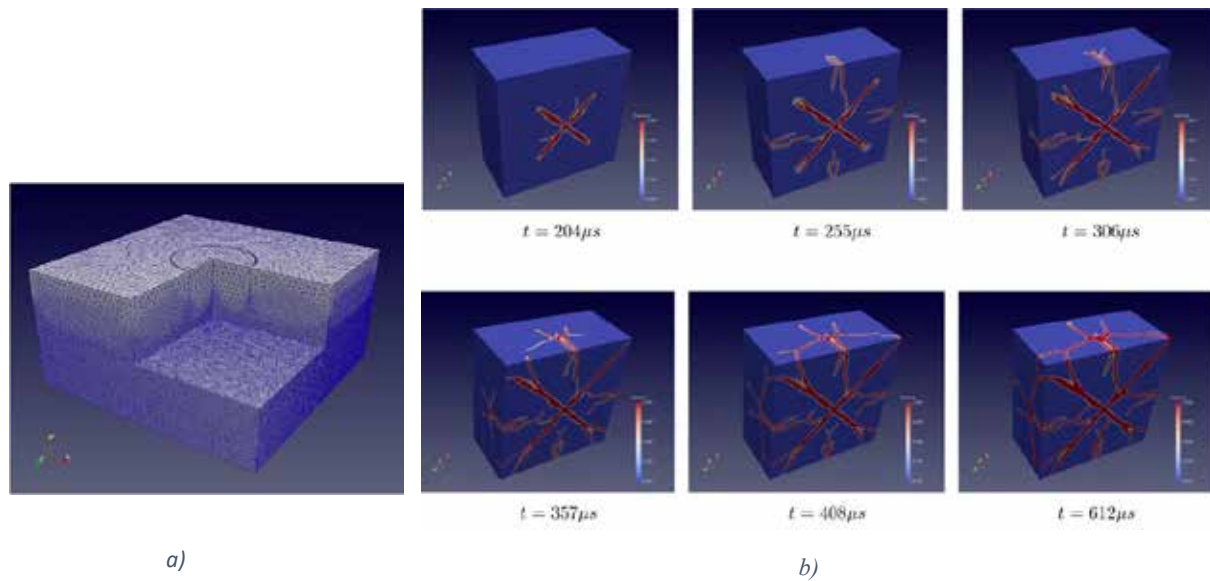


Figure 1. a) Mesh of the domain with cut to show the interior elements, b) Phase field for impact velocity $v = 16.5\text{m/s}$.

References

- [1] Miehe C, Welschinger F, Hofacker M. Thermodynamically consistent phase- field models of fracture: variational principles and multi-field FE implementations. *Int J Numer Meth Eng* 2010; 83(10):1273–311.
- [2] Miehe C, Hofacker M, Welschinger F. A phase field model for rate-independent crack propagation: robust algorithmic implementation based on operator splits. *Comput Methods Appl Mech Eng* 2010; 199(45-48):2765–78.
- [3] Swope WC, Andersen HC, Berens PH, Wilson KR. A computer simulation method for the calculation of equilibrium constants for the formation of physical clusters of molecules: Application to small water clusters. *J Chem Phys* 1982; 76(1):637–49.
- [4] Bonet J, Marriott H, Hassan O. An averaged nodal deformation gradient linear tetrahedral element for large strain explicit dynamic applications. *Int J Num Method Biomed Eng* 2001; 17(8):551–61.
- [5] Ren HL, Zhuang XY, Anitescu C, Rabczuk T. An explicit phase field method for brittle dynamic fracture. *Comp & Struct*. 2019; 217:45–56.



François Moussy

Eng. École Centrale Paris/
Retired

Former activities:

1974-1989. IRSID. French Iron and Steel Research Institute.

Head of Forming Department.

Cold formability, drawability, machinability, tribology.

Deformation and fracture mechanisms. Role of inclusions.

Damage mechanisms : observations and quantification.

Evaluation of fracture criteria.

1990-2009. RENAULT. Materials Engineering Department.

Renault expert for Metallic Materials.

Project Leader for 3 European projects linked to lightening of cars:

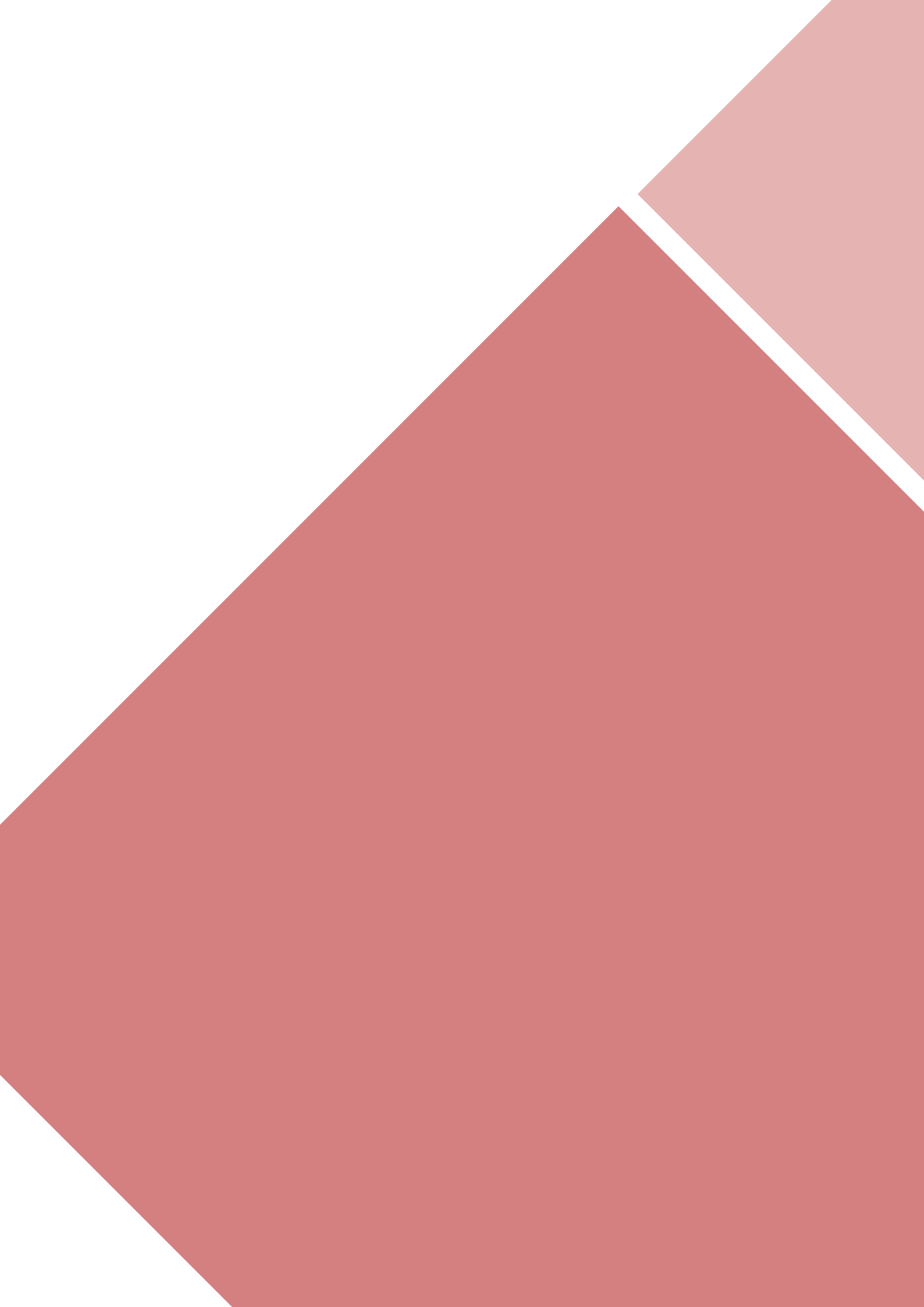
- MOSAIC (EUREKA) : Metallic Materials Aspect

- LWV (BRITE). Low Weight Vehicle. Manufacturing Aspects.

- FOMM (BRITE). Forming Of new Metallic Materials.

Fields of research : quasi-static (deep drawing) and high strain rates (crash) constitutive equations for FEM simulations : experimental and identification developments.

For these two activities at IRSID and RENAULT: Transfer of these research developments for solving industrial problems.



ABSTRACTS

The background of the page features a series of overlapping geometric shapes in various shades of red and pink. These shapes, which include diamonds and triangles, are arranged in a way that creates a sense of depth and movement. The colors range from a light, dusty rose to a deep, vibrant red. The shapes are positioned diagonally across the page, with some appearing in the foreground and others receding into the background.

3rd International Conference on Impact Loading of Structures and Materials
ICILSM 2022

Modeling the Interaction of a Generic Hollow Projectile with Different Types of Masonry

Andreas Heine,^{a,*} Christoph Sauer,^a Werner Riedel^a

^aFraunhofer EMI, Ernst-Zermelo-Str. 4, 79104 Freiburg, Germany

Abstract

We present experimental and numerical results on the interaction of a generic hollow steel projectile with two different types of masonry. The experiments comprise impact tests performed with finite-thickness targets at impact velocities where the projectile still behaves elastically or shows marginal plastic flow. That regime was chosen in order to avoid unnecessary complications with the modeling of the projectile material and to focus the investigations on capturing the response of the target materials in numerical models. The two considered target materials are lightweight adobe and fired clay masonry. The behavior of both materials is described with the RHT concrete model and appropriate parameters are obtained from material testing, independent ballistic validation experiments, and subsequent iterative parameter studies. It is shown that for both materials a reproduction of the experimental results is mostly possible for the response of the solid brick material toward ballistic impact. For projectile impact against brick wall elements, limitations are identified that can be explained by still inadequate modeling of the behavior of the mortar joints and their bonding to the bricks. Nonetheless, for two building materials simulation models for ballistic impact are obtained. This conference presentation partly summarizes prior work on lightweight adobe [1] and fired clay masonry bricks [2]. It also provides additional experimental results available for validation purposes.

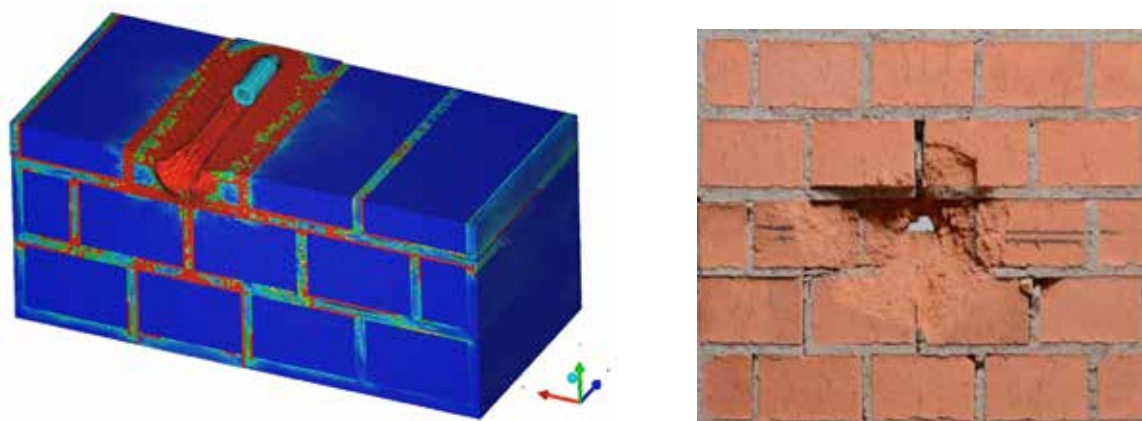


Figure: Exemplary results from simulation and experiments.

References

1. C. Sauer, A. Heine, W. Riedel, *Comprehensive study of projectile impact on lightweight adobe masonry*, International Journal of Impact Engineering **125** (2019) 56-62.
2. C. Sauer, A. Heine, F. Bagusat, W. Riedel, *Ballistic impact on fired clay masonry bricks*, International Journal of Protective Structures **11** (2020) 304-318.

* Corresponding author. Tel.: +49-761-2714-435; fax: +49-761-2714-81-435.
E-mail address: andreas.heine@emi.fraunhofer.de

3rd International Conference on Impact Loading of Structures and Materials
ICILSM 2022

Experimental investigation under laser-driven shocks of the dynamic behavior of materials for beam-intercepting devices in particle accelerators

Lucie Baudin ^{a*}, Carlotta Accettura ^a, Alberto Morena ^b, Leonard Wegert ^c, Artem S. Martynenko ^c, Paul Neumayeur ^c, Marilena Tomut ^{c,d}, Alessandro Bertarelli ^a, Federico Carra ^a, Lorenzo Peroni ^b, Martina Scapin ^b, Christian Brabetz ^c

^a CERN, Esp. des Particules 1, 1211 Meyrin, Switzerland

^b Politecnico di Torino, Corso Duca degli Abruzzi 24, 10129 Turin, Italy

^c GSI Helmholtzzentrum für Schwerionenforschung GmbH, Planckstraße 1, 64291 Darmstadt, Germany

^d Institute of Materials Physics, University of Münster, Wilhelm-Klemm Str. 10, 48149 Münster, Germany

Abstract

A laser-shock experimental campaign, named “P219”, was performed in the framework of the H2020 European project ARIES in February 2022. ARIES, and more specifically its Work Package 17, aims at studying innovative advanced materials used for beam intercepting devices, such as collimators absorber blocks and dumps, in high energy particle accelerators.

Safety protection devices must be able to intercept highly energetic particle beams travelling in the particle accelerators, such as the CERN Large Hadron Collider (LHC). The materials must withstand severe thermo-mechanical conditions due to the quasi-instantaneous energy deposition while also meeting drastic requirements in term of electrical conductivity, ultra-high vacuum compatibility, deformations, to avoid perturbing the accelerator operation. The constraints related to an affordable and large-scale industrial feasibility must also be accounted. Carbon-fibre Carbon (CFC) composite and isotropic polycrystalline graphite were used at CERN, in LHC collimators and other beam intercepting devices.

Programs aiming at increasing the beam energy in particle accelerators, such as the implementation of the High-Luminosity LHC upgrade (HL-LHC) or the study on the Future Circular Collider (FCC), urge the development and characterization of novel materials able to handle even more severe conditions, in particular, in extreme accidental scenarios. CERN has launched an R&D program to develop in install materials fitting the requirements of HL-LHC collimator absorbers. Graphite-matrix composites reinforced with Molybdenum carbides (MoGr) have been installed but several others are still under investigations: Chromium Carbide – Graphite (CrGr), metal-graphite composite (CuGr) and copper-diamond.

In this context, a wide range of specimen targets made of relevant materials and coatings for the use in beam intercepting devices, were submitted to laser-driven shocks to contribute to their thermo-mechanical characterization under severe loading conditions.

High-power laser pulses irradiating thin targets can lead to their fragmentation under tensile stresses. Indeed, the plasma expansion, resulting from the laser/matter interaction for sub-picosecond laser pulses, triggers a planar compression wave on the front surface of the specimen. The shock wave travels across the target until it reaches the back surface and is reflected as a tensile wave. As a result, a high-strain tensile stress is generated a few hundreds of micrometers below the back surface.

* Corresponding author. Tel.: 0041 22 7662896
E-mail address: lucie.baudin@cern.ch

When changing the intensity of the laser irradiation, and therefore the amplitude of the compression applied on the front surface, as well as the thickness of the specimens, a large range of tensile stresses applied beneath the back surface can be investigated. If this stress reaches the spall strength of the material, the material breaks and a spall can be ejected.

This study provides an overview of the P219 experimental campaign conducted at the PHELIX high energy laser facility at the GSI in Darmstadt. The laser produced square temporal pulses of 1.5 ns at a wavelength of 527 nm (2nd harmonic), delivering energy in the range of 50 to 60 J, with a focal spot obtained by a phase plate of 1 mm diameter, resulting in a laser intensity in the range of 3.4 to 5.9 TW/cm².

After calibration shots at copper and aluminum targets, 46 specimens made of fine-grained nuclear isotropic graphite, Carbon-fibre Carbon (CFC) composite, metal-carbide graphite (MoGr, CrGr), metal-graphite composite (CuGr) and copper-diamond were irradiated under vacuum. Targets were 10-mm-diameter discs with thicknesses ranging from 0.75 to 3.5 mm.

Carbide-graphite composites are mainly composed of oriented graphite, therefore they exhibit an orthotropic behavior, as well as CFC composites. The dynamic behavior of those anisotropic materials was investigated in both directions, in-plane and through-plane, when cutting the specimens and applying the pressure conditions (laser and shock wave propagation directions are respectively parallel and perpendicular to basal planes).

In addition, the adhesion of the thin-film (such as 6- μ m-thick Molybdenum or 3- μ m-thick copper) deposited on the collimators of the LHC to enhance electrical conductivity was investigated taking advantage of irradiation conditions close to those of a LASer Shock Adhesion Test (LASAT) used to assess the bonding strength of coating and adhesives.

For this P219 experimental campaign, both, on-line and post-mortem diagnostics were used:

Photonic doppler laser velocimetry (PDV) was pointing at the back surface of the specimen. In addition of the measurement of the surface velocity, such PDV could measure the velocity of the ejected fragments in the range of several hundreds of meters per second, nevertheless the temporal resolution was limited to 55 ns. Facing the challenges due to the low reflectivity of the target, several methods were used to enhance the return signal in the 1.5-mm-diameter PDV probe: surface polishing, 1- μ m-thick aluminum flash coating, or application of reflecting silver color ink. A fine adjustment of the alignment of the incident and reflected probe beam was also required.

In addition, a streak camera was also pointed at the back surface. Streak images, recorded with a 16 bits CDD with 1344*1024 pixels could show when the shock break out on the back surface of the specimen with a temporal resolution in the range of 65 to 120 ns, depending on the choice of the sweep window. Parallely, the exact time of the high energy laser beam impact on the front surface is known thanks to the synchronisation system between the laser facility and the diagnostic. The break time of the shock wave across the specimen could therefore be determined.

High speed systems based on shadowgraphy, was implemented for transverse imaging of the debris ejection. With photo diode enlightenment, the camera took 26.6- μ m-pixel-size pictures of the cloud of debris, every 1.7 to 5.4 μ s. Opening and closing time of the shutter were recorded on oscilloscope to determine the exact time of the capture.

Ejected debris were collected on a transparent PMMA plate placed at 12 mm from the back surface. The shape and size of debris will be analyzed by microscopy. Ultimately, post-mortem microscopy and tomography of the specimens submitted to laser impact will be deployed to measure the crater on the front surface, the spallation depth on the back surface and to localize the subsurface cracks.

Assisted by numerical simulation, such diagnostics should both, allow to evaluate the loading conditions into the targets and get an insight into the resulting damage phenomena in materials under high-strain stresses.

To conclude, the P219 experimental campaign provided large amount data to cross-check and validate the models implemented for laser matter interaction, shock wave propagation and spall strength concerning a wide range of materials, all relevant for the use in beam intercepting devices of particle accelerators.

3rd International Conference on Impact Loading of Structures and Materials
ICILSM 2022

New insights into the role of porous microstructure on dynamic shear localization

A. R. Vishnu, M. Marvi-Mashhadi, J. C. Nieto-Fuentes, J. A. Rodríguez-Martínez*

Department of Continuum Mechanics and Structural Analysis. University Carlos III of Madrid. Avda. de la Universidad, 30. 28911 Leganes, Madrid, Spain

Abstract

This work provides new insights into the role of porous microstructure on dynamic shear localization. For that purpose, we have performed 3D finite element calculations of electro-magnetically collapsing thick-walled cylinders. The geometry and dimensions of the cylindrical specimens are taken from the experiments of Lovinger et al. [1], and the loading and boundary conditions from the 2D simulations performed by Lovinger et al. [2]. The mechanical behavior of the material is modeled as elastic-plastic, with yielding described by the von Mises criterion, an associated flow rule and isotropic hardening/softening, being the flow stress dependent on strain, strain rate and temperature. Moreover, plastic deformation is considered to be the only source of heat, and the analysis accounts for the thermal conductivity of the material. The distinctive feature of this work is that we have followed the methodology developed by Marvi-Mashhadi et al. [3] to incorporate into the finite element calculations the actual porous microstructure of 4 different additively manufactured materials –aluminium alloy AlSi10Mg, stainless steel 316L, titanium alloy Ti6Al4V and Inconel 718– for which the initial void volume fraction varies between 0.001% and 2%, and the pores size ranges from $\approx 6 \mu\text{m}$ to $\approx 110 \mu\text{m}$. The numerical simulations have been performed using the Coupled Eulerian-Lagrangian approach available in ABAQUS/Explicit, which allows to capture the shape evolution, coalescence and collapse of the voids at large strains. To the authors' knowledge, this work contains the first finite element simulations with explicit representation of the material porosity which demonstrate that voids promote dynamic shear localization, acting as preferential sites for the nucleation of the shear bands, speeding up their development, and tailoring their direction of propagation. In addition, the numerical calculations bring out that for a given void volume fraction more shear bands are nucleated as the number of voids increases, while the shear bands are incepted earlier and develop faster as the size of the pores increases.

References

- [1] Lovinger, Z., Rittel, D., Rosenberg, Z., 2015. An experimental study on spontaneous adiabatic shear band formation in electro-magnetically collapsing cylinders. *Journal of the Mechanics and Physics of Solids* 79, 134-56.
- [2] Lovinger, Z., Rittel, D., Rosenberg, Z., 2018. Modeling spontaneous adiabatic shear band formation in electro-magnetically collapsing thick-walled cylinders. *Mechanics of Materials* 116, 130-145. IUTAM Symposium on Dynamic Instabilities in Solids.
- [3] Marvi-Mashhadi, M., Vaz-Romero, A., Sket, F., Rodríguez-Martínez, J.A., 2021. Finite element analysis to determine the role of porosity in dynamic localization and fragmentation: Application to porous microstructures obtained from additively manufactured materials. *International Journal of Plasticity* 143, 102999.

* Corresponding author. Tel.: +34 91-624-9904.
E-mail address: jarmarti@ing.uc3m.es

3rd International Conference on Impact Loading of Structures and Materials
ICILSM 2022

The behavior of ceramics and geomaterials during impact events

K.T. Ramesh^{a*}

^aHopkins Extreme Materials Institute, Johns Hopkins University, 3400 North Charles St., Baltimore, MD 21218

Abstract

We present a constitutive model that captures the major deformation and failure mechanisms active within ceramics and geomaterials during a major impact event. The model is based on experimental and computational investigations of the behavior of brittle and quasi-brittle materials over multiple scales in both length and time, and in this sense is an integrated multiscale model. Our approach captures the fundamental mechanisms of amorphization and dislocation plasticity under pressure, dynamic fracture and fragmentation, and granular flow of the fragmented material. Each mechanism is described in terms of a physics-based submodel, and the coupling of mechanisms is explicitly considered. The approach is developed primarily for advanced structural ceramics and geomaterials.

The model has been implemented in a variety of codes for large-scale simulations. While these simulations are generally more expensive than is the case for phenomenological models, the model itself does not need to be reparameterized when the loading conditions change. We describe some applications of the model to impact problems at several different scales.

* Corresponding author. Tel.: +0-000-000-0000 ; fax: +0-000-000-0000 .
E-mail address: author@institute.xxx

3rd International Conference on Impact Loading of Structures and Materials
ICILSM 2022

Sensitivity analysis of analysis program to crash analysis results of the aircraft engine for the spent fuel transport cask

Jong-Sung Kim^{a*}, Min-Sik Cha^b

^aSejong University, 205 Neungdong-ro, Gwangjin-ku, Seoul, Republic of Korea, kimjsbat@sejong.ac.kr

^bGraduate School, Sejong University, 205 Neungdong-ro, Gwangjin-ku, Seoul, Republic of Korea, popag55@naver.com

Abstract

It is expected that the transport of spent nuclear fuel will occur frequently in the future, and various types of casks will be used for such transport. After the 9.11 attack, it has been required to prepare for a sabotage attack on nuclear materials, including spent nuclear fuel. As part of this preparation, the structural integrity of the cask should be verified analytically or experimentally when an aircraft engine crashes into a spent fuel transport cask. In the nuclear industry, verification and validation related to structural integrity analysis are a fundamental process that should be performed. Analysis programs are also subject to evaluation in this verification and validation process.

In the study, when an aircraft engine collides with a spent fuel transport cask, the structural integrity of the cask was evaluated using three analysis programs: Autodyn, Speed, and ABAQUS explicit version. As a result of all analysis, it was confirmed that no penetration occurred in the cask wall. However, even though the same finite element model and analysis conditions were used, it was identified that there were significant differences in analysis variables such as von Mises effective stress and equivalent plastic strain among the programs.

3rd International Conference on Impact Loading of Structures and Materials
ICILSM 2022

Performance of a Welded Steel Component Under Shock Loading

Matthew Cotton^{a,*} and Andrew Whorton^a

^aAWE Aldermaston, Reading, Berkshire, RG7 4PR, UK.

Abstract

Welding is used extensively throughout manufacturing as a reliable and low cost joining technique for a range of metals. The methods employed vary depending on the material, geometry and application of the product, but in most situations characterization of the welded material is an important step in certifying the final component. This is particularly crucial where the component in question is likely to be exposed to conditions of impact or blast loading which have the potential to initiate failure processes. The most ubiquitous example of such a scenario is a vehicle collision, but these considerations are also important for many products designed for use in defence applications such as armour systems. In these situations the weld may offer a preferential location for damage nucleation relative to the surrounding material which may reduce the overall performance or reliability of the component.

Testing of welded parts under representative conditions is important part of any certification process, but the cost involved in repeated testing of large assemblies can be significant. This can be mitigated to some extent by a greater reliance on small scale testing in simple geometries coupled with simulations. Gas gun plate impact experiments offer one route for testing which can deliver the pressures and strain rates relevant to blast and impact scenarios. It also has the benefit of providing a simplified loading geometry in which the forces applied to the weld can be easily linked to observed experimental phenomena.

In order to better understand the behaviour of welded material under conditions of shock loading, a series of gas gun plate impact experiments have been conducted on steel plates over a range of impact velocities. Samples with full and partial penetration laser butt welds aligned with the loading direction were investigated alongside unwelded control samples to look for evidence of localized changes in response around the weld. Data was gathered using multiple velocimetry channels to record transmitted wave profiles at various positions across the sample rear surface, with an emphasis on detecting perturbations during the period of 1D uniaxial strain conditions in the sample. Additional data was supplied from metallographic examination of the shocked samples, using optical imagery of the weld region to look for signs of preferential damage nucleation in the region of the weld.

UK Ministry of Defence © Crown Owned Copyright 2022/AWE

* Corresponding author.

E-mail address: matthew.cotton@awe.co.uk

3rd International Conference on Impact Loading of Structures and Materials
ICILSM 2022

Studying Dynamic Fragmentation of Metallic Rings Using a Single-stage Gas Gun: A Novel Experimental Approach

J.C. Nieto-Fuentes ^{a*}, N. Jacques ^b, J.A. Rodríguez-Martínez ^a

^a*Department of Continuum Mechanics and Structural Analysis, University Carlos III of Madrid, Avda. de la Universidad, 30, 28911, Leganés, Spain.*

^b*ENSTA Bretagne, CNRS UMR 6027, IRDL, 2 rue François Verny, F-29806 Brest Cedex 9, France*

Abstract

The ring expansion test developed by Niordson in 1965 was a turning point in the experimental research on dynamic localization and fragmentation of metallic materials. In this impact experiment, a circular ring specimen is expanded at large velocities by detonation of an explosive charge or application of transient magnetic fields. While magnetic loading technique has become more popular than explosive loading schemes, it shows the drawback that Joule heating effects occur in the sample material. The complexity of performing fragmentation tests of rings, cylinders, and hemispheres, has led to the development of alternative techniques to conduct fragmentation experiments using gas guns, providing greater control over the strain rates in the specimen.

Here, we have developed and demonstrated a novel ring expansion experiment which uses a light-gas gun to fire a conical projectile that impacts axially on a thick-walled cylindrical tube. A metallic ring, located concentrically to the tube on the outside, is expanded radially by the tube until multiple necks and fractures appear along the circumference of the specimen at large strains. The impact velocities have been varied from 150 to 400 m/s, leading to strain rates in the ring that range between 10000 to 25000 s⁻¹. We have tested samples made of Ti6Al4V and AlSi10Mg alloy, with different nominal diameters and cross sections. To collect the fragments ejected after impact a neoprene case was located around the specimen. Due to the large radial velocities reached during the tests, most of the fragments were flying in the radial direction towards the stopping case, thus they could be recovered for a later statistical study. Considering the soft nature of the collecting device, it was ensured that after the first impact no further fragmentation occurred. The recovered fragments were sized and weighted, and the influence of the impact velocity, and the specimen thickness and radius were studied.

* Corresponding author. Tel.: +34 91 624 9588
E-mail address: junietof@ing.uc3m.es

3rd International Conference on Impact Loading of Structures and Materials
ICILSM 2022

A distribution model for low-velocity impact tests on Kevlar-epoxy composites reinforced by nanoparticles

Dayou Ma^{a*}, Sandro Campos Amico^b, Marco Giglio^a, Andrea Manes^a

^aPolitecnico di Milano, Department of Mechanical Engineering, via la Masa, 1, 20156, Milan, Italy. dayou.ma@polimi.it; andrea.manes@polimi.it; marco.giglio@polimi.it

^bMaterials Engineering Department, Federal University of Rio Grande do Sul, Av. Bento Gonçalves, 9500, Porto Alegre/RS, Brazil. amico@ufrgs.br

Abstract

Fibre-reinforced polymers enriched with nanoparticles have attracted great attention due to their good performance under impact loading and their potential application on health monitoring. However, the random, not homogenous distribution of nanoparticles (NPs) inside the polymer matrix represents a challenge: if predictive modelling approaches are used for optimal design. Finite Element (FE) modelling of such materials on the nanoscale poses several issues to modelling, as widely recognized in the literature [1,2]. Not only does the presence of NPs increase the complexity of modelling strategies, especially for the determination of a damage model when both macroscale and mesoscale are taken in account, but more so microscale modelling is in fact not feasible for complex loading conditions (*e.g.* impact cases) due to the massive computational cost and thus the effect of NPs have to be considered in a higher modelling scale. The modelling of the heterogeneous distribution of NPs is hence a key aspect to advance the understanding of the damage mechanism of this enriched composite for application purpose. Therefore, an investigation into reliable and efficient modelling strategies is an actual task.

In order to find an efficient method to simulate dynamic response under low-velocity impact (LVI), a hybrid method is herein investigated. This approach consists in developing a macroscale modelling but with a statistical discrete distribution of the mechanical properties, which addresses the random distribution of NPs. The global model simulates a Kevlar-epoxy composite with 0.5wt.% NPs and has been employed as a case study for LVI. Initially, a FE model of the impacted panels was created and the material properties, calibrated from tensile, compressive and shear tests on Kevlar-epoxy composites with 0; 0.5; 1.0 or 2.0 wt.% of NPs, were assigned to each element. Figure 1 shows the detailed model built for LVI, in which the use of boundary conditions in the red region replicates the rigid-window clamps in the tests. According to [1,2], the distribution of NPs in cured polymer obeys a normal distribution, thus, Poisson distribution, as a discrete format of Normal distribution, was employed to describe the probabilistic distribution of NPs in the Kevlar-epoxy composite. Herein, each element of the FE model was regarded as a homogeneous material with 0; 0.5; 1.0 or 2.0 wt.% of NPs. The material properties of all data-available weight fractions in the present study, *i.e.* 0; 0.5; 1.0 and 2.0 wt.% were statistically assigned according to the Poisson distribution in order to capture this particular effect of a non-homogeneous distribution. Nevertheless, the total weight fraction of NPs in the FE model was kept around 0.5 wt.% by controlling the mean value of the Poisson distribution. The mechanical response in the present model was simulated using MAT_054/055 in Ls-dyna for all weight fractions. On the other hand, a uniform-distribution model was created to compare the mechanical properties of all the samples from numerical models with

* Corresponding author. Tel.: +39 02 2399 8474; fax: +39 02 2399 8630.
Email address: dayou.ma@polimi.it

data from material tests for the 0.5 wt.% nanocomposite. Two different impact energies, 15 J and 30 J, were evaluated in the present work to analyse the effect of the impact energy and damage morphology for uniform and non-uniform distributions. The quantitative analysis of the damage volume shows that the normal-distributed models stand in better agreement with experimental data than the results obtained from the uniform model, which predicts a larger damage volume indicating more absorbed energy. Also, the damage shape obtained with the distribution model reproduces experimental data with regards to damage size, especially for the impact energy of 30 J, more accurately.

In sum, the proposed distribution model is able to replicate the damage behaviour of nanocomposites under low-velocity impact, especially the accumulation of intra-laminar cracking. Furthermore, the progressive damage behaviour for nanocomposites under LVI is sensitive to the distribution of NPs and this effect of the NPs' distribution decreases when the impact energy is higher. Furthermore, the difference between loading history of the models is less significant at a higher impact energy, most likely due to the fact that this energy level accelerates the damage process and decreases the effect of the NPs' not homogenous distribution. On the contrary, at lower energy levels (15 J), a large fluctuation is visible for different distributions.

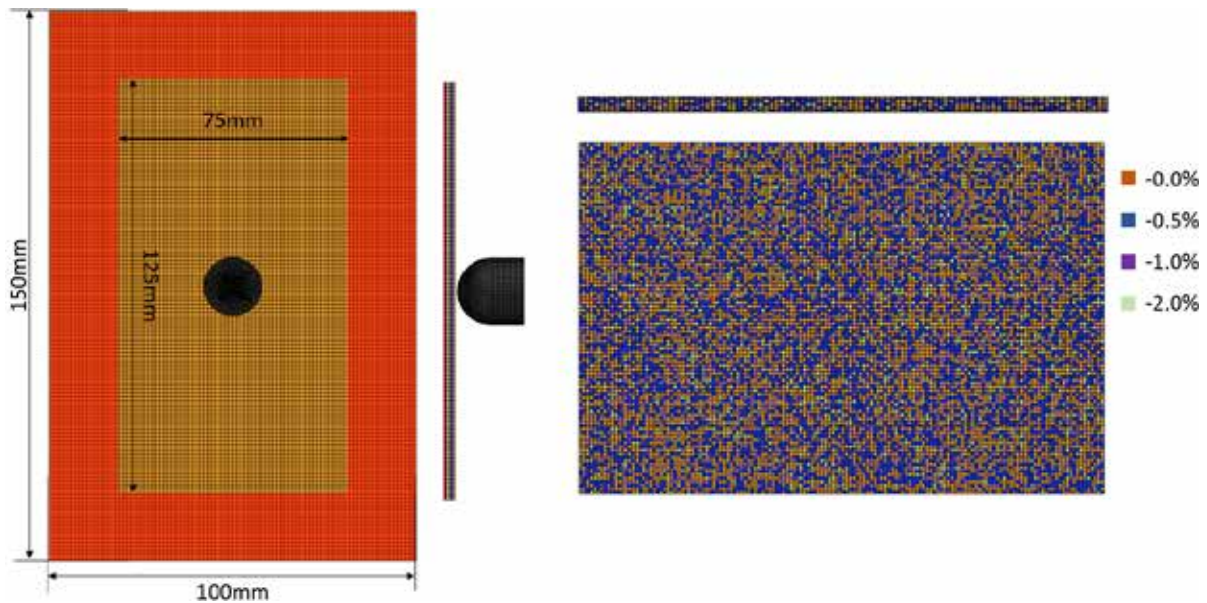


Figure 1. FE model with the most probable probabilistic distribution of NPs under low-velocity impact.

Reference

- [1] Mecklenburg M, Mizushima D, Ohtake N, Bauhofer W, Fiedler B, Schulte K. On the manufacturing and electrical and mechanical properties of ultra-high wt.% fraction aligned MWCNT and randomly oriented CNT epoxy composites. *Carbon*, 2015, 91:275–290. doi: 10.1016/J.CARBON.2015.04.085.
- [2] Chiu J J, Kim B J, Yi G R, Bang J, Kramer E J, Pine D J. Distribution of nanoparticles in lamellar domains of block copolymers. *Macromolecules*, 2007, 40(9): 3361–3365. doi: 10.1021/ma061503d.

3rd International Conference on Impact Loading of Structures and Materials
ICILSM 2022

Deformation and energy absorption characteristics of 3D-printed polymeric lattices under static and impact compression

Z.P. SUN^b, Y.B. GUO^b, V.P.W. SHIM^{a,b} *

^aKey Laboratory of Impact and Safety Engineering (MOE), Ningbo University, Ningbo, Zhejiang 315211, China

^b Impact Mechanics Laboratory, Department of Mechanical Engineering, National University of Singapore, 9 Engineering Drive 1, Singapore 117575

Abstract

Lightweight additively-manufactured lattices have attracted increasing interest because their uniform and regular unit cell topologies can be specifically tailored to fulfil customised requirements [1]. For example, axial-loading dominated lattices (e.g. Octet, Fig.1a) possess high stiffness and strength, which are desirable for load-bearing applications, while bending dominated lattices (e.g. Rhombic Dodecahedron (RD), Fig.1b) display a stable post-yield stress plateau during gross crushing [2], which is advantageous for energy absorption. However, intrinsic limitations of these conventional lattices, such as the significant post-yield stress fluctuations for the octet and the low plateau stress level for the RD, constrain them from maximising their energy absorption capacities. In an earlier study, a hybrid lattice (HS, Fig. 1c) that comprises an axial-loading dominated octahedron identical to the octet (highlighted in red), linked to external bending dominated struts similar to those in an RD (highlighted in blue), was formulated. This resulted in favourable mechanical properties – a high strength comparable to that of the Octet and a relatively stable post-yield stress response, similar to that of the RD. These endow it with better energy absorption characteristics than its two parent topologies – the Octet and RD (Fig. 1d).

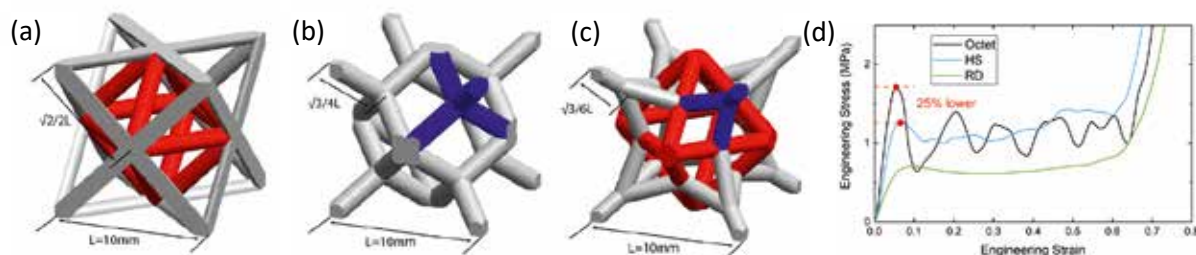


Fig.1. Schematic diagram of unit cells of an (a) Octet, (b) Rhombic Dodecahedron and (c) proposed hybrid structure; (d) overall stress-strain responses of the three lattices under quasi-static compression

The present study yields a deeper understanding of this hybrid lattice, particularly under dynamic compression, in terms of the overall deformation and failure characteristics, stress-strain response and energy absorption performance. Two aspects are examined in detail with respect to their influence on the gross crushing response: i) deformation rate, and ii) loading direction.

* Corresponding author. Tel.: +65 6516-2228.

E-mail address: vshim.mc@nus.edu.sg

Theoretically, the hybrid lattice, Octet and RD, should all possess identical responses for compression along their three respective principal orthogonal directions – i.e. the rise (vertical printing) direction, and the directions transverse to this – if all their struts have similar mechanical properties. However, the 3D layer-by-layer fabrication process causes cell struts printed at various inclinations to the printing bed to have different properties, as shown in Fig. 2a. This introduces anisotropy into their mechanical response, which this investigation examines.

To identify the effects of deformation rate and loading direction, samples of the three lattice types were fabricated using Fused Deposition Modelling (FDM), and subjected to quasi-static and dynamic compression along different directions (i.e. rise and transverse directions) using a universal testing machine and a drop tester respectively. The results demonstrate that the hybrid lattice yields the most desirable response in terms of energy absorption, regardless of deformation rate and loading direction. Although it possesses a slightly lower strength than the Octet, it displays a more stable post-yield response, with much smaller stress fluctuations. Compared to the RD, it has a significantly higher initial yield strength and post-yield plateau stress level. The hybrid lattice achieves a good balance between crushing strength and stress stability after yield, endowing it with the best energy absorption attributes. With respect to deformation rate, similar trends are observed for the three lattices – i.e. their strengths increase with the rate of compression, but deformation within them becomes more localised, generating larger fluctuations in the post-yield stress response and fracture in more struts. In terms of loading direction, compression along the transverse direction is characterised by a lower strength and larger post-yield stress fluctuations. Of the three lattices, the axial-loading dominated Octet exhibits the greatest direction-dependence – it is significantly weaker along the transverse direction (Fig. 2b) compared to the rise direction; moreover, the overall deformation mode changes from horizontal layer-by-layer crushing for compression along the rise direction (Fig. 2c), to inclined shear-band-like deformation for compression along the transverse direction (Fig. 2d). The responses of the bending dominated RD lattice and the hybrid lattice are less sensitive to loading direction – the RD is little affected by loading direction, while the hybrid lattice is slightly weaker for compression along the transverse direction.

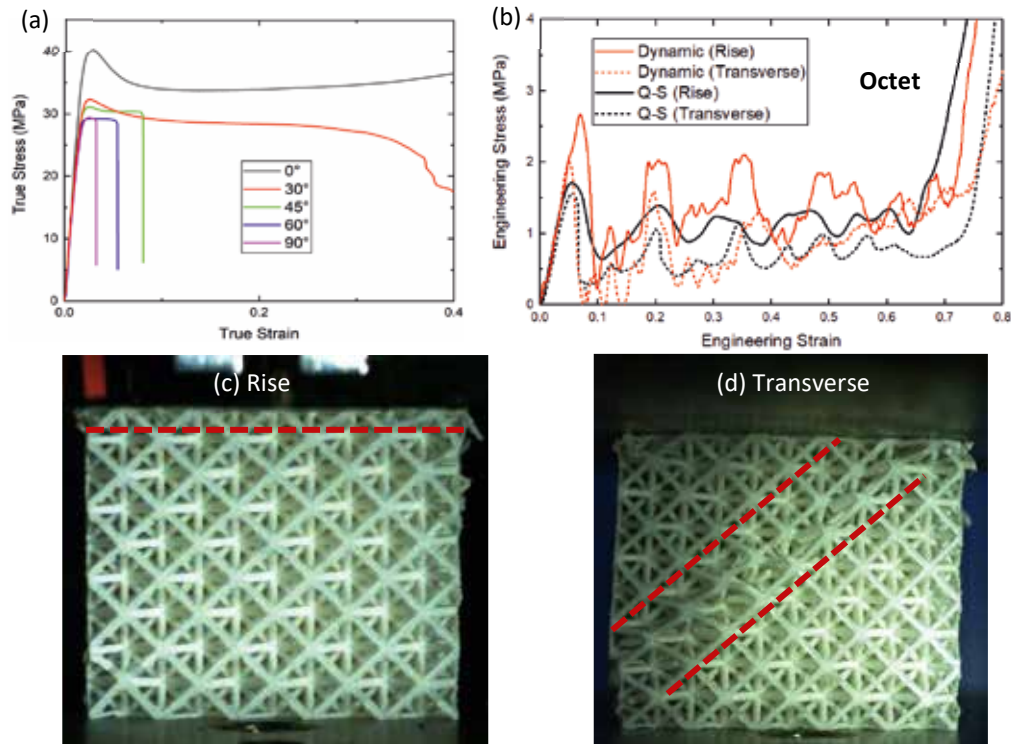


Fig.2. Anisotropic mechanical properties of lattices arising from 3D-printing process – (a) quasi-static stress-strain response of tensile test specimens printed at various inclinations to the printing bed; (b) global stress-strain response of Octet compressed along the rise and transverse directions; (c, d) effect of loading direction on cell deformation modes in an Octet lattice: (c) horizontal layer-by-layer crushing for compression along the rise direction; (d) inclined shear-band-like localised deformation for transverse compression.

References

- [1] R. Gümrük, R. A. W. Mines, and S. Karadeniz, "Static mechanical behaviours of stainless steel micro-lattice structures under different loading conditions," *Materials Science and Engineering: A*, vol. 586, pp. 392-406, 2013.
- [2] T. Tancogne-Dejean and D. Mohr, "Stiffness and specific energy absorption of additively-manufactured metallic BCC metamaterials composed of tapered beams," *International Journal of Mechanical Sciences*, vol. 141, pp. 101-116, 2018.

3rd International Conference on Impact Loading of Structures and Materials
ICILSM 2022

Data-driven approach to account for fluid-structure interaction effects on blast loaded steel plates

Luca Lomazzi^{a,*}, Andrea Manes^a, Francesco Cadini^a, David Morin^{b,c}, Vegard Aune^{b,c}

^aPolitecnico di Milano, Dipartimento di Meccanica, Via La Masa 1, Milano, 20156, Italy

^bStructural Impact Laboratory (SIMLab), Department of Structural Engineering, Norwegian University of Science and Technology (NTNU), NO-7491 Trondheim, Norway

^cCentre for Advanced Structural Analysis (CASA), NTNU, Trondheim, Norway

Abstract

The dynamic response of blast-loaded structures has been largely investigated in the last fifty years by means of analytical, experimental and numerical methods [1]. Historically, based on experimental observations, empirical models were developed both to predict the properties of blast waves generated by high explosive (HE) detonations and as fast running engineering predictive tools to describe the behaviour of simple circular and quadrangular metal plates [2]. Moreover, similar considerations also came from properly developed analytical models describing the response of plate-like structures subjected to dynamic loading conditions [3]. More recently, exploiting the constantly increasing availability of computational resources, numerical methods have been employed to simulate the response of structures to blast events. Compared to analytical and empirical methods, this approach allows studying structures characterized by complex geometry and made of any material. Such numerical methods may be mainly classified into two groups, i.e., uncoupled and coupled methods [4]. Uncoupled methods consist in the description of the structural domain by employing elements with Lagrangian formulation, on which blast pressure is exerted as prescribed pressure load. Pressure load properties are commonly determined either through empirical models or by means of pure Eulerian analyses, where the pressure exerted on the structure is predicted by explicitly simulating the blast wave generation and propagation. Instead, coupled methods simultaneously describe in the same analysis both the Eulerian fluid domain and the Lagrangian structural domain. Although coupled methods are computationally demanding, to date they represent the only satisfactorily accurate solution to account for fluid-structure interaction (FSI) effects. In fact, analytical models accounting for such effects have been proposed in the literature, but their applicability is still limited to simplified scenarios, such as free-standing plates subjected to blast loading conditions, since the underlying physics is complex and still partially unknown [5].

Hence, there is a lack of fast and reliable methods to account for FSI effects in uncoupled numerical simulations. This work will address this challenge by exploring the opportunities of data-driven approaches to predict FSI effects during the dynamic response of blast-loaded steel plates. To this purpose, the database presented in [4] is employed to train and test a properly developed feed-forward neural network (NN). The database consists in results from uncoupled and coupled numerical simulations of thin steel (Docol 600DL) plates subjected to five different blast loading conditions. Specifically, the NN operates on nodes arranged in layers to process the numerical results element-by-element. The NN considered in this work consists of (i) three nodes in the input layer, i.e., element maximum velocity, element displacement when the plate center reaches the maximum displacement over time and peak overpressure from the uncoupled analysis, (ii) two hidden layers with five and three nodes, respectively, and (iii) one output node, i.e., the correction factor between the displacement values predicted in uncoupled and coupled simulations. The results from four blast loading conditions are used for training and validation, while the remaining loading scenario is used for testing. The NN performances are shown in Figure 1.

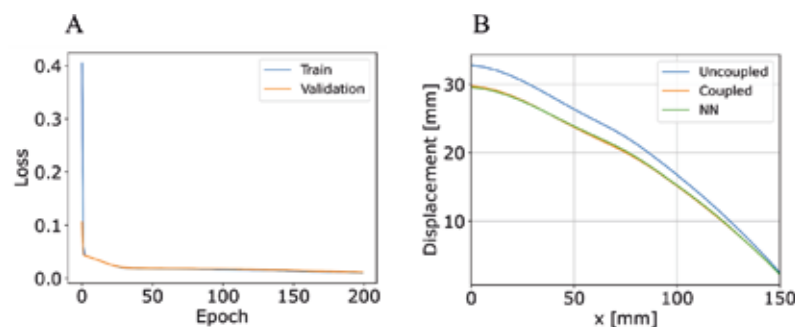


Figure 1. NN performances. A: Training performances. B: predicted half plate cross-section when the plate center reaches the maximum displacement over time - test data.

Based on the test performances (Figure 1B), it seems that the NN successfully learned to predict the results of coupled simulations by applying a correction factor to the results obtained from uncoupled simulations. Thus, in other words, the NN is capable of predicting the FSI effects. Moreover, in order to better interpret the NN behavior, a function-based explainability algorithm is developed to identify the most relevant input parameter driving the NN prediction, i.e., the direction along which a function resembling the NN behavior shows the steepest gradient. The results of the explainability analysis are shown in Figure 2, where two displacement values are considered as reference values to show the influence of peak overpressure and maximum element velocity on the NN prediction.

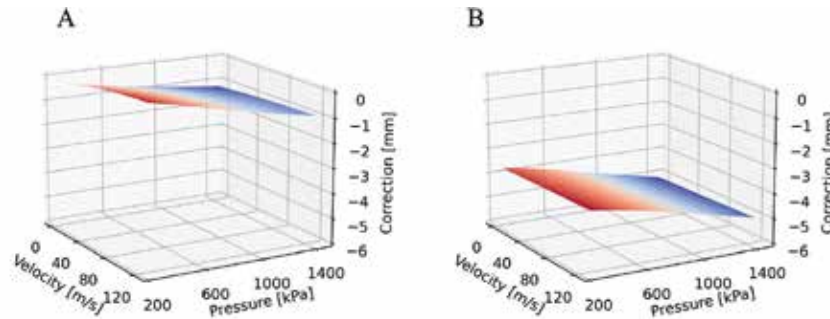


Figure 2. Explainability results, the NN prediction is shown on the vertical axis. A: Element maximum displacement of 7mm. B: Element maximum displacement of 42mm.

It turns out that at small element deflections both velocity and pressure drive the NN prediction through similar gradients, while at large element deflections the gradient smooths out along the velocity direction, meaning that only pressure drives the prediction. This result suggests that FSI effects are independent of the deflection velocity at large deflections. Moreover, in uncoupled analyses the element velocity intrinsically depends on the plate material properties, while the exerted pressure is independent of the material the plate is made of. Thus, since at large deflections only pressure seems to drive the NN prediction, in such conditions generalization capabilities on different materials are likely to be shown by the data-driven approach. Hence, generalization capabilities are tested by considering the same blast loading conditions presented in [4], but using different steel materials, i.e., Docol 1000DP and Docol 1400M. The results of the generalization tests are shown in Figure 3 for some reference cases, proving that the NN may successfully predict FSI effects also when applied to plates made of steel materials different from the one used to build the training database.

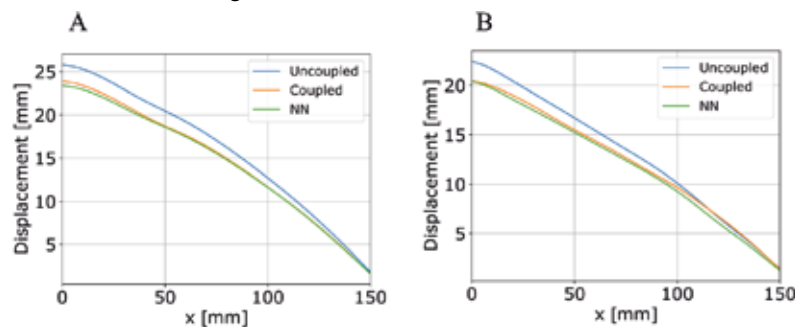


Figure 3. Results of the generalization tests. A: Docol 1000DP. B: Docol 1400M.

Further work is required to test the generalization capabilities of the proposed data-driven approach on metal materials different from steel, such as aluminum and titanium. Moreover, given the promising performances of the proposed framework in predicting FSI effects starting from the results of uncoupled numerical simulations, it may be worth investigating if such an approach may also be used to indicate the underlying physics governing other effects related to the interaction between blast waves and structures. To this purpose, the authors are currently implementing a data-driven approach inspired to the method presented in this work into a finite element software, so that FSI effects may be predicted iteration-by-iteration, thus making it possible to study the influence of such effects on more complex structural behaviors, such as damage onset and properties.

References

- [1] Lomazzi L, Giglio M, Manes A. Analytical and empirical methods for the characterisation of the permanent transverse displacement of quadrangular metal plates subjected to blast load: Comparison of existing methods and development of a novel methodological approach. *Int J Impact Eng* 2021;154:103890. <https://doi.org/10.1016/J.IJIMPENG.2021.103890>.
- [2] Nurick GN, Martin JB. Deformation of thin plates subjected to impulsive loading—A review: Part I: Theoretical considerations. *Int J Impact Eng* 1989;8:159–70. [https://doi.org/10.1016/0734-743X\(89\)90014-6](https://doi.org/10.1016/0734-743X(89)90014-6).
- [3] Jones N. *Structural impact*. 2nd ed. 1997.
- [4] Aune V, Valsamos G, Casadei F, Langseth M, Børvik T. Fluid-structure interaction effects during the dynamic response of clamped thin steel plates exposed to blast loading. *Int J Mech Sci* 2021;195:106263. <https://doi.org/10.1016/J.IJMECSCI.2020.106263>.
- [5] Kambouchev N, Radovitzky R, Noels L. Fluid–StructureInteraction Effects in the Dynamic Response of Free-Standing Plates to Uniform ShockLoading. *J Appl Mech* 2007;74:1042–5. <https://doi.org/10.1115/1.2712230>.

3rd International Conference on Impact Loading of Structures and Materials
ICILSM 2022

Adiabatic Shear Failure of Lightweight Materials: From Titanium Alloys to PA66-GF30 Composite

Longhui Zhang^a1, David Townsend^a

^a*Department of Engineering Science, University of Oxford, Parks Road, Oxford, OX1 3PJ, UK*

Abstract

Titanium alloys and short fibre reinforced polymeric composites, with excellent high strength-to-weight ratio, have been widely employed in aerospace engineering and automotive engineering applications. The metal and composite are usually jointly used in the structural components in service, which would be subjected to impact loading. Consequently, it is important to understand the mechanical behavior of titanium alloys and fibre reinforced polymeric composites under high rate deformation.

This work studies the dynamic failure of titanium alloys (Ti3Al2.5V and Ti6Al4V) and a PA66-GF30 composite (30 wt % glass fibre reinforced polyamide 66) in aerospace engineering applications.

A series of dynamic compression tests have been performed for titanium alloys, using a high-speed infrared detector synchronized with a split Hopkinson pressure bar. Until the final collapse of the titanium specimens, the overall temperature rise remains quite modest.

For PA66-GF30, the micro crack, due to the brittle failure of glass fibre, has already formed in dynamically deformed PA66-GF30 beyond the maximum stress. This corresponds to the macro strain localization observed from the high speed images. However, the PA66-GF30 with lateral confinement shows adiabatic shear failure, with glass fibres coated by the severe shear matrix facets and evenly distributed filaments. This is different from the unconfined PA66-GF30 which shows the glass fibres pull-out in the fractured matrix.

Microstructural examination reveals that both titanium alloys and the confined PA66-GF30 fail in a similar way of adiabatic shear localization, which is associated with intensive adiabatic temperature rise.

* Corresponding author. Tel.: +44-7570538761
E-mail address: longhui.zhang@eng.ox.ac.uk

3rd International Conference on Impact Loading of Structures and Materials
ICILSM 2022

Snow Avalanche Impact Loads: Work-Energy Methods to Calculate Impulsive Pile-Up and Deflection Forces with Shear Traction

Perry Bartelt¹, Joël Borner and Andrin Caviezel

WSL Institute for Snow and Avalanche Research SLF, Flüelästrasse 11, CH-7265, Davos, GR, Switzerland

Abstract

The calculation of impact loads caused by snow avalanches has been a central problem in natural hazards research in mountainous areas. In Switzerland impact loads are used to delineate mountain land into different danger zones and is therefore associated with land use restrictions, typically building constraints. Buildings, and other mountain infrastructure such as ski-lift pylons or power-line transmission towers, cannot withstand the massive forces of direct, high-speed avalanche impact. Therefore, engineering guidelines are primarily used to calculate impact forces when the avalanche has reached the runout zone and is moving at much lower velocities. Often this impact is accompanied by an intense air-blast. Much damage can be mitigated by careful object placement, deflection structures or appropriate building reinforcement.

Over the years different methods have been developed to predict avalanche impact forces. The primary problem is that avalanche snow, at impact, is a highly compressible and deformable material. It behaves both as a solid and a fluid. Impact of wide structures (walls) leads to “pile-up”. Large impulsive forces arise from stopping snow directly at the obstacle. The stopping distance, and therefore the magnitude of the impulsive force, is given by the compactibility and upward deformation of the moving snow. Moving snow is deflected around narrow objects, causing a combination of deflection forces and shear tractions. The deflective forces are impulsive in nature as they are produced by changing the flow direction of the flowing snow; shear tractions arise from jamming effects when the deflected snow is introduced back into the surrounding flow. This creates a shear zone near the obstacle edges. The viscous shear forces that arise from this process are taken up by the obstacle at the edges, often leading to damage and collapse. Although pressure sensors have been introduced into avalanche flows to quantify these forces, measurements are fraught with technical problems including sensor shape and size-effects, and the lack of overall structural forces (reactions) that would provide insight into total loads, including edge forces.

The most widely applied methods to estimate impact loads are based on kinematic models that avoid using essentially unknown constitutive parameters to describe flowing snow. Material parameters such as compactive viscosity and snow elasticity vary by orders of magnitude over the relevant strain-rate and density ranges. Although they can be estimated at low strain rates, and small deformations, they are hard to predict in actual avalanches. As such, simulation models (FE or DEM) are seldom applied for actual case-studies. In this paper we show how work-energy methods can be effectively applied to predict avalanche forces, but require a careful selection of the kinematic assumption describing how snow deforms at impact. To complete the overview of the avalanche impact problem, we conclude with a brief overview of impact forces caused by the avalanche air-blast.

¹* Corresponding author. Tel.: +41 81 417 0251
E-mail address: perry.bartelt@slf.ch

3rd International Conference on Impact Loading of Structures and Materials
ICILSM 2022

Comparison of drone collision and bird strike on aircraft radome using experimental and simulation methods

Sebastian Heimbs^{a,*}, Jannik Hansen^a, Malte Woitdt^a

^aTechnische Universität Braunschweig, Institute of Aircraft Design and Lightweight Structures, Hermann-Blenk-Straße 35, 38110 Braunschweig, Germany

Abstract

The number of lightweight hobby drones in public airspace is constantly increasing. Despite regulatory and technical measures, a collision of lightweight drones with larger aircraft or helicopters cannot be ruled out, especially if they operate beyond restricted commercial flight paths [1]. The collision with other foreign objects like birds is indeed a load case that is taken into account in the design of forward-facing aircraft structures and safety demonstration is even part of the certification process requested by Airworthiness Authorities. In this context, the question arises, how the collision of a lightweight hobby drone compares to the collision with a bird of similar mass and impact velocity.

In order to answer this question, an extensive research study has been conducted, addressing both impact load cases using experimental and numerical simulation methods and a specific aircraft structure use case. This use case is a generic radome for satellite communication (SatCom radome) as it may come into operation in a MALE (medium altitude long endurance) RPAS (remotely piloted aircraft system), such as the Eurodrone [2]. It is supposed to demonstrate bird strike resistance under impact of a 2 lbs = 0.9 kg bird [3]. For a direct comparison, the DJI Mavic 2 Zoom drone was selected for this study, as it is one of the most sold consumer products in the quadcopter segment and has an identical weight of 0.9 kg (Fig. 1).

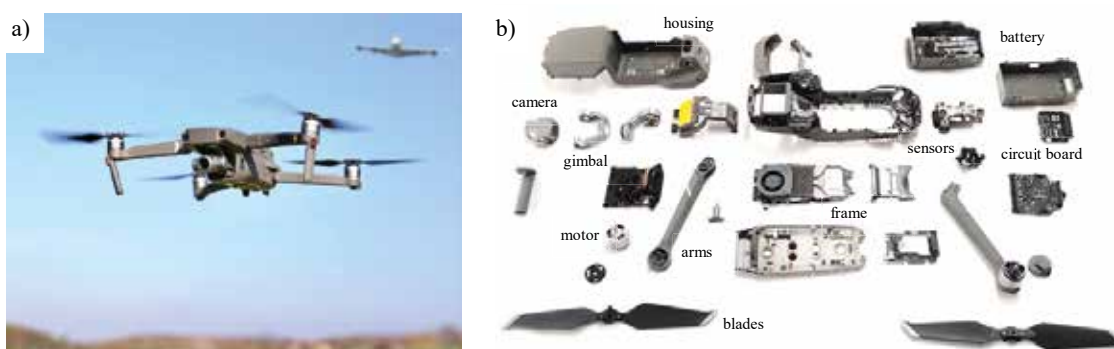


Figure 1: a) Typical lightweight drone (DJI Mavic 2 Zoom) imposing risk of aircraft collision, b) drone components for characterization

An experimental high-velocity impact test campaign, typically involving a gas gun that propels the projectile against the target structure at the velocities of interest, would be a straight-forward approach for this comparison. However, in contrast to established bird strike test procedures, it is not as easy to perform drone strike tests, because the dimensions of the drone with extracted arms surpass by far the diameter of typical gas guns. Therefore, simulations supported by tests were selected as the appropriate method for the drone collision study, while the bird strike was performed both in test and simulation.

To develop accurate and predictive numerical simulation models (using the commercial finite element (FE) software Abaqus/Explicit in this study), it is common practice to follow the building block approach with experimental tests on material coupon and component level to feed and validate the simulation models [4]. Extensive test campaigns were conducted in this context: The fluid modelling of the bird using Smoothed Particle Hydrodynamics (SPH) is calibrated based on bird strike tests on instrumented plates and structures. The drone components were also characterized experimentally in compression tests of the motors, the battery, the camera as well as bending and fracture tests of the arms, frame and housing (Fig. 2a-c). An optical 3D scanning system was used to derive accurate geometrical data of the drone components as basis for a highly realistic drone simulation model (Fig. 2d). The aircraft radome consists of a sandwich structure with quartz fiber-reinforced skins and a

* Corresponding author. Tel.: +49-531-391-9901; fax: +49-531-391-9904.
E-mail address: s.heimbs@tu-braunschweig.de

honeycomb core. In addition to the full experimental characterization of these materials under quasi-static and high-rate dynamic conditions, impact tests on flat and curved sandwich panels were performed for a sufficiently large database for FE model validations. Finally, a bird strike test with a full-scale radome prototype of 3 m length was performed. This allowed for the accurate validation of the high-velocity bird impact simulation model to be used as basis for predictive drone impact simulations (Fig. 3).

There is a substantial difference between these two projectiles: while the bird behaves as a fluid and significantly spreads during impact and flows along the structure's surface, the drone consists of many hard, metallic components that are prone to induce local failure and penetration of the thin-walled sandwich structure. While for lower impact velocities the global structural response and indentation of the radome is similar for both load cases showing no penetration, differences occurred when increasing the impact velocity. The limit velocity, when penetration of the sandwich structure occurs, turned out to be much lower for the drone. Fig. 3 shows two simulations with identical impact velocity and impact energy, where the bird flows along the surface but the drone penetrates. The assessment of structural damage of these simulations reveals further differences. While the area of honeycomb core shear damage is significant for both load cases and slightly differs in size and shape, fracture damage of the composite skin only occurs in the drone collision load case. Since such high impact velocities are at the limit or exceeding the sum of typical MALE RPAS speed and maximum drone speed, it is worth mentioning that the initial radome design is resistant against both impact load cases.

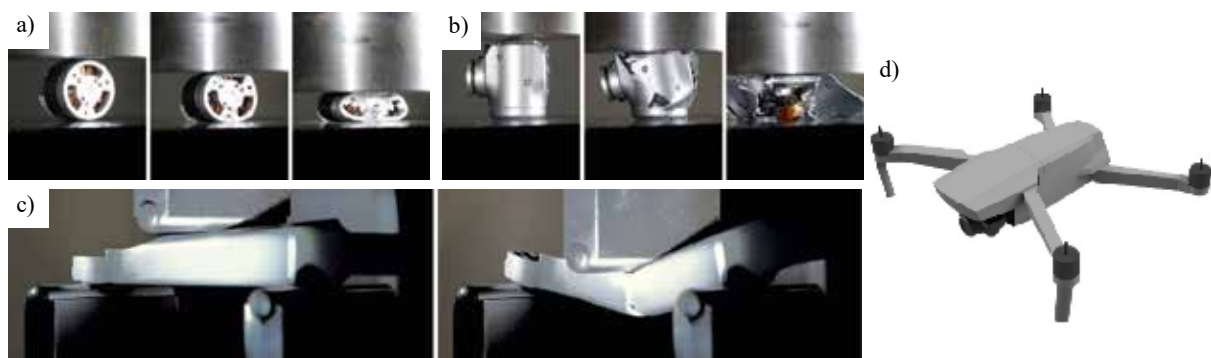


Figure 2: a) Compression testing of drone motor, b) compression testing of drone camera, c) bending and fracture testing of drone arm, d) accurate drone simulation model development

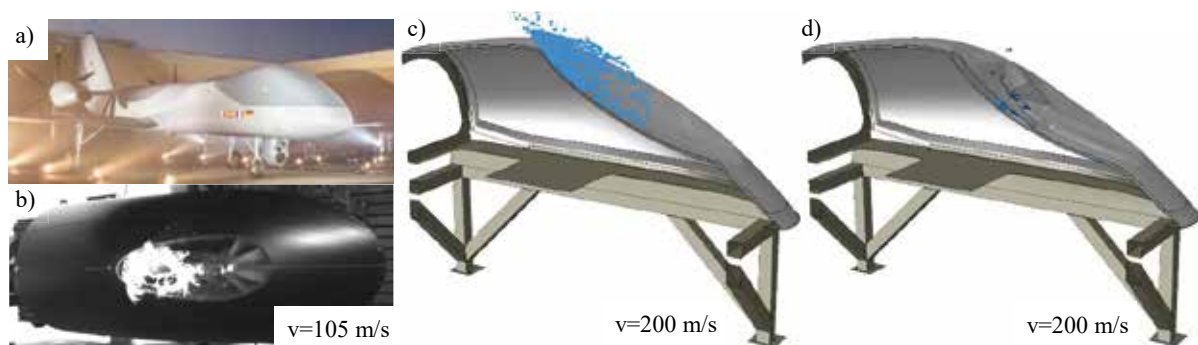


Figure 3: a) MALE RPAS aircraft (Photo: airbus.com, Max Thum), b) bird strike test on radome, c) sectional view of bird strike simulation showing no penetration, d) sectional view of drone collision simulation with penetration of sandwich skin

References

- [1] Drone Collision Task Force – Final Report, European Aviation Safety Agency (EASA), 2016
- [2] Meister, H.; Brand, C.; Starke, P.; Doll, G.; Mosch, J.; Christ, U.; Krell, T.: Radomes – Large sized composite structures with multi-disciplinary requirements for unmanned reconnaissance air platforms. ECCM-17, Munich, June 2016
- [3] Meister, H.; Brand, C.; Calomfirescu, M.; Rothenhäusler, M.; Schlick, M.; Karch, C.; Heimbs, S.; Wagner, T.: Nachweis der technologischen Reife von SatCom Radomen für MALE Flugzeuge. DLRK 2019, Darmstadt, September 2019
- [4] Heimbs, S.; Wagner, T.; Meister, H.; Brand, C.; Calomfirescu, M.: Bird strike on aircraft radome: Dynamic characterisation of quartz fibre composite sandwich for accurate, predictive impact simulations. EPJ Web of Conferences 183, 01007, 2018

Acknowledgements

This study builds upon the collaborative research project “FFS – Fortschrittliche Flugzeugstrukturen (Advanced Aerostructures)” led by Airbus Defence & Space, where this radome structure was developed and tested. Sincere thanks are given to project leader Mircea Calomfirescu for supporting this study by providing data generated in that project.

3rd International Conference on Impact Loading of Structures and Materials
ICILSM 2022

Behaviour of multi-layered plates impacted by high-velocity projectiles

Maxim Yu Orlov, Viktor P. Glazyrin, Talgat V Fazylov

National Research Tomsk State University, 36, Lenin Avenue, Tomsk, 634050, Russia

Abstract

At present, the creation of new protective structures is a very complex problem. The constant improvement of kinetic impact projectiles causes developers to search for a new way to strengthen protective structures. The simplest is to add a new layer if possible. Therefore, numerical simulation methods must be developed for high informativity and low cost compared to traditional experimental methods. At the same time, the results obtained experimentally remain decisive in the verification of any phenomenological model and computational algorithms. At the development stage of any protective structure, developers use both commercial software packages, including ABACUS, AUTODYNE, and IMPETUS Afea Solver, and non-commercial computer codes. Some numerical results obtained with computer codes are presented in [1]. In the present research, perforation of a multi-layered target impacted by elongated high-velocity projectiles is investigated with the non-commercial code Impact 2D [2].

A mathematical model enables describing the destruction of solids at explosive and shock loads. The governing equations are based on the fundamental laws of conservation of mass, momentum, and energy. A complex model of continuum mechanics was used to describe the material's behaviour under dynamic load. The material modelled was a porous, compressible medium, taking into account strength properties, shock-wave phenomena, and event of fracture material. The material was modelled by an elastic plastic medium. To describe the shear strength of a body, the Prandtl–Reuss constitutive equations and the von Mises yield condition were used. The equation of state was the Mie–Grüneisen. The mathematical model allows using various equations of state, including a wide-range equation of state. Pressure in detonation products was described using the Landau–Stanyukovich polytropic [3]. In the process of material fracture under dynamic loading, new free surfaces, including fragmentary events, were allowed.

The system of equations for a 2D axisymmetric approach is solved by the modified method in [4], one based on a Lagrangian approach to the description of the motion of continuous media. Any Lagrangian method has problems with penetration and perforating tasks, including deep penetration of a protective structure by a projectile with complex geometry. To overcome this, an algorithm for erosion elements, an algorithm for splitting nodes, and an algorithm for constructing the free surface were introduced.

In accordance with [5], a quantitative test was conducted to demonstrate the capabilities of the numerical method and the correctness of some computational algorithms. The task of deep penetration by an ogival projectile into a semi-infinite metal target was chosen. The subject of comparison was the depth of penetration of the projectile into the target. Qualitative and internal tests in this article were not considered. The projectile was the core of the B-32 bullet (Russia), length 30 mm and weight 5.5 g. The target was a semi-infinite aluminum plate. In a numerical experiment, the target diameter was more than 10 times that of the projectile diameter. The initial velocity was 336 m/s. The subject of comparison was the depth of penetration of

the projectile into the plate. Discrepancy was 5% between the experimental and numerical data. Figure 1 displays the cross-sectional configuration of the projectile and the aluminum target at the end of the perforation process (left picture).

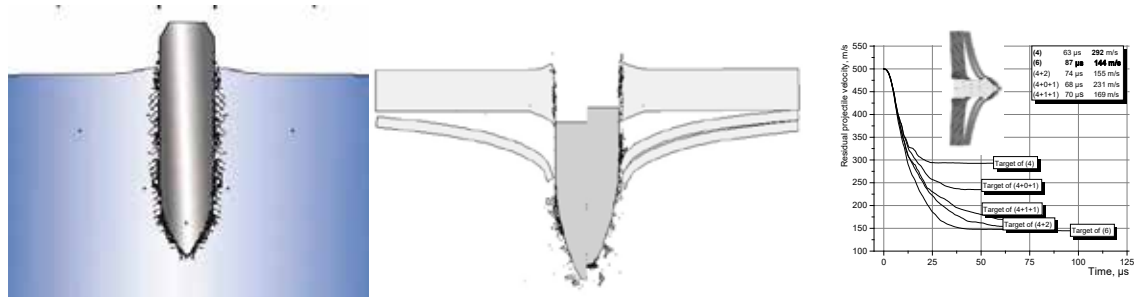


Figure 1. The numerical results obtained the computer code developed by Yu. Orlov

In the present research, the behaviour of a multi-layered target impacted by elongated high-velocity projectile was predicted. Three steel projectiles of the same mass were used, each with a 6.1 mm diameter. The projectiles had an ogival, conical, and flat-nosed part. Initial velocity was 500 m/s. A series of numerical experiments aimed to investigate the pinching effect, defined as an interaction of the cylindrical part of a projectile with the inner surface of the hole in the target. Specially for it, monolithic, two-layered, and three-layered plates and plates with an air gap between layers were considered.

The results of numerical simulation are presented as computed values of duration of perforation, holes in impacted targets, and damage level of material. Numerical simulation found that an ogival projectile acted as a "needle". During perforation of the target with conical and blunt projectiles, a plug knock-out mechanism also occurred. An air gap between layers arose during the perforation process, and the targets had much permanent deformation. Therefore, the ballistics performances of some targets declined. The tips of conical and blunt projectiles were plastically deformed, but the tip of the ogival projectile was slightly eroded (see picture in the middle). According to the projectile history, at the beginning of the process the ballistic performance of all targets were similar (see right picture). Thus, we found that a pinching effect occurred only in multi-layered targets impacted by an ogival projectile.

References

1. Glazyrin V, Orlov M (2007) Dynamics of deformation and fracture of inhomogeneous materials during impact. In: Gerasimov A (Ed) Theoretical and experimental studies of the interaction of solids, Tomsk State University Publishing House, Tomsk, p.459
2. Orlov YN, Glazyrin VP, Orlov My (2016) Explosion, Smoothing the contact boundary. Certificate of state registration of computer program. Patent 2016663830, 31 Oct 2016
3. Zukas J, Nicholas T, Swift HF, Greszczuk LB, Curran DR (eds) (1982) Impact Dynamics. Wiley, USA
4. Olovsson L, Limido J, Lacomme JL, et al (2015) Modeling fragmentation with new high order finite element technology and node splitting. EPJ Web of Conferences, 94: 04050 DOI: 10.1051/epjconf/20159404050
5. Selivanov V, (Ed) (2008) Means of destruction and ammunition, Bauman Moscow Technical University Publishing House
- 6.

This study was supported by the Tomsk State University Development Programme (Priority-2030).

3rd International Conference on Impact Loading of Structures and Materials
ICILSM 2022

Carbon fibre composite exposed to blast loading: A preliminary study.

R. del Cuvillo¹, M. Costas^{2,3}, V. Aune^{2,3}, T. Børvik^{2,3},
J. A. Artero-Guerrero¹, J. Pernas-Sánchez¹, J. López-Puente¹

¹University Carlos III de Madrid, Avenida de la Universidad, 30, 28911, Leganés, Madrid, Spain

²Structural Impact Laboratory (SIMLab), Department of Structural Engineering
NTNU – Norwegian University of Science and Technology, Trondheim, Norway

³Centre for Advanced Structural Analysis (CASA), NTNU, Trondheim, Norway

Abstract

Nowadays, composite materials have consolidated their position as one of the most important in terms of design and manufacture of structures with high requirements. Thanks to their great versatility with uncountable different combinations of materials, stacking sequences and manufacturing processes, they can ensure stiffness and good strength-to-weight ratio in many fields. However there are still certain loading conditions where the confidence of its use is still low, and deep studies are needed.

Regarding Carbon Fibre Reinforced Plastic (CFRP) materials, woven laminates employed in the manufacturing process of the Airbus 350 got deeply analyzed previously from the mechanical point of view by the authors at the University Carlos III de Madrid. Quasi-static loading, low velocity impacts (LVI) and high velocity impact of soft projectiles tests were performed. After this extensive experimental campaign, the response, final damage and residual properties of the material are well known and can be predicted for this kind of events. Afterwards, it is necessary to investigate the response of the same material against extreme loads such as explosions.

To that end, a wide experimental campaign in the SIMLab Shock Tube Facility (SSTF), was performed in this work. 300 mm x 300 mm panels were tested under different pressures to investigate the laminates from the elastic behavior to the total failure. With this purpose, 3D Digital Image Correlation (3D-DIC) was employed during blast tests in order to obtain out-of-plane displacements. Later, a non-destructive inspection (NDI) with ultrasounds was also done to obtain the non-visible internal damage. Results show an increase of the maximum out-of-plane displacement with pressure, and so for the damage.

However, the latest failure was always found at the clamps and does not allow to analyze the crack propagation. Consequently, three different slits were machined at the center of the plates to enforce a chosen failure start point and propagation. Horizontal/vertical slits, rotated slits and a 5 mm hole were made to subject these machined specimens to the same pressures as those employed for unmachined.

Additionally to the experimental campaign, numerical models for all configurations were also developed and validated the experimental data. Thanks to the vumat user subroutine developed in the Lightweight Structures Dynamics Group from the University Carlos III de Madrid, both out-of-plane displacement and crack propagation were very well reproduced. This work could lead further studies seeking to increase the confidence on composite structures subjected to extreme dynamic conditions.

3rd International Conference on Impact Loading of Structures and Materials
ICILSM 2022

Effects of Ship Collision on Offshore Wind Turbines

N. Mehreganian^a, G.K. Boiger^b, Y. Safa^b, A.S. Fallah^{c,*}

^a Department of Civil and Environment Engineering, University of Massachusetts Dartmouth, North Dartmouth, 02747 MA, United States of America

^b Institute of Computational Physics, Zürich University of Applied Sciences (ZHAW), Winterthur 8400, Switzerland

^c Department of Mechanical, Electronic, and Chemical Engineering, OsloMet, Pilestredet 35, St. Olavs plass, Oslo NO-0130, Norway

Abstract

Offshore wind turbines (OWT) are being continuously constructed and installed due to the promising market segmentation for renewable energy, abundant, favourable, and steady flow of wind at sea, as well as concerns over land use, visual impact, and noise levels of their onshore counterparts. While their functionality has been encouraging of their application, the structural integrity of these systems is of prime significance. Problems may arise due to extreme environmental conditions, the complexities of offshore design loads, as well as the significant dynamic stresses generated by extreme accidental loads. The latter encompass blast and impact phenomena, which can cause catastrophic failure and collapse of such structures. The detrimental damage brought about by such extensive loads emanates from either the large inelastic localised deformations with potential perforation due to blast or impact of mass through the thickness of structural members or to global rotations, leading to the collapse and turning over of the OWT. In some circumstances, however, the combination of the two is imminent.

In this work, we examine two scenarios of impact and blast phenomena on the OWT. In the first, the damage to the OWT when struck by a commercial ship is assessed using the numerical Finite Element (FE) methods. The influence of the vessel's initial momentum on the localised and global mode of response is discussed. A dimensionless kinetic energy parameter is proposed which serves as a threshold highlighting the two failure zones of damage with distinguishable differences: (i) total collapse of the wind turbine upon ship impact, and (ii) localised plastic failure in the contact interface with a safe level of global deformations. In the second scenario, we develop a mathematical model to delineate the dynamic plastic collapse of unstiffened long cylindrical shells utilised in the OWT foundation (monopile or jacket). The shell material is presumed as rigid, perfectly plastic, insensitive to strain rate effects, and subjected to a localised blast pressure load. Through multiplicative decomposition of the load into a spatial part with constant magnitude and a temporal part characterised by a piecewise continuous function, an analytical solution is sought for a kinematically admissible displacement field in the two distinguishable phases of motion. The validation of the analytical model with the FE one shows the capability of the former to capture the dynamic plastic collapse of the shell with a good degree of accuracy. The influence of pulse shape on the permanent deformation of the shell is also discussed in the context of the problem.

Keywords: limit analysis, pulse pressure load, ship collision, offshore wind turbine

*Corresponding author. Tel.: +4767236765
Email address: arashsol@oslomet.no

3rd International Conference on Impact Loading of Structures and Materials
ICILSM 2022

Experimental and Numerical Investigation of High-Density Polyurethane Foam for Impact Against Metallic Target Plates

Dhruv Narayan^a, Makhan Singh^a, Naresh Bhatnagar^a

^a *Mechanical Engineering Department, Indian Institute of Technology, Delhi, India*

Abstract

The strain rate sensitivity of a high-density polyurethane foam is examined by performing quasi-static and high strain rate compression tests. Split Hopkinson Pressure Bar is used to perform high strain rate compression tests. Based on the experimental results, parameters for the material model (MAT_MODIFIED_CRUSHABLE_FOAM) are derived. Numerical simulations using LS-DYNA are performed using experimentally derived material model of the foam. The foam is modelled as a projectile and fired on different metallic targets to visualize the force-time history. The force with which PU foam strikes the target is calculated numerically. The obtained results are compared with actual force measured by a force sensor when the foam projectile is fired through an airgun using high pressure air at speeds around 400m/s.

3rd International Conference on Impact Loading of Structures and Materials
ICILSM 2022

A state of the art review of numerical models for Hyper Velocity Impacts in Space

Tiziana Cardone ^{a,b}, Chiara Bisagni ^a

^a*Delft University of Technology, Faculty of Aerospace Engineering, Kluyverweg 1, 2629 HS Delft, The Netherlands*

^b*ESTEC, European Space Agency, Keplerlaan 1, Noordwijk 2201 AZ, The Netherlands*

Abstract

All S/C orbiting in space are exposed to several impacts of meteoroids and human-made objects during their lifetime, especially in Low earth Orbit (LEO). The number of impacts depends on the orbital altitude and the impactor diameter.

Collisions in LEO are becoming a main issue and a great threat for our space missions, since the Chinese anti-missile test in January 2007 and Iridium / Cosmos 2251 collision in February 2009. Envisat over its entire lifetime has performed several collisions avoidance maneuvers, which are accompanied by a sharp increase of collision alarms.

The criticality rises with the impact energy. The consequences of collisions depend also on the mass of the target object. When an energy-to-target-mass ratio (EMR) of 40J/g is exceeded, collisions are believed to be of catastrophic nature.

In catastrophic collisions, the shockwave travelling through the satellite structure contains enough energy to shatter the whole object into pieces. The larger the satellite mass, the larger the shock wave amplitude needs to be for the same effect (which is represented through a fixed energy-to-target-mass ratio). Catastrophic collisions have several implications:

- They contribute to an increase in the overall future collision rate (Kessler Syndrome).
- They may have an important environmental impact,
- Due to their clear traceability by surveillance systems, they can be proven (and they might generate liability discussions).

Four cases of such collisions are known today:

- 1996: Cerise – Fragment of an Ariane-1 Upper stage
- 1991: Cosmos 1934 – Cosmos 926 Fragment
- 2005: Thor Burner IIA Upper stage – Fragment of a CZ-4B (third stage)
- 2009: Iridium 33 – Cosmos 2251 (generated ca. 2000 trackable fragments = ca. 10% of the known population).

Tools available nowadays can simulate the flux of impacting particles on orbital surfaces throughout a spacecraft lifetime.

Based on those tools, one can estimate how many impacts a S/C will most probably encounter and the dimension of the impactors. One example is the ESA's Meteoroid and Space Debris Terrestrial Environment Reference model (MASTER), which provides population inputs to long-term environment evolution analyses.

The effects of hypervelocity impacts are a function of projectile and target material, impact velocity, incident angle and the mass and shape of the projectile.

Beyond 4 km/s (depending on the materials), an impact will lead to a complete break-up and melting of the projectile. Typical impact velocities are around 14 km/s for space debris, and significantly higher for meteoroids.

At low velocities, plastic deformation normally prevails. With increasing velocities the impactor will leave a crater on the target. Beyond 4 km/s (depending on the materials), an impact will lead to a complete break-up and melting of the projectile, and an ejection of crater material to a depth of typically 2–5 times the diameter of the projectile.

In hypervelocity impacts, the projectile velocity exceeds the speed of sound within the target material. The resulting shockwave that propagates across the material is reflected by the surfaces of the target, and reverses its direction of travel. The

superimposition of progressing and reflected waves can lead to local stress levels that exceed the material's strength, thus causing cracks and/or the separation of spalls at significant velocities.

With decreasing target thickness, the effects will range from cratering, via internal cracks, to spall detachment to, finally, clear-hole perforations.

In this view, the effect of Hyper Velocity Impacts (HVI) is of paramount importance to understand if the S/C can survive the impact and/or if the mission will be compromised.

Some data regarding HVI are available in literature [RD-01]. Very often, those data are transformed into a generalised damage equation that can determine the failure response of the particular item for a range of impact conditions. A Ballistic Limit Equation (BLE) is the most common form of damage equation. It is usually developed by drawing a curve through a set of pass/fail impact test data. Thus, a BLE provides a simple means of assessing whether a surface (or collection of surfaces) has been penetrated, and therefore it has become the main technique employed by almost every impact risk assessment code. However, BLEs have some important limitations.

This paper presents an overview of BLE and their limitations together with a review of all numerical models currently in use to understand the physics of fragmentation after an HVI. Hydrocodes models are first discussed. These have been developed from the physics of fragmentation and conservation principles. They are generally used to perform complex first principles analyses to help understand the basic phenomenology of a break-up. Following this discussion, a simpler approach to modelling the physics of a break-up is summarised, i.e. the so-called engineering model. Next, the most commonly-used models – those based purely on empirical data – are discussed. The review then looks at semi-empirical models, which are a hybrid of conservation laws and empirically-derived relationships.

Finally, tools recently developed in Europe for simulating the effects of HVI on a S/C are also presented. The capabilities of the different methods are presented and their limitations are discussed.

[RD01] Formation and Description of Debris Clouds Produced by Hypervelocity Impact, A.J. Pickutowski

3rd International Conference on Impact Loading of Structures and Materials
ICILSM 2022

Low-velocity impact on aluminium plates with geometric defects. An experimental and numerical study.

Vetle Espeseth^{a,*}, Tore Børvik^{a,b}, Odd Sture Hopperstad^{a,b}

^a Structural Impact Laboratory (SIMLab), Department of Structural Engineering, NTNU – Norwegian University of Science and Technology, NO-7491 Trondheim, Norway.

^b Centre for Advanced Structural Analysis (SFI CASA), NTNU, NO-7491 Trondheim, Norway.

Abstract

The use of thin-plate structures of steel or aluminium alloys is widespread in the aviation, automotive and marine industries. The integrity of such structures is highly sensitive to crack formation and propagation, and their performance can be substantially reduced during e.g. impact loading. The ability to predict material failure can therefore be a crucial factor in the design of such structures.

In this study, an experimental and numerical program investigating low-velocity impact (≤ 10 m/s) on 1.5 mm thick AA6016 aluminium plates in the three different heat treatments T4 (natural aged), T6 (peak-aged) and T7 (overaged) is presented. The heat treatments result in materials with different strength, work-hardening, and ductility. The impact tests are carried out in a drop tower, shown to the right in Figure 1, where the force and plate deformation are continuously monitored. Crack formation

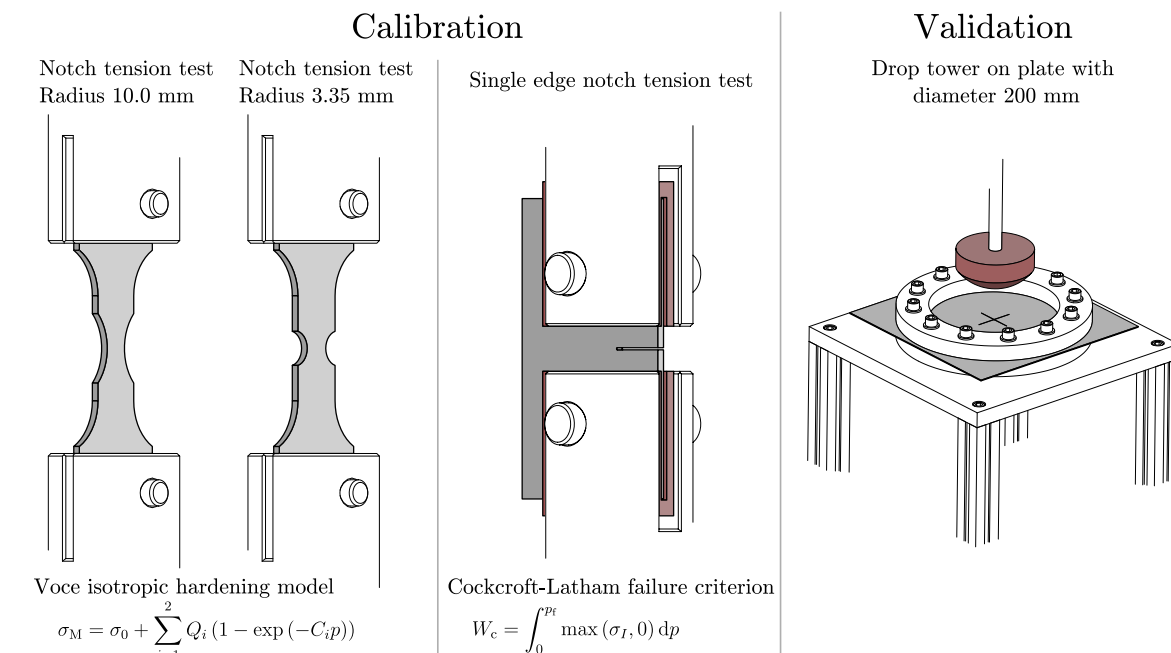


Figure 1 – Illustration of the notched specimens used in the calibration of the isotropic hardening model, the single edge notch tension (SENT) specimen used in the calibration of the Cockcroft-Latham failure criterion and the drop-tower specimen used in the validation of the numerical model.

* Corresponding author. Tel.: +47 954 65 995
E-mail address: vetle.espeseth@ntnu.no

is provoked by geometric defects in the form of pre-cut slits in the centre of the plates (see Figure 1). The force-displacement response of the impact experiments is shown by dashed lines in Figure 2. Though a high-strength material often yields high resistance to impact loads, geometrical defects such as a sharp notch may result in a stress concentration that leads to early crack initiation and growth. Experimental findings show that high ductility is often preferred in these cases as crack growth is more restrained. Since strength and ductility are generally mutually exclusive properties, one should carefully select the correct material based on the application. Quasi-static push-through experiments on the same plates with slits show a significant reduction in force for plates in temper T6 and T7 and only a slight change in force level for plates in temper T4, seen as the grey curves marked “QS” in Figure 2. There are clear indications that this change in peak force is mostly related to the behaviour of the material under high strain rates, while the inertia effects are only minimal.

The experiments are complemented by nonlinear finite element simulations using linear solid elements with reduced integration in Abaqus/Explicit. An isotropic hardening law is calibrated from the notch tension tests. Global response from single edge notch tension (SENT) tests is used to calibrate the Cockcroft-Latham failure criterion. The specimens used in the calibration are shown to the left in Figure 1. The numerical model accurately captures the response and crack propagation of the SENT tests. The dynamic simulations of low-velocity impacts on plates with defects agree with the observed quasi-static response, as shown by the solid lines in Figure 2. For temper T6 and T7, however, the force level is generally underestimated when compared to the dynamic experiments. For plates in temper T4, the predicted response also agreed with the dynamic experiments. A strain rate dependence of the fracture parameter might be necessary to capture the experimental results, but only for tempers T6 and T7.

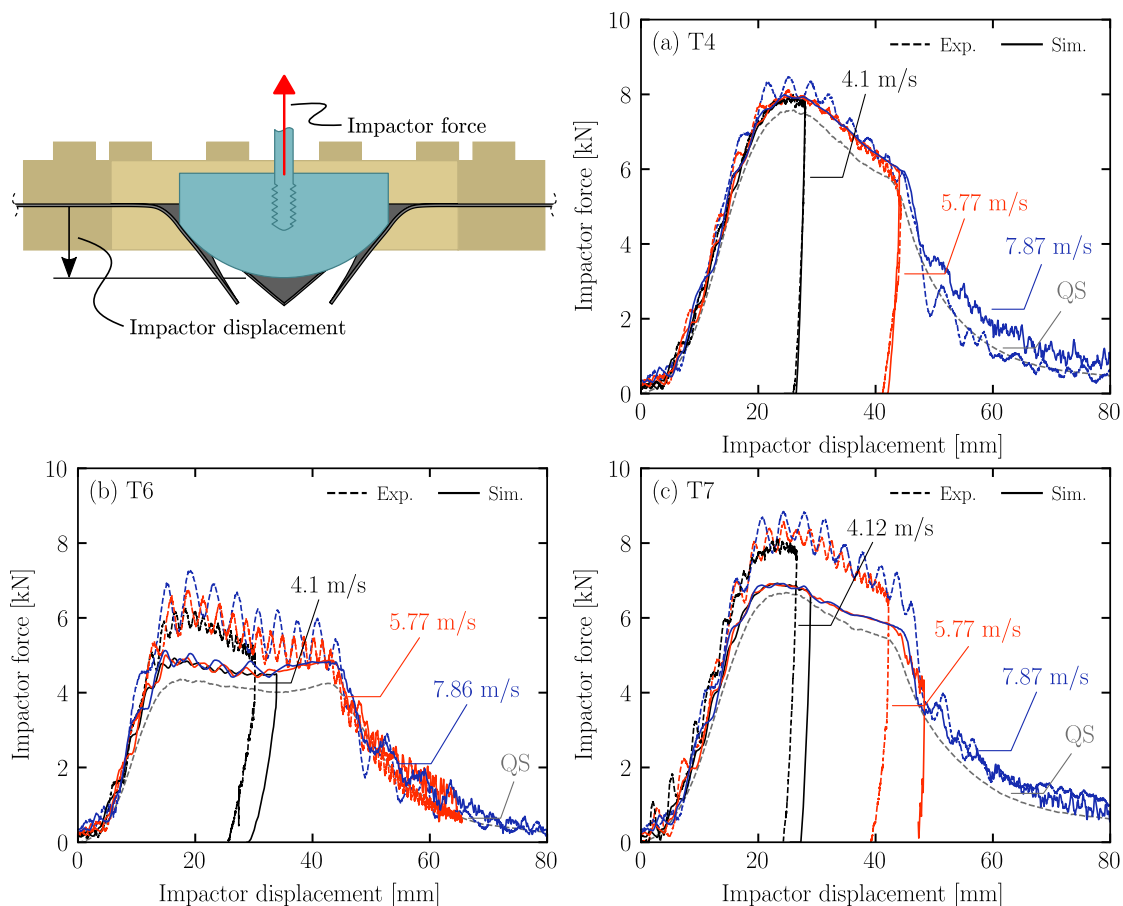


Figure 2 – Resisting force from the target on the impactor as a function of the displacement of the impactor for temper (a) T4, (b) T6 and (c) T7. All measurements are defined in the upper left figure. Different colours define the measured initial velocity before impact. The quasi-static push-through response is shown by grey curves and given the label “QS”. Solid and dashed lines correspond to results from simulations and experiments, respectively.

3rd International Conference on Impact Loading of Structures and Materials
ICILSM 2022

Blast resistance of pre-damaged steel plates

Benjamin. S. Elveli^{a,*}, Torodd Berstad^a, Tore Børvik^a, Vegard Aune^a

^aSFI CASA and SIMLab, Department of Structural Engineering, NTNU – Norwegian University of Science and Technology, NO-7491 Trondheim, Norway

Abstract

Blast waves caused by industrial accidents, military actions or terrorist attacks may subject surrounding structures to extreme loadings. Additionally, the blast wave can accelerate objects in its proximity to high velocities. Such fragments typically originate from a fractured casing of the explosive (typically a shell or a vehicle), or it could be a result of parts initially contained in the explosive device (e.g., ball bearings). These fragments may impact the structure before, during, or after the arrival of the blast wave [1]. A fragment perforation prior to the arrival of the blast wave may reduce the load carrying capacity of the structure. Hence, the combination of fragment impact and blast loading may be more severe than the two loading cases acting alone [1].

In previous studies [2-5], the effect of fragment impact prior to the arrival of the blast wave has been investigated through pre-cut holes of idealized geometries. In more realistic scenarios, a fragment impact may lead to complex hole geometries, accompanied by surrounding material damage such as cracks and plastic deformations. This study aims to evaluate the effect of the hole geometry on the blast resistance of thin steel plates. This is done by subjecting plates with either a pre-formed circular hole or a ballistic hole to the same blast intensities. The ballistic impact was performed using a fixed smooth-bore Mauser rifle, firing 7.62 mm APM2 projectiles, and the blast loading was generated using a shock tube facility [6]. Both the ballistic impact and blast loading events were recorded using two high-speed cameras and several pressure sensors, allowing for a well-documented experimental procedure. Numerical simulations were conducted in LS-DYNA to address potential challenges in the modelling of the combined effect of the ballistic impact and the blast loading, as well as to evaluate the predictive capacities in such models.

Fig. 1a-c shows three representative images of the observed fracture mode from the ballistic impact event. It is seen that all steel plates fractured by petaling. During blast loading, it was found that the steel plates exposed to ballistic impact consistently fractured at lower blast intensities than the plates containing pre-cut circular holes. Moreover, it was also observed that both the crack initiation and crack propagation were significantly affected by the petaling cracks at the ballistic hole. In fact, for the blast tests on plates with ballistic impact holes, all cracks were initiated from the petaling cracks (see Fig. 1d).

* Corresponding author. Tel.: + 47 40 40 05 67
E-mail address: Benjamin.s.elveli@ntnu.no

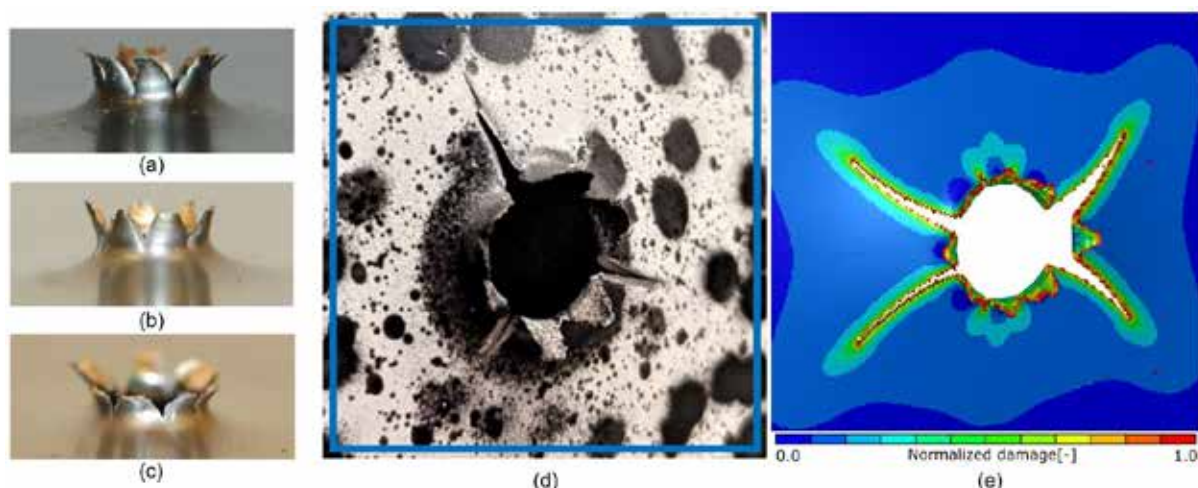


Figure 1: Three representative images of the ballistic impact holes in (a-c), and a comparison of experimentally and numerically obtained crack propagations in (d) and (e).

All numerical simulations showed a good agreement with the experimental findings (see Fig. 1e). However, some challenges were encountered in the trade-off between a sufficiently fine discretization for numerical accuracy during the ballistic impact, and at the same time obtain reasonable computational costs during subsequent simulation of the blast loading. This was particularly the case for the ballistic simulations, where the excessive compression experienced by some elements around the nose-tip of the projectile requires some special attention in the fracture modelling. This motivated the use of two fracture criteria in the ballistic simulations. That is, the Cockcroft-Latham failure criterion was used in combination with an additional strain-based fracture criterion. The physical interpretation of this approach is a strain-capped CL-criterion. This proved as a very successful modelling approach to overcome the numerical challenges associated with significantly distorted elements during compression-dominated stress states.

References

- [1] U. Nystrom, K. Gylltoft, Numerical studies of the combined effects of blast and fragment loading. *International Journal of Impact Engineering* 36 (2009) 995-1005.
- [2] K.G. Rakvag, N. J. Underwood, G.K. Schleyer, T. Børvik, O.S. Hopperstad. Transient pressure loading of clamped metallic plates with pre-formed holes. *International Journal of Impact Engineering* 53 (2013) 44–55.
- [3] V. Aune, G. Valsamos, F. Casadei, M. Langseth, T. Børvik. On the dynamic response of blast-loaded steel plates with and without pre-formed holes. *International Journal of Impact Engineering* 108 (2017) 27-46.
- [4] H. Granum, V. Aune, T. Børvik, O. S. Hopperstad, Effect of heat-treatment on the structural response of blast-loaded aluminium plates with pre-cut slits. *International Journal of Impact Engineering* 132 (2019) 103306.
- [5] B. S. Elveli, M. B. Iddberg, T. Børvik, V. Aune. On the strength-ductility trade-off in thin blast-loaded steel plates with and without initial defects – an experimental study. *Thin-walled Structures* 171 (2022) 108787
- [6] V. Aune, E. Fagerholt, M. Langseth, T. Børvik. A shock tube facility to generate blast loading on structures. *International Journal of Protective Structures* 7 (2016) 340-366.

3rd International Conference on Impact Loading of Structures and Materials
ICILSM 2022

Mechanical behavior of Ultra High Molecular Weight PolyEthylene for blast and ballistic protection

M. Arrigoni*, M. Castres, A. El Malki Alaoui

ENSTA Bretagne, IRDL, 2 rue François Verny, 29806 Brest Cedex 09, France

** Corresponding author. Tel.: +33298348978.
E-mail address: michel.arrigoni@ensta-bretagne.fr*

Abstract

The design and development of ballistic protections is a constantly evolving field. One of their major challenges are protection efficiency, compactness and lightweight solution. Over the last decennies, various materials have been used to meet these challenges depending on physical mechanisms involved for the kinetic energy dissipation: metallic or ceramic materials. However, these materials have many drawbacks such as their weight penalty, their fragility or their durability.

Nowadays, composite materials have proven their value in term of lightweight ballistic protection [1]. Glass fiber reinforced composites were the first composites used for ballistic applications. Since then, many more efficient composite materials have been developed based on polypropylene fibers, aramid fibers, or high density polyethylene fibers. Even though they are not sufficient to stop most vulnerant bullets, Ultra High Molecular Weight PolyEthylene (UHMWPE) shows good performances with respect to compliance with NIJ and STANAG standards.

UHMWPE remains available from several manufacturers, under various variants. Among them, Tensylon® is a good compromise between cost and efficiency. Previously, the interaction of a FMJ 7.62x39 mm bullet interacting with a Tensylon® panel was described [2], a first quasi static characterisation of plies was proposed in [3], and its delamination under ultra high strain rate was prospected in [4].

However, the manufacturing steps of a UHMWPE panel involve several process parameters like temperature and pressure. In order to assess the influence of these parameters, two panels were cured with a different cycle with a maximum pressure of 60 and 230 bar. Quasi-static characterisations were performed with conventional tensile machine at ENSTA Bretagne at [0°/90°] and [±45°] in particular uniaxial monotonic tensile tests and load/unload tests. In addition, dynamic tests with Split Hopkinson Tensile Bar were conducted in order to assess the strain rate sensitivity. At a higher strain rate, impact experiments of steel balls on Tensylon panels were performed to obtain a dynamic deformation of the panel. In order to determine the shock equation of state, plate impact experiments were performed up to 1000 m/s. To complete the description of damage, laser induced shock wave delamination were also conducted to evaluate the delamination threshold. Also, both materials exhibit a sensitivity to strain rate.

For the quasi static tests, in general, it was observed that Young's modulus increase with the strain rate. A similar observation is made for yield stress (fig1). The influence of the manufacturing process on the elastic properties of the material has also been underlined. It has been shown the Young Modulus and the yield stress also increases with the pressing pressure. From the load/unload tests, the damage evolution has been described versus stress for [0°/ 90°] and [±45°]. Hopkinson tests also reveal the strain rate sensitivity of UHMWPE at higher strain rate, up to several hundreds of s⁻¹ (fig.1).

Steel ball impacts brought interesting final state after impact by a simple projectile (elastic, spheric) what will be very useful for further investigation by Finite Element Methods.

Plate impact experiments and laser induced shock wave experiments helped determining the shock equation of state and delamination (or spall) strength at high strain rate of those two Tensylon variants.

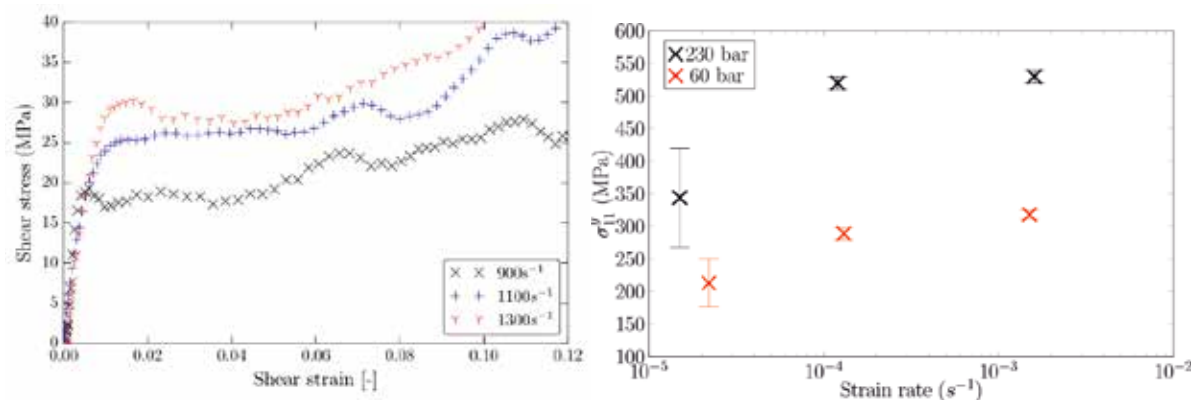


Figure 1 : (left) Stress-strain relation for $[\pm 45^\circ]$ in tension. (right) yield stressin function of strain rate for two different pressing pressure of Tensylon.

References :

- [1] Mawkhlieng, U., Majumdar, A., & Laha, A. (2020). A review of fibrous materials for soft body armour applications. RSC Advances, 10(2), 1066-1086.
- [2] Alil, L. C., Arrigoni, M., Badea, S., Ginghină, R., Matache, L. C., & Mostovykh, P. (2018). Ballistic study of Tensylon®-based panels. Express Polymer Letters, 12(6), 491-504.
- [3] Alil, L. C., Arrigoni, M., Badea, S. M., Barbu, C., Istrate, M., & Mostovykh, P. S. (2017). On the constitutive law for the mechanical quasi-static response of criss-cross composites (on the example of UHMWPE). Human Factors and Mechanical Engineering for Defense and Safety, 1(1), 1-12.
- [4] Alil, L. C., Arrigoni, M., Deleanu, L., & Istrate, M. (2018). Assessment of delamination in Tensylon® UHMWPE composites by laser-induced shock. MATERIALE PLASTICE, 55(3), 364.

3rd International Conference on Impact Loading of Structures and Materials
ICILSM 2022

The challenge of accurate strain measurement during dynamic testing of fibrous composites in the split Hopkinson bar technique

Amos Gilat, Jeremy Seidt, and Mark Konieczny

*Department of Mechanical and Aerospace Engineering, The Ohio State University
Columbus, OH 43210, USA*

Abstract

The Split-Hopkinson Bar (SHB) technique is frequently used for testing metals at high strain rates in the range of 500 to 5,000 s⁻¹. In this technique a short specimen is placed (compression) or attached (tension) between two metal bars (incident and transmitter). The specimen is loaded by a wave that is generated in the incident bar. Once the specimen is loaded, most of the wave is reflected back to the incident bar and part of the wave passes through the specimen to the transmitter bar. Traditionally, the strain in the specimen during the test is determined from analyzing the reflected wave in the incident bar. The amplitude of this wave is proportional to the difference between the particle velocities of the ends of the incident and transmitter bars where the specimen is placed. The average strain rate in the specimen is the difference in the particle velocity divided by the specimen's gage length. The strain is obtained by integrating the strain rate. This determination is accurate if the relative motion between the ends of the bars is identical to the change in length of the specimen (no relative motion between the specimen ends and the bars), and if the strain in the specimen is uniform. The force in the specimen is determined from the wave measured in the transmitter bar. Compression tests are the easiest to conduct with the SHB technique since the specimen is just placed between the two bars. In tension the specimen geometry is more complicated (dog-bone shaped) such that the motion between the incident and transmitter bar cannot be all attributed to deformation in the gage section of the specimen. In addition, the specimen has to be attached to the bars. This can affect the state of stress and deformation in the specimen and might disturb the transmission of the waves. In recent years the Digital Image Correlation (DIC) technique has been introduced for accurate non-contact full-field measurement of strains directly on the surface of specimens. The technique has been used in the SHB experiment for testing a ductile material (copper) in compression and tension by Gilat et.al. (2009). The results show that in compression at strains larger than about 0.02 the strains determined from the waves agree with the DIC measured strains. In tension there are large discrepancies that depend on the specimen geometry.

Testing of fibrous composites with the SHB technique requires special attention due to the nonhomogeneous structure of the material, the requirement of specimens of small size, and the brittleness of the material. Small fibrous composite specimens are difficult to machine and attach to the testing apparatus. Brittle composites fracture at strain of less than 5% and sometimes at strains of the order of 1% or less. Determining such small strains in SHB experiments from the waves in the bars is not accurate due to wave dispersion and the effects of the specimen boundary and attachment method on the waves.

The present paper examines the challenges in obtaining accurate stress strain curve when testing fibrous composite using the split Hopkinson bar technique. The focus is on the measurement of strain and strain rate. The strain and strain rate are measured on the surface of the specimen by using DIC and the measurements are compared with the ones that are determined in the traditional way from the recorded waves. The DIC measurements are done by using Shimadzu HPV-X2 high-speed video cameras (frame rate of up to 5,000,000 fps and 400×250 pixel resolution). Compression tests have been done with specimens machined from T800/F3900 unidirectional laminates in the 0° and 90° directions, and tensile tests have been done with specimens machined in the 90° direction.

As an example, Figure 1 shows the waves recorded in a compression SHB test with specimens machined in the 0° direction. The recorded wave in the transmitter bar, which correspond to the force in the specimen, shows that the specimen fractures 19 μs after the loading starts. This means that when using the traditional SHB analysis the strain rate and strain are determined from the first 19 μs of the reflected wave in the incident bar. This initial portion of the wave might not accurately

correspond to the actual deformation of the specimen. The strain rate, strain, and stress that are determined from the waves are displayed in Figure 2. The figure shows also the strain that is measured by DIC. It can be seen that there are significant differences between the two measurements. The stress strain response from this test is shown in Figure 3. The figure shows the curves that use the strain determined by the wave and strain measured by DIC. The figure also shows stress strain curves from quasi-static tests. The stress strain curve that is determined from the reflected wave shows a significant strain rate sensitivity with higher stiffness (which is not realistic) and higher stress. The stress strain curve that is determined from the DIC measurement has the same stiffness as the quasi-static curves with slightly higher maximum stress.

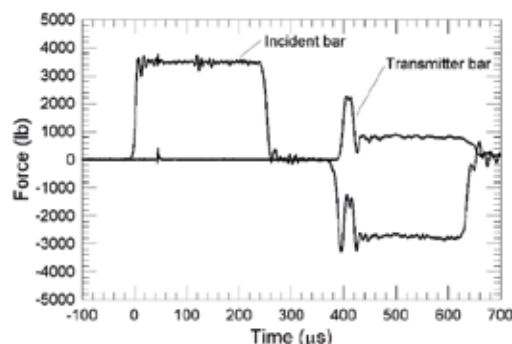


Figure1: Waves recorded in a test.

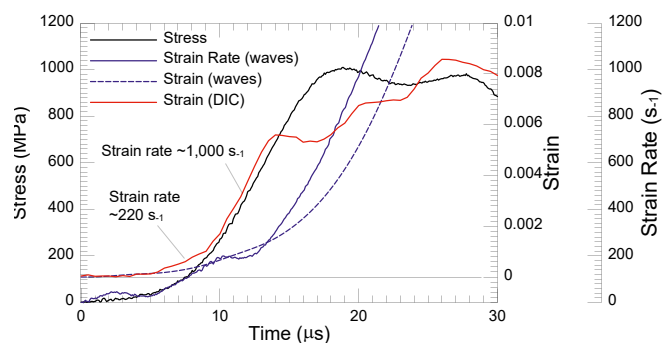


Figure 2: History of stress, strain rate and strain.

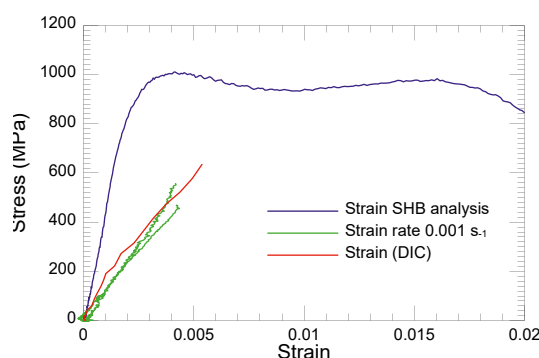


Figure 3: Stress strain curves from compression test of T800/F3900 unidirectional laminates in the 0° direction.

Compression and tensile SHB tests in the 90° direction also show significant differences between the strain that is determined from the waves and the strain measured with DIC which consequently affect the stress strain curves. The differences in the stress strain curves are shown in Figures 4 and 5.

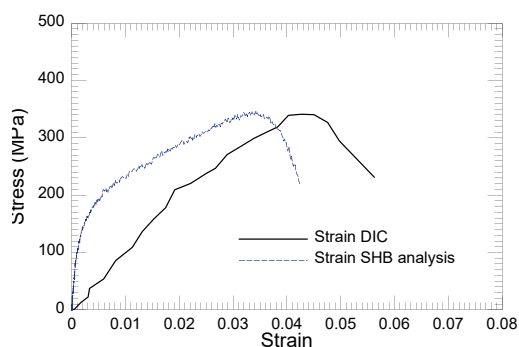


Figure 4: Stress strain curves from compression SHB test in the 90° direction.

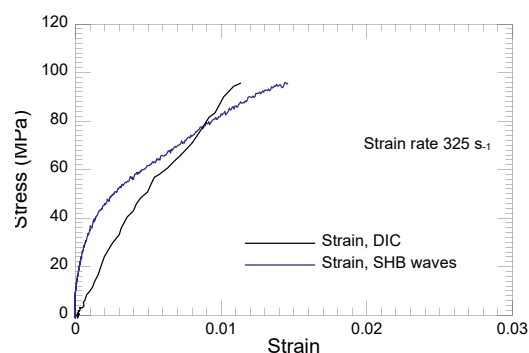


Figure 5: Stress strain curves from tensile SHB test in the 90° direction.

In summary, testing fibrous composites at high strain rate with the SHB technique requires the use of DIC for measuring the strain directly on the surface of the specimen. Due to the difficulties of attaching the specimens to the bars, and since the material is very brittle, the strain that is determined from the waves recorded on the bars is not the actual strain in the specimen.

Reference

A. Gilat, T.E. Schmidt, and A.L Walker (2009) "Full Field Strain Measurement in Compression and Tensile Split Hopkinson Bar Experiments," *Experimental Mechanics* Vol. 49, pp 291–302.

3rd International Conference on Impact Loading of Structures and Materials
ICILSM 2022

Failure characterization for polymers at different strain rates and temperatures

V. Dorléans^{b*}, R. Delille^a, F. Lauro^a, D. Notta-Cuvier^a, G. Haugou^a, E. Michau^b

*

^aUniversity Polytechnique Hauts de France LAMIH, UMR CNRS 8201, Valenciennes, F- 59 313, France

^bFAURECIA Interior system, Méru, France

Abstract

In the automotive industry, the plastic materials are used in the design of interior parts. This is true in particular for dashboards, door panels or center consoles. These materials bring many advantages compared to the steels. Indeed, they are less costly, less noise, lighter and give to the designers a significant latitude on the drawings of the parts. Some thermoplastics should also offer some interesting mechanical properties such as a high capacity of plastic deformation. Thus, one refers of ductility. This ability to reach so high levels of plastic deformation allow them to absorb kinetic energy before to fail. They are deployed in different components of interior vehicle like the top covers. These parts can be submitted to Europeans safety regulations always more and more stringent such as the ECE21. The ECE21 is a physical test which allow to simulate the impact of the head of a passenger against a dashboard at 24.1km/h. To avoid internal injuries in the brain, the deceleration of the head doesn't exceed 80g beyond 3ms during the shock. No protruding edges should be recognized after the test in the impact area because the rupture of a component of the dashboard might cause the occupant.

It is therefore essential to characterize with accuracy the behavior of thermoplastics until the failure in order to meet the regulatory requirements for the homologation of the vehicle such as the ECE21. As the polymers are very sensitive to the strain rate and the temperature, it is necessary to characterize at first the viscoelastic and viscoplastic properties over such wide strain rate and temperature ranges (0 to 300s-1/-30°C to +85°C).

In the context of the study, the material chosen is a copolymer propylene ethylene mineral (talc) filled with 15% impact modified. The work done by [1][2] have shown that for this type of material, in a specific range of application, the principle of time temperature superposition is applicable in the viscoelastic domain and the viscoplastic domain by using the same shift factor determined in viscoelasticity. This approach of the interdependence between time and temperature has been implemented thereafter in association with viscoelastic, non-associative viscoplastic constitutive law and non-local damage model [3][4][5].

The field observations carried out on this material suggest a new test procedure of characterization which allowing to reduce significantly the number of tests and reduce the costs. But what about the failure of thermoplastics with high ductility?

Currently in the industry sector, the characterization of the failure is usually limited to a global estimation of a percentage of plastic strain at room temperature whatever the strain rate and the temperature. From dynamic uniaxial tensile tests done on a

* Corresponding author. Tel.: +33 3 44 52 53 16.
E-mail address: vincent.dorleans@faurecia.com

classic sample, a value of plastic strain failure is determined and applied on the behavior law. However, this criterion is not unfortunately sufficient to describe with accuracy the stress state of the material.

It is necessary to integrate a failure criterion dependent of the stress triaxiality and the strain rate in a phenomenological approach to be exploited from the industrial point of view. From 2008, some authors [6] have developed some new failure models with considering the stress triaxiality effect. More recently in 2011, the computing code Ls Dyna proposes also a failure model based on the coupling between the accumulation of damage and a failure curve which is a function of the triaxiality and the strain rate. It is the GISSMO model (Generalized Stress State Dependent Damage Model) [7]. In simulation this model is retained to describe the failure behavior of the studied material

In this paper, we present the results of experimental tests carried out on specific geometries of samples (notched/shear/biaxial) for different levels of triaxiality and strain rates at room (23°C) and cold (-30°C) temperatures. Once the Gissmo model is tuned, a correlation study is done on samples. It follows a validation on a new demonstrator.

- [1] Dorléans, V., Delille, R., Lauro, F., Notta-Cuvier, D., Bourel, B., Haugou, G., Bennani, B., Morvan, H., Michau, E., 12th European LS-Dyna Conference 2019, Koblenz, Germany.
- [2] Dorléans V., Delille R., Notta-Cuvier D., Lauro F., Michau E. (2021). Time-temperature superposition in viscoelasticity and viscoplasticity for thermoplastics, *Polymer Testing*. Vol 101.
- [3] Balieu, R., Lauro, F., Bennani, B., Delille, R., Matsumoto, T., Mottola, E., A fully coupled elastoviscoplastic damage model at finite strains for mineral filled semi-crystalline polymer, *International Journal of Plasticity*, 51, 241-270, 2013.
- [4] Balieu, R., Lauro, F., Bennani, B., Matsumoto, T., Mottola, E., Non-associated viscoplasticity coupled with an integral-type nonlocal damage model for mineral filled semi-crystalline polymers, *Computers and Structures*, 134, 18-31, 2014.
- [5] Balieu, R., Lauro, F., Bennani, B., Haugou, G., Chaari, F., Matsumoto, T., Mottola E., Damage at high strain rates in semi-crystalline polymers , *International Journal of Impact Engineering*, 76, 1-8, 2015.
- [6] Wierzbicki. (2008). A new model of metal plasticity and fracture with pressure and Lode dependence. *International Journal of Plasticity*, 2008, vol.24, pp.1071-1096.
- [7] Andrade, F.X.C., Feucht, M., Haufe, A., Neukamm, F., An incremental stress state dependent damage model for ductile failure prediction. © Springer Science+Business Media Dordrecht 2016

3rd International Conference on Impact Loading of Structures and Materials
ICILSM 2022

Mechanical response of an armour steel alloy under combined condition of elevated temperature, high strain rate and triaxiality

Ezio Cadoni*, Matteo Dotta, Daniele Forni

University of Applied Sciences and Arts of Southern Switzerland, Via Flora Ruchat-Roncati 15, Mendrisio 6850, Switzerland

Abstract

Armour steels are extensively used to protect vehicles, structures and personnel from threats involving impact and explosion. To improve the reliability and degree of protection and to provide new safety solutions is of capital importance to know the mechanical response of armour steels in typical conditions present in serious dynamic events.

With the aim to investigate these aspects a comprehensive experimental study on different armour steels is presently running at the DynaMat Laboratory.

This work analysis the dynamic behaviour of Armox®500T steel in a large range of strain rate, temperature and triaxiality by means of a Split Hopkinson Tensile Bar (SHTB) (Fig. 1a). To investigate the combined effects of temperature and high strain rate the SHTB was equipped with an Ambrell compact EASYHEAT induction water-cooled heating system with maximum power of 2.4 kW. This non-contact induction heating is ideal for heating parts of many geometries and compositions with precise power control within 25 W resolution and is able to supply energy only to the part and the zone to be heated, as shown in Fig. 1b [1].

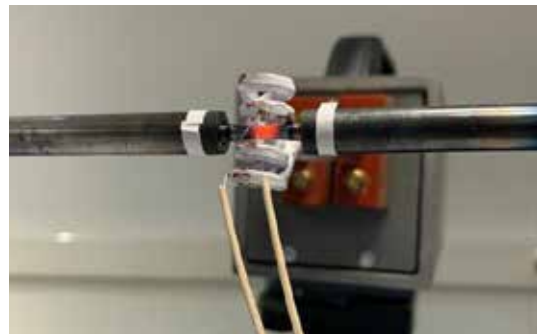


Fig. 1 – Experimental set-up: a) SHTB; b) heating system

* Corresponding author. Tel.: +41-58-666-6377
E-mail address: ezio.cadoni@supsi.ch

This steel is characterised by a quite high density and outstanding mechanical properties. Tests at high strain rate at elevated temperature show an increment of the plastic strain rate with increasing temperature. The dynamic behaviour has been studied in a temperature range from 20°C to 900°C by keeping same dynamical initial condition (30kN preload). The results highlighted a decrement of the strength capacity and an increment of the deformation with increasing temperatures. Analysing the ductility parameters as reduction of the cross-area at failure or the ratio between UTS and yield strength, a significant increase has been recorded. The dynamic reduction factors for the yield and ultimate tensile strength have been evaluated, it seems that the reduction follows a linear trend.

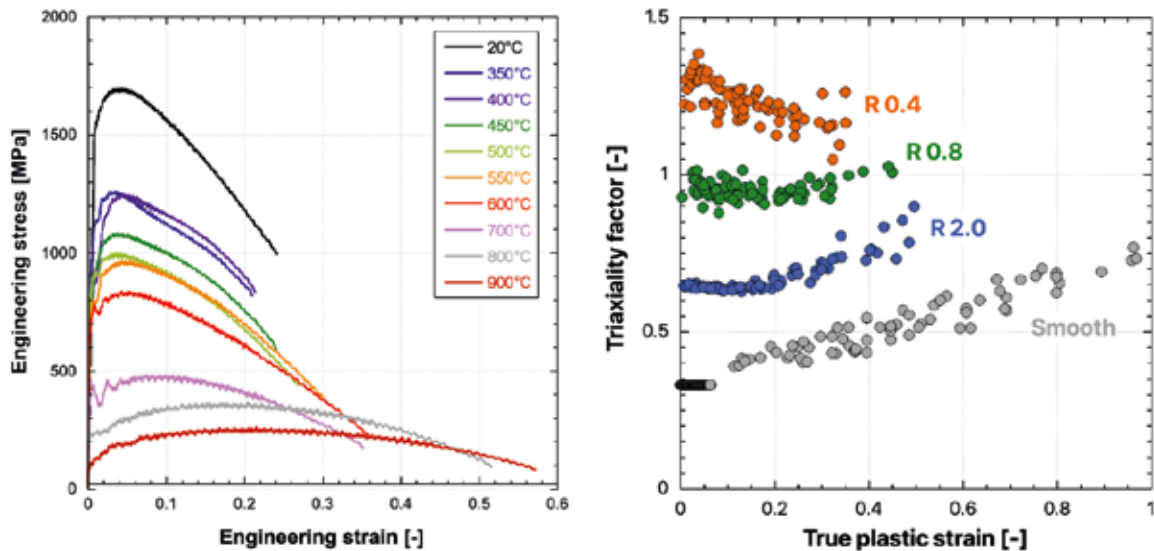


Fig. 2 – a) Engineering stress-strain curves at high strain rate as a function of temperature; b) Triaxiality factor versus true plastic strain curves.

In order to analyse the triaxiality effects four types of samples have been used. They were extracted from 8 mm thick steel plate in two different orientations, i.e. along and transversely to the rolling direction.

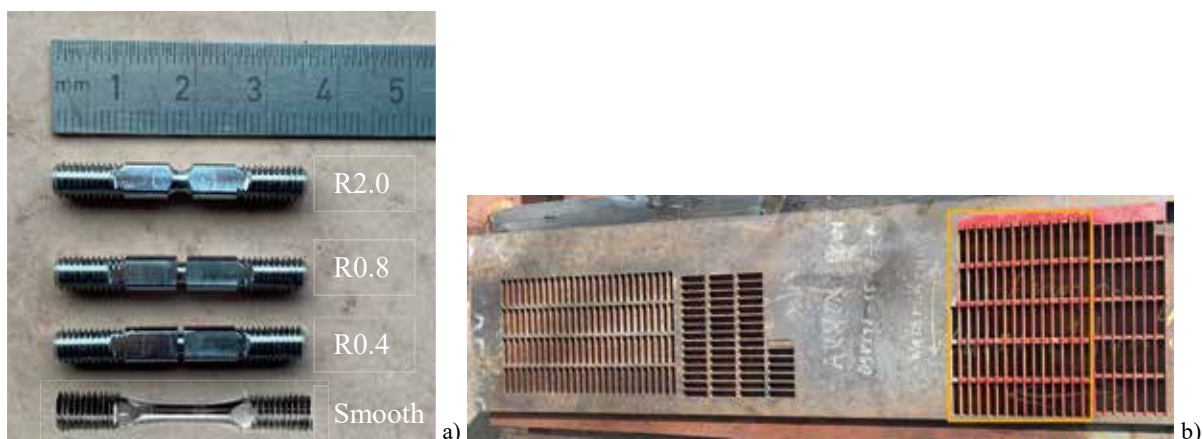


Fig. 3 – Specimen types (a) and photo of the Armox500T plate 8mm thick (b).

Different triaxialities were investigated through the true tensile strength as a function of the triaxiality as depicted in Fig. 2a, where the smooth specimen has triaxiality $\tau = 0.33$, whilst the specimens with notch radius equal to 2.0mm, 0.8mm and 0.4mm have $\tau = 0.652$, $\tau = 0.955$ and $\tau = 1.389$, respectively. These data have been used to calibrate the widely used constitutive laws such as Johnson-Cook relationship.

References

[1] Cadoni, E. and Forni, D. (2019), 'Mechanical behaviour of a very-high strength steel (S960QL) under extreme conditions of high strain rates and elevated temperatures', Fire Safety Journal, 102869.

3rd International Conference on Impact Loading of Structures and Materials
ICILSM 2022

A simplified approach in the design of energy absorbing cellular structures by means of the efficiency curves

Massimiliano Avalor^{a*}

^a*Dipartimento di Ingegneria Meccanica, Energetica, Gestionale e dei Trasporti,
Università di Genova, Via all'Opera Pia 15/A, 16145 Genova, Italy*

Abstract

The concept of efficiency curves introduced many years ago [1] and widely considered also in other works by the same author of this paper [2] introduces a very convenient tool to assess the energy absorption capacity of foamed, cellular, materials. In practice it was explained in [1] for a given absorbed energy there is a condition of minimum stress, or vice versa once a limit is given on the maximum stress the highest absorbed energy is obtained. This optimum condition coincides with the maximum of a parameter called efficiency which is the amount of absorbed energy divided by the stress. Efficiency plotted against the stress itself, or the compression strain, always has a maximum: curves of maximum efficiency against the foam density allowed in [2] to propose a method for the selection of the best density for a given type of foam for a specific application.

An equivalent method known as cushioning is also known for packaging applications. The method is also standardized by ISO 2248, 1985 *Packaging-complete, filled transport packages*. Vertical impact test by dropping and ASTM D1596 97(2003) Standard test methods for dynamic shock cushioning characteristic of packaging material. Recently an in-depth analysis of the method for simplifications was given by C. Ge in [3]. The cushion curves considered by the mentioned standard require a large amount of data obtained by loading samples of the energy absorbing material in several conditions of impact energy and speeds.

At the end the two methods are equivalent: with the efficiency curves the maximum is considered, corresponding to the minimum load, while in the cushioning method the minimum acceleration is found.

Following the analysis reported in [4] the compression stress-strain curves of many different cellular materials, both metallic [4] and polymeric based [5] can be described by a general relation as follows:

$$\sigma(\varepsilon) = \sigma_p [1 - \exp(-m\varepsilon)] + \sigma_s \varepsilon + \sigma_D \varepsilon^n \quad (1)$$

$$\sigma_p = \sigma_{p,0} \left[1 + \left(\frac{\dot{\varepsilon}}{\dot{\varepsilon}_0} \right)^p \right] f_p(\rho) \quad \sigma_s = \sigma_{s,0} \left[1 + \left(\frac{\dot{\varepsilon}}{\dot{\varepsilon}_0} \right)^p \right] f_s(\rho) \quad \sigma_D = \sigma_{D,0} \left[1 + \left(\frac{\dot{\varepsilon}}{\dot{\varepsilon}_0} \right)^p \right] f_D(\rho) \quad (2)$$

With σ_p plateau stress level, σ_s linear hardening slope in the intermediate phase, σ_D Rusch, densification parameter, m linear-plateau transition constant, n Rusch densification exponent, $\dot{\varepsilon}_0$ reference strain-rate value, p strain-rate exponent. Constants with lowered zero correspond to the reference strain-rate value.

* Corresponding author. Tel.: +39-010-3532241; fax: +39-010-3532241.

E-mail address: massimiliano.avallo@unige.it

By integrating the previous equation (1) it is possible to write an expression for the absorbed energy:

$$w(\varepsilon) = \int_0^\varepsilon \sigma \frac{d\varepsilon}{d\varepsilon} d\varepsilon = \sigma_p \left\{ \frac{(m-2) + \exp(-\varepsilon) [1 - m + \exp(-\varepsilon)^m]}{m-1} \right\} + \sigma_s [1 - (\varepsilon+1)\exp(-\varepsilon)] + \sigma_D \gamma(n+1, \varepsilon) \quad (3)$$

Where γ is the lower incomplete gamma function. The expression of the efficiency can be written as the ratio of (3) divided by (1). Equating the derivative of the efficiency function to zero, the maximum efficiency can be found and described as a function of the material parameters, in particular the density dependence can be explicated.

By analyzing experimental results from compression testing of different types of foams used in energy management applications, an interesting, serendipitous aspect was observed: maximum efficiency occurs for roughly a unit value of true compression strain (some examples for different cellular materials are in Fig. 1). This approximate but repeatable result is very important because it can be used to greatly simplify the design process based on the efficiency diagrams. In fact, once the foam parameters of equations (1)-(2) are identified, the curves of maximum efficiency as a function of the density are quickly obtained and plotted. To build selection diagram for a given class of cellular materials is a straightforward process by directly expressing absorbed energy and stress for the maximum efficiency.

$$\sigma(E_{\max}) = \sigma(\varepsilon = 1) = \sigma_p \left[1 - \frac{1}{e} \right] + \sigma_s + \sigma_D \quad (4)$$

$$w(E_{\max}) = w(\varepsilon = 1) = \frac{\sigma_p}{m-1} \left\{ (m-2) + \frac{1}{e} \left[1 - m + \frac{1}{e} \right] \right\} + \sigma_s \left[1 - \frac{2}{e} \right] + \sigma_D \gamma(n+1, 1)$$

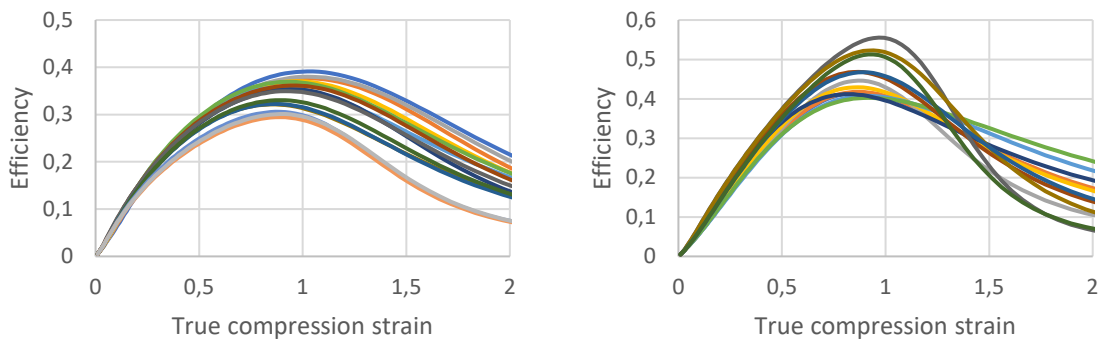


Fig.1 Efficiency curves for EPP (left, densities from 35 to 105 g/l) and PUR (right, densities from 60 to 100 g/l).

The relations between compression stress at the maximum efficiency, the corresponding specific energy absorbed, and the relative density [2] can be obtained directly from the identified material parameters [5] (Fig. 2).

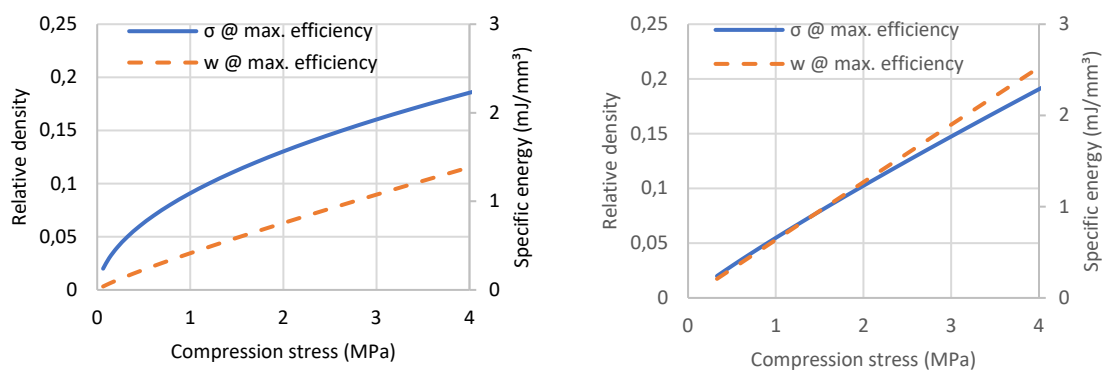


Fig.2 Optimal foam selection charts for EPP (left) and EPS (right).

References

- [1] L. J. Gibson, M. F. Ashby, Cellular Solids: Structure and Properties, Cambridge University Press, 1999.
- [2] M. Avallé, G. Belingardi, R. Montanini, Int. J. Impact Eng. 2001, 25, 455.
- [3] C. Ge, Packag Technol Sci. 2019; 32:185–197
- [4] M. Avallé and G. Belingardi, Adv Eng Mat. 2018, 1800457.
- [5] M. Avallé and G. Belingardi, ICILSM 2018.

3rd International Conference on Impact Loading of Structures and Materials
ICILSM 2022

Blast Attenuation in Cohesive Soils

Arthur van Lerberghe^a, Sam Clarke^a, Andrew D. Barr^a & Stephen L. Kerr^b.

^a*University of Sheffield, UK*

^b*Defence science and technology laboratory (Dstl), UK*

Abstract

Soil-filled wire and geotextile gabions are commonly used to construct defensive infrastructure in military bases, where the attenuating properties of soil are used to protect personnel and key assets from the effects of blast and fragmentation. The behaviour of cohesive soils in these extreme loading environments is unknown, and so designers require data at these high pressures and strain rates in order to develop robust soil constitutive models and adapt to new threats. Currently, the cohesive soils mostly used in experimental testing are kaolin clay, adobe clay, London clay and silt. The dry density, moisture content and Atterberg limits of these soils are contrasted between numerous different literature sources. The results reveal a lack of consistency in the recording of the parameters necessary to convincingly understand the material's performance under different loading conditions. Testing at high strain rates, a characteristic of blast and impact events, has required the development of specialised experimental methods such as the Split-Hopkinson pressure bar. Yet, no extensive applications have been conducted on cohesive soils. Additionally, testing at low strain rates using triaxial and oedometer apparatuses are important to understand the overall behaviour of cohesive soils, creating a complete soil profile of the material. This work will focus on presenting an overview of the current work which has been completed using low and high strain rate tests on cohesive soil samples, highlighting initial findings, and introducing future work opportunities.

3rd International Conference on Impact Loading of Structures and Materials
ICILSM 2022

Polymer testing with a pre-tensioned steel split-Hopkinson bar

Einar Schwenke^{a,b,c,*}, David Morin^{a,b}, Arild Holm Clausen^{a,b}

^a*Structural Impact Laboratory (SIMLab), Department of Structural Engineering,
Norwegian University of Science and Technology (NTNU), NO-7491 Trondheim, Norway*
^b*Centre for Advanced Structural Analysis (CASA), NTNU, NO-7491 Trondheim, Norway*
^c*Inventas AS, NO-7014 Trondheim, Norway*

Abstract

High-rate testing of polymeric materials is known to be a challenging task, but it is nevertheless required for numerical simulations of components subjected to rapid deformations. The most common tool for material testing at high strain rates is the split-Hopkinson bar. Many variants of the Hopkinson bar exist, but common for them all is that the load is applied in the form of a stress wave.

The impedance and flow strength of polymers is often much lower than that of the Hopkinson bars. The measured signal from the strain gauges on the bars is therefore weaker compared to the inherent noise within the signal and the gauges. The traditional bar material is steel, but several researchers have utilized lower impedance materials such as aluminum or nylon to increase the signal-to-noise ratio. These alternatives have proven useful, but they also introduce new challenges relative to the steel bars.

The objective of this study is to evaluate whether the use of steel bars yields acceptable results for the testing of semi-crystalline polymers. A cross-linked polyethylene has been tested with an in-house pre-tensioned steel split-Hopkinson bar. One major advantage of this test set-up is that a long duration stress wave of 3.4 ms is achieved. This enables acquisition of high strains compared to other designs, which is particularly useful for testing of ductile polymers. A detailed description of the set-up was given by Chen et al. [1].

Numerical simulations were performed for the full test set-up, also including the generation and propagation of the stress waves. This enabled investigation of both the performance of the bar and the response of the specimen. A good correspondence was found with the experimental results. The comparison serves as a mutual validation of both the numerical model and the experimental test set-up.

* Corresponding author. Tel.: +47 97 66 49 41.
E-mail address: Einar.schwenke@ntnu.no

REFERENCES

- [1] Y. Chen, A. H. Clausen, O. S. Hopperstad, and M. Langseth, "Application of a split-Hopkinson tension bar in a mutual assessment of experimental tests and numerical predictions," *Int. J. Impact Eng.*, vol. 38, no. 10, pp. 824–836, 2011.

3rd International Conference on Impact Loading of Structures and Materials
ICILSM 2022

Impact of Full-field Measurement Biases on Identification of Anisotropic Material Behavior Model

Jean-David THOBY^{a,b,c}, Thomas FOUREST^a, Delphine NOTTA-CUVIER^{c,d},
Eric MARKIEWICZ^{b,c}, and Bertrand LANGRAND^{a,c*}

^aDMAS, ONERA, F-59014 Lille - France

^bUniversity Polytechnique Hauts-de-France, F-59313, Valenciennes, France

^cLAMIH, CNRS, UMR 8201, F-59313, Valenciennes, France

^dINSA, Hauts-de-France, F-59313 Valenciennes, France

Abstract

Commercial aviation industry is facing important challenges regarding the reduction of CO₂ emissions. In addition to studies on propulsion systems, aircraft manufacturers are consistently improving manufacturing techniques, part design and selection process of new lightweight materials to reduce the weight of aircraft. The majority of studies in these topics uses numerical modelling and simulations based on Finite Element Analysis (FEA). The relevance of these simulations depends partly on the accuracy of constitutive equations used for material behaviour modelling, which can be complex.

For instance, the AA2198-T351, studied in this work, is a recent aluminium-copper-lithium alloy developed by Constellium. This material has low density, good strength and resistance to mechanical damage [1], and is used to manufacture commercial aircraft fuselage skin and wings components. However, the AA2198-T351 shows strong anisotropic behaviour that requires the definition and characterization of appropriate yield criteria, such as that developed by Bron and Besson [2,3]. This yield criterion is able to simulate the angular variation in the stress space of the initial yield stress, σ_0 , and the Lankford coefficient, r (ratio between longitudinal and through-thickness plastic strain). Identifying the constitutive material parameters with standard procedure requires numerous statically determined uniaxial tensile tests, performed in different loading directions with respect to the rolling direction of laminated material (Figure 1) and at different displacement rates to analyse strain rate dependency. Moreover, post-treatment of such statically determined tests requires to ensure spatial homogeneity of stress and strain fields and strain rate during the tests. Such homogeneity is obviously violated as soon as localisations appear, thus limiting the exploitation of tests to a restricted strain range.

On the other hand, inverse identification methods such as the Virtual Fields Method (VFM) allow the exploitation of heterogeneous mechanical fields, which may significantly reduce the amount of tests required for the identification of complex behaviour [4]. Aiming at identifying the parameters of an anisotropic yield criterion in a single test, numerous stress states must be generated through the specimen to vary the local mechanical responses (*i.e.*, tension, shear, compression). However, the design of such specimen geometry remains an open problem [4]. In the literature, it was numerically proven that some geometries can expand the range of generated stress states during a single tensile test. Yet, the impact of the biases introduced by full-field measurement in real conditions (noise, resolution, biased data close to the edges etc.) was not taken into account.

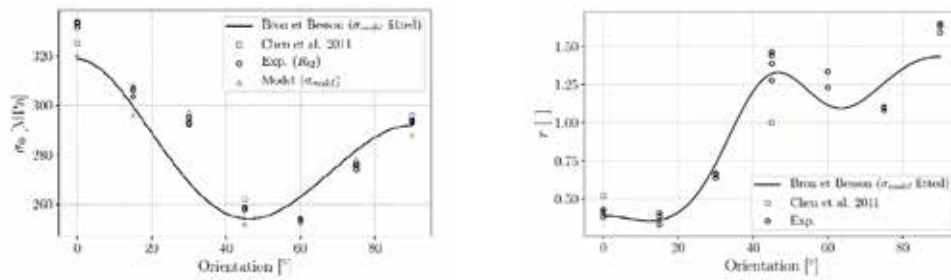


Fig. 1. Angular variation of the initial yield stress (left) and the Lankford coefficient (right)

This study aims to develop a numerical procedure to evaluate the impact of full-field measurement during the selection process of the most suitable specimen geometry, *i.e.* in terms of accuracy of identification of parameters of material constitutive model. Marek *et al.* [5] tested a notched specimen. Kim *et al.* [6] and Jones *et al.* [7] designed more complex geometries, called “ Σ ”-shape and “D”-shape specimens respectively. Barroqueiro *et al.* [8] used topological optimization to generate a more complex specimen shape (Figure 2). In the present work, the FE method is used to simulate tensile tests on these specimens. Then, a set of synthetic images [9] is generated and the Digital Image Correlation (DIC) method is applied to compute kinematic fields from these images. The impact of biases introduced by DIC, such as effect of sensor noise, speckle pattern and edge reconstruction, are analysed based on two indicators. The first one is an indicator of the heterogeneity of the stress fields [10] obtained by FE simulations. The second one quantifies the error in the identification procedure with the VFM due to measurement biases.

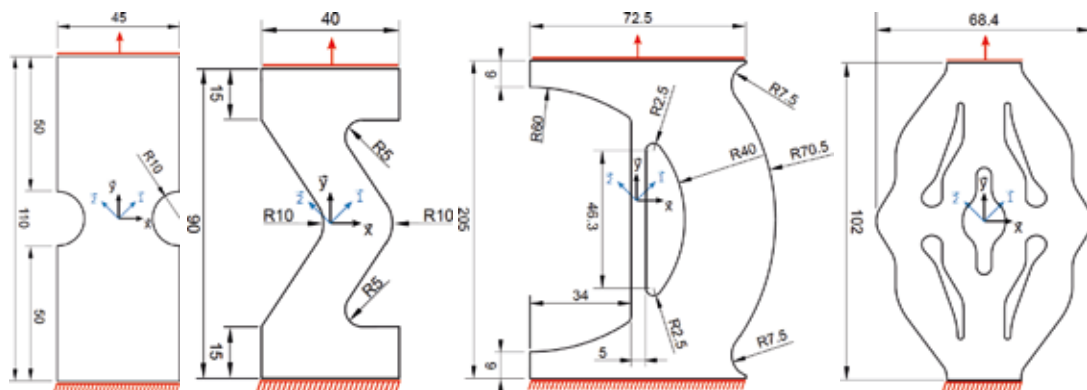


Fig. 2. Specimen geometries. From left to right: notched, “ Σ ”-shape, “D”-shape and optimized specimens

Then, experiments are performed using the four specimens machined in AA2198-T351 aluminium alloy. DIC is used to compute strain fields with the algorithm folkiD developed by Onera [11] and the VFM is applied to identify the parameters of the Bron and Besson model. Several optimisation algorithms are compared. Finally, the results obtained by the two methods (synthetic images and experimental images) are discussed.

Acknowledgements

The authors are grateful to ONERA and the Région Hauts-de-France for co-funding this project. Also, the authors would like to express their sincere gratitude to Constellium and more specifically to Dr. Jean-Christophe Ehrström for supporting this study and providing the aluminium alloy sheet.

References

- [1] J. Chen, Y. Madi, T. F. Morgeneyer, J. Besson, *Comput. Mat. Sci.*, **50**, 1365-1371 (2011)
- [2] D. Banabic, *Plastic Behaviour of Sheet Metal* (2010)
- [3] F. Bron, J. Besson, *Int. J. Plasticity*, **20**, 937-963 (2004)
- [4] F. Pierron, M. Grédiac, *The Virtual Fields Method* (2012)
- [5] A. Marek, F. M. Davis, M. Rossi and F. Pierron, *Int. J. Mat. Forming*, **12**, 457-476 (2019)
- [6] J.-H. Kim, F. Barlat, F. Pierron, M.-G. Lee, *Exp. Mech.*, **54**(7), 1189-1204 (2014)
- [7] E. M. C. Jones, J. D. Carroll, K. N. Karlson, S. L. B. Kramer, R. B. Lehoucq, P. L. Reu, D. Z. Turner, *Comput. Mat. Sci.*, **152**, 268-290 (2018)
- [8] B. Barroqueiro, A. Andrade-Campos, J. Dias-de Oliveira, R. A. F. Valente, *Int. J. Mech. Sci.*, **181** (2020)
- [9] P. Bouda, B. Langrand, D. Notta-Cuvier, et al, *Comput. Mech.*, **64**, 1639-1654 (2019)
- [10] N. Souto, S. Thuillier, A. Andrade-Campos, *Int. J. Mech. Sci.*, **101-102**, 252-271 (2015)
- [11] G. Le Besnerais, Y. Le Sant, D. Lévêque, *Strain*, **52**, 286-306 (2016)

3rd International Conference on Impact Loading of Structures and Materials
ICILISM 2022

A numerical modelling and generative deep learning approach to the ballistic impact resistance of additive manufactured maraging steel plates

Maisie Edwards-Mowforth^{a,*}, Samuel Thompson^a, Miguel Costas^b, Martin Kristoffersen^b, Tore Børvik^b,
Filipe Teixeira-Dias^a

^aInstitute of Infrastructure and Environment (IIE), School of Engineering, The University of Edinburgh, Edinburgh, UK

^bStructural Impact Laboratory (SIMLab), Department of Structural Engineering, NTNU – Norwegian University of Science and Technology, Trondheim, Norway

Abstract

Improved performance of protective structures is critical to keep pace with demand for lightweight and mobile fortification. Additive manufacturing (AM) can be used to enhance performance-to-weight ratios of armour systems. AM maraging steel draws extreme strength during heat treatment from intermetallic precipitates, and has recently demonstrated potential for superior ballistic perforation resistance, provided that an optimisation of strength versus ductility can be achieved. Testing of high-strength AM materials, however, escalates the complexity and cost of experimental campaigns. As a result, optimisation tasks become increasingly dependent on numerical modelling and predictive technologies. Advancements in deep learning methods, computational systems that employ artificial neural networks (ANNs), have recently found utility in high-dimensional design processes with limited experimental training data. This feature of generative adversarial networks (GANs) and transfer learning holds potential to accelerate developments in innovative ballistic protection. A set of numerical models are presented, that accurately reproduce perforation processes seen in experimental tests for as-printed AM maraging steel, although falling short for the ultra high-strength heat treated material. The latter is attributed to an inability of the material model to capture projectile fracture; the mechanism that gives superior ballistic performance to the material. A GAN model is proposed and accurate quantitative predictions of ballistic limit velocity for both heat treated and as-printed maraging steel datasets are demonstrated, surpassing that of the FE models. Lingering issues of convergence and stability are addressed with a “fine tuned” GAN architecture, in which an analytical ballistic curve is incorporated by means of a variational autoencoder (VAE) secondary model. The FE simulation results are a step toward a functional model of AM maraging behaviour during ballistic penetration, but nevertheless highlight the drawbacks of methods reliant on empirical data, lacking at present due to experimental limitations. Upon exposure to variations of material composition and geometry, the proposed GAN architecture could be an important tool in drawing upon the flexible and customisation possibilities of AM, diminishing of the cost and resources required in the development stage of maraging steel for armour systems.

*Corresponding author: m.edwardsmowforth@gmail.com

3rd International Conference on Impact Loading of Structures and Materials
ICILSM 2022

Modelling of concrete subjected to projectile impact

Sumita Dey^{a,*}, Martin Kristoffersen^b, Oda Toreskås^a, Tore Børvik^{a,b}

^aDepartment of Research and Development, Norwegian Defence Estates Agency, NO-0103 Oslo, Norway

^bSFI CASA and SIMLab, Department of Structural Engineering, NTNU – Norwegian University of Science and Technology, NO-7491 Trondheim, Norway

Abstract

Concrete is the most widely used building material in the world and is thus much used in protective structures exposed to extreme loadings such as explosion or ballistic impact. Studies on ballistic impact of concrete typically concern either deep penetration or perforation. For the former, where a high level of confinement is present, the compressive strength of the concrete has been shown to be the primary variable. For the latter, the process is more complex and the concrete experiences multiple damage and failure mechanisms, including spalling, tunnelling, and scabbing. Analytical and/or empirical approaches were formerly used extensively for modelling problems of this kind, but with the rapid increase in computational power, more and more studies are now carried out using numerical simulations. Several concrete models are available in various commercial finite element solvers [1], each with their strengths and weaknesses. A model may for example be easy to calibrate but lack the sophistication to capture all relevant phenomena accurately, and vice versa. In this study, a modified version of the Holmquist-Johnson-Cook (MHJC) model [2] is validated for dynamic loading of three concrete qualities. This model is easy to calibrate and implement, and may serve as an engineering compromise between simplicity and accuracy.

To validate the MHJC-model, the ballistic perforation resistance of 50 mm thick concrete slabs impacted by 20 mm diameter ogive-nose steel projectiles is studied both experimentally and numerically. Three types of commercially produced concrete with nominal unconfined compressive strengths of 35, 75 and 110 MPa were used to cast material test specimens and slabs. After curing, ballistic impact tests were carried out in a compressed gas gun facility to determine the ballistic limit velocity and curve and for each slab quality. Figure 1 shows typical time lapses of the penetration and perforation process based on high-speed camera images from impact tests of the different concrete qualities [3]. All tests are at impact velocities close to their respective ballistic limits. Since one camera was focused on the front side and the other camera was focused on the back side of the concrete slabs, both spalling and scabbing could be studied. Alongside the impact tests, material tests were conducted to assess the mechanical properties of the materials. Finite element models using input from the material tests were established in LS-DYNA [3]. The constitutive behaviour of the concretes was predicted by the MHJC model.

Numerical simulations of the ballistic impact tests were carried out and the results were in general found to be in good agreement with the experimental data. The MHJC model was calibrated based on quasi-static material tests (i.e., cube compression, cylinder compression and tensile splitting), data from the literature and inverse modelling of the cylinder compression tests based on DIC measurements. The calibrated and validated MHJC model was

* Corresponding author. Tel.: + 47 97 53 15 80
E-mail address: sumita.dey@forsvarsbygg.no

then used in a 2D axisymmetric model of the ballistic impact tests. Figure 3 shows typical fringe plots of the volumetric strain at selected times during perforation of a C75 concrete slab together with a comparison between experimental and numerical ballistic limit velocities as a function of cube compressive strength. As shown, the MHJC model provided in general good and conservative results, even though the slope of the $f_{cc} - v_{bl}$ curve differs somewhat between tests and simulations. Based on these results, it seems safe to conclude that the MHJC-model provides a reliable alternative to more advanced concrete models for which accurate material parameter sets may be difficult to obtain.

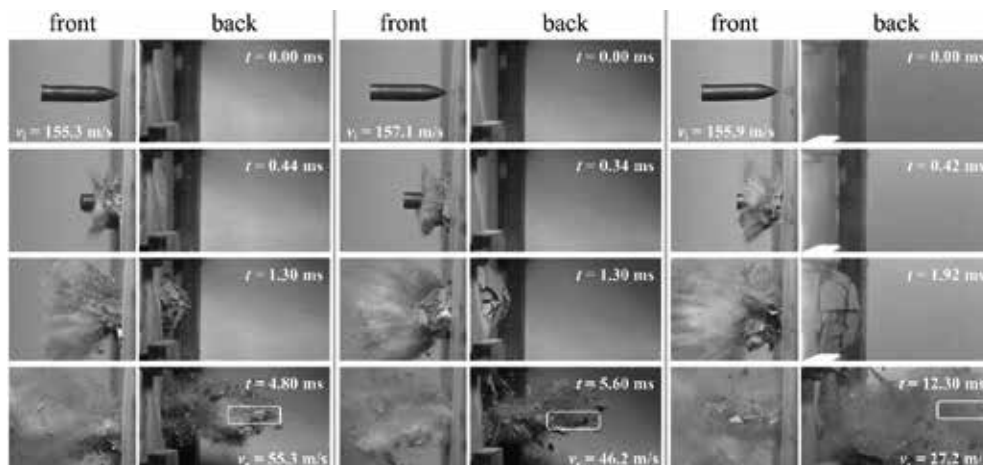


Figure 1: Time lapse from impact tests on C35 (left column), C75 (centre) and C110 (right) [3].

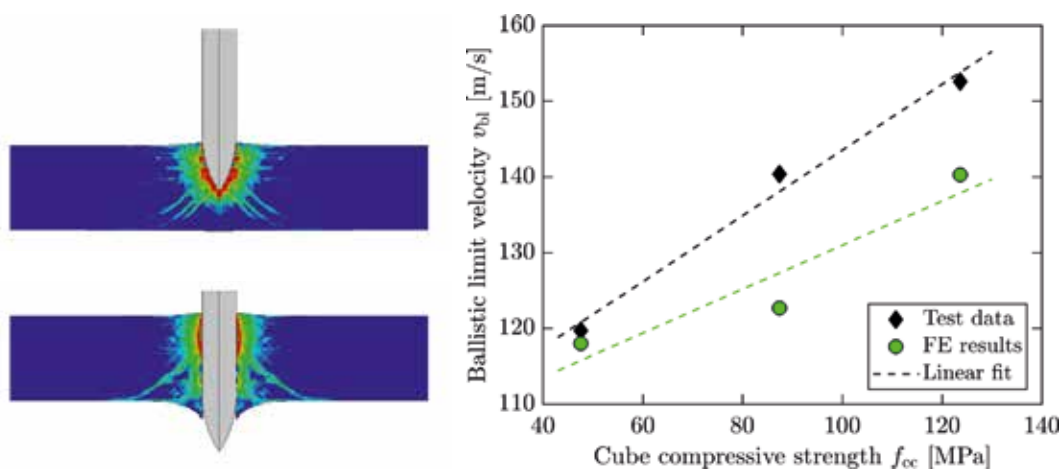


Figure 2: Fringe plots of volumetric strain at selected times during perforation of a C75 concrete slab (left) and comparison of experimental and numerical ballistic limits as function of cube compressive strength (right) [3].

References

- [1] Antoniou A, Kristoffersen M, Børvik T. Survey of four material models for ballistic simulations of high-strength concrete. Proceedings of 13th European LS-DYNA Conference, October 5-6, 2021, Ulm, Germany.
- [2] Polanco-Loria M, Hopperstad OS, Børvik T, Berstad T. Numerical predictions of ballistic limits for concrete slabs using a modified version of the HJC concrete model. International Journal of Impact Engineering 2008;35:290-303.
- [3] Kristoffersen M, Toreskås OL, Dey S, Børvik T. Ballistic perforation resistance of concrete slabs impacted by ogival projectiles. International Journal of Impact Engineering 2021;156:103957.

3rd International Conference on Impact Loading of Structures and Materials
ICILSM 2022

Characterization with LASer Shock Adhesion Test of the interface strength of a
HDPE composite coated with ceramic

R. Ben Saada^{a*}, A. El Malki Alaoui^a, G. Darut^b, J. Le Clanche^a, M. Arrigoni^{a c}

^aENSTA Bretagne, IRDL, UMR 6027 CNRS, 29806 Brest, France

^bICB UMR 6303, CNRS, Université Bourgogne Franche-Comté, UTBM, F-90010 Belfort, France

Abstract

In the last decades, many progresses are achieved concerning the materials development for defence applications, especially for ballistic protection. In this context, the composite materials present obvious advantages in comparison with the conventional materials i.e. metals and ceramics given their interesting strength/weight ratio. However, the protection efficiency of material assemblies could be improved in term of manufacturing and mass reduction.

In the present contribution, an Al₂O₃ coating is deposited on an HDPE-based composite i.e. Tensylon® using thermal spray coating. In order to obtain the expected multi-material, a metallic undercoat between the composite and the coating is necessary. Otherwise, the composite degrades and melts. Henceforth, the Tensylon/Al₂O₃ coating assembly could be characterized from a mechanical point of view. Firstly, observations under optical microscope are done in order to obtain the preliminary information on the coating microstructure (roughness, porosity, ...). These parameters could play a key role on the coating strength. The adhesion of the assembly is subsequently tested using the LASAT (LASer Adherence Test) technique which is a contactless test involving high strain-rates (10⁶ s⁻¹). The uncoated composite is considered as a control sample. This test is a means of evaluating the cohesion of Tensylon® only. Then shots are performed on the 50 x 50 mm sample of Tensylon® coated with the alumina coating of approximately 0.3 mm thick. Each shot is performed with a 4 mm focal spot (shocked area) on the Tensylon® side. A spacing of 5 mm between the edges of the target and the edge of the focal spot and between two focal spots in order to avoid edge effects due to the sample geometry. The energy of the shot is increased from one shot to the next. For each impact, a laser Doppler interferometer based on the Photonic Doppler Velocimetry measurement (PDV probe) of the speed of the free surface with respect to the impact is measured during the experiment. From the analysis of these signals, a diagnosis of the decohesion of the interface is proposed.

Through this technique, a delamination limit stress can be estimated, which offers the prospect of identify the key parameters of the spraying method in order to optimize the level of adhesion of the coating on its substrate.

* Corresponding author

3rd International Conference on Impact Loading of Structures and Materials
ICILSM 2022

Static and dynamic characterization of UHMWPE with nanoparticles

Alia Ruzanna Aziz, Haleimah Alabdouli, Abdulla Alshehhi, Monserrat Gutierrez,
Rafael Santiago, Zhongwei Guan

Advanced Materials Research Center, Masdar City, Abu Dhabi PO Box 9639, United Arab Emirates.

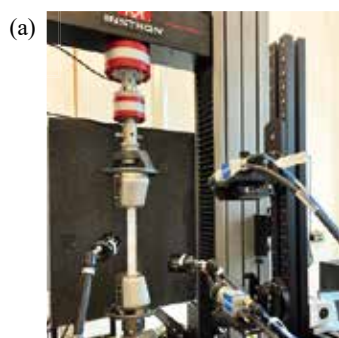
Abstract

There has been a significant increase in the use of ultra-high molecular weight polyethylene (UHMWPE) composites for ballistic and impact protection applications, mainly due to their excellent strength-to weight ratio. The UHMWPE fibers can be up to 15 times stronger than steel and up to 40% stronger than aramid fibers (Kevlar) of the same weight [1]. Thus, there is a need to characterize UHMWPE composites at different strain rates to provide an in-depth understanding and modelling for impact purposes. Only few efforts have been reported aiming to explore the mechanical response of UHMWPE composites under quasi-static and dynamic loadings, and, apparently, the existing literature showed inconsistent and conflicting results. This can be probably due to the challenges faced in gripping the specimens that are related to the poor adhesion between the fibre-matrix interface and low coefficient of friction of the polymer [2]. Furthermore, composites using nanoparticles such as carbon nanotubes (CNT) have demonstrated to reinforce the fibers without adding weight and keeping the flexibility the fiber [3]. A good dispersion of CNT plays a very important role to obtain the desired mechanical properties; in this work we propose to disperse them by using ultrasonic deposition of a fluoropolymeric matrix with the nanoparticles embeded on it. The fluoropolymer has been study to enhance mechanical properties of body armors [4]; at the same time the matrix helps to improve the adhesion between UHMWPE layers.

The purpose of this study is to develop a comprehensive material characterization of UHMWPE composites at strain rates ranging from 0.001 s^{-1} up to 1000 s^{-1} using innovative techniques and to investigate the effect of the fluoropolymer fluoroethylene vinyl ether (FEVE) on the mechanical properties. Three grades of UHMWPE composite systems supplied by DSM were investigated in the study, with details listed in Table 1. Initially, the quasi-static tensile strength, Young's modulus and failure strain were determined from the measured stress-strain curves using a specially designed grips attached to an Instron 5982 universal testing machine with 100 kN load cell. The strain distribution data were measured using a digital image correlation (DIC) system, as shown in Figure 1a. Subsequently, dynamic tensile behaviour at intermediate and high strain rates were carried out for the same set of samples using a servo mechanical device and Split Hopkinson pressure bar, combined with high-speed cameras and DIC for the strain tracking, as shown in Figures 1b and c respectively. The testing results showed that the material is highly dependent on the fiber/matrix combination and UHMWPE exhibits an evident strain rate dependency.

Grade	Fiber type	Matrix type	Thickness (mm)	Configuration
HB26	Dyneema SK76	Polyurethane-based (PADP)	0.26	$[0^\circ/90^\circ]_2$
HB210	Dyneema SK99	Polyurethane-based	0.14	$[0^\circ/90^\circ]_2$
HB212	Dyneema SK99	Rubber based	0.14	$[0^\circ/90^\circ]_2$

Table 1: Details of the UHMWPE composite systems investigated.



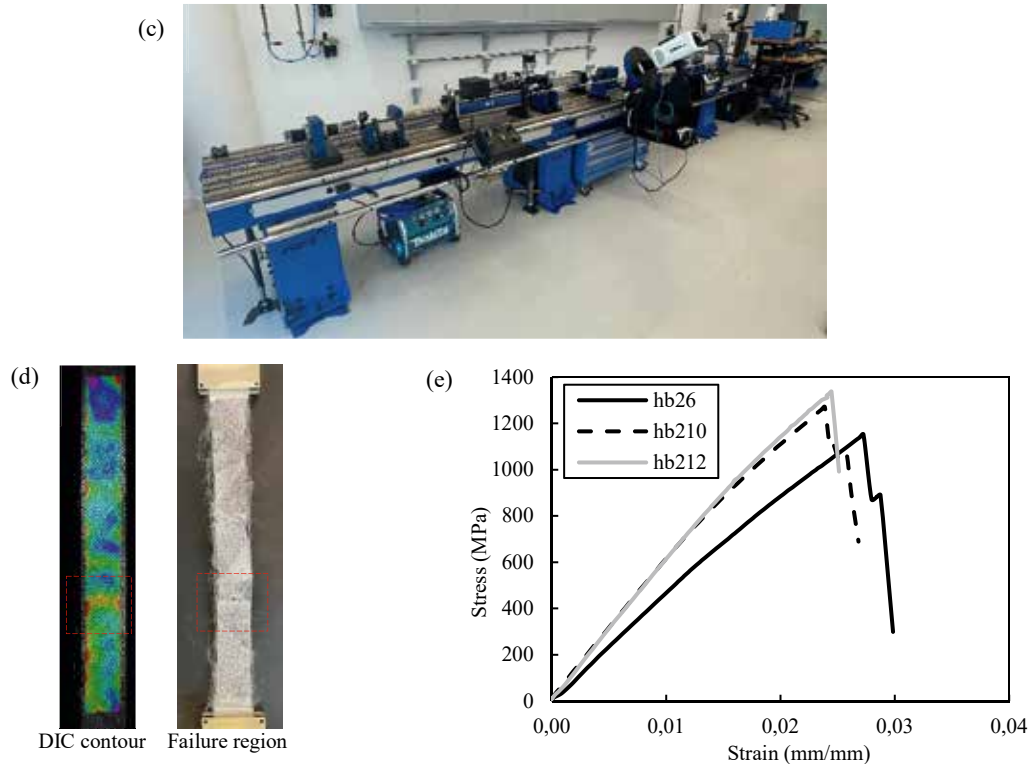


Figure 1: (a) Setup of quasi-static tensile test with digital image correlation (DIC) system, (b) Servo Mechanical rig, (c) Split Hopkinson Pressure bar, (d) longitudinal strain distribution for HB210 sample prior and following failure within the gauge length. (e) The measured stress-strain curves of the UHMWPE samples.

Following this, UHMWPE panels, Figure 2a, were manufactured using various combinations of nanoparticles and fluoropolymer matrix to improve the composite interlaminar strength. The panels were manufactured by hot-pressing at 16.5 MPa at 125°C, as per the supplier recommendations, being the nanofillers dispersed in FEVE matrix at different concentrations. The panels were then tested in a drop weight rig Instron 9450, Figure 2b, at the impact velocity of 2 m/s and 3 kg mass. Preliminary results points to an optimum combination of nanoparticles/matrix that improves the impact strength of UHMWPE laminates.

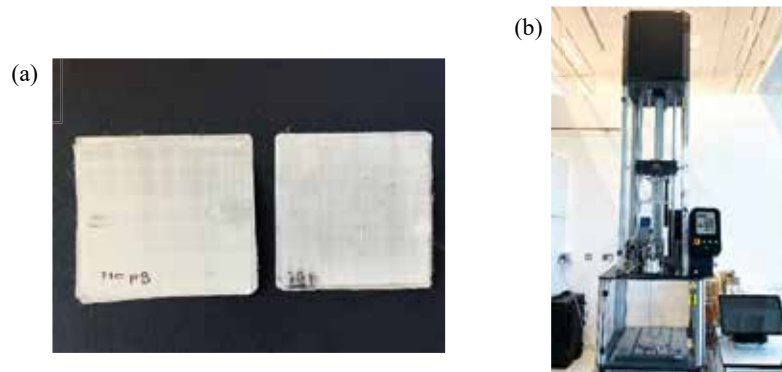


Figure 2: (a) UHMWPE panels manufactured using various combinations of nanoparticles and (b) drop weight rig Instron 9450 used to test the panels.

References

- [1] H. Wang et al, Tensile properties of ultra-high-molecular-weight polyethylene single yarns at different strain rates, *Journal of Composite Materials*, 54, 2020, pp1453–1466.
- [2] H. Van Der Werff and U. Heisserer, *High-performance ballistic fibers: Ultra-high molecular weight polyethylene (UHMWPE)*. Elsevier Ltd, 2016.
- [3] A. M. K. Esawi and M. M. Farag, Carbon nanotube reinforced composites : Potential and current challenges, *Materials & Design*, 28, 2007, pp2394–2401.
- [4] B. Dyatkin and R. M. Gamache, Ballistic performance of front-facing fluoropolymer-coated armor composites, *International Journal of Impact Engineering*, 114, 2018, pp63–68.

3rd International Conference on Impact Loading of Structures and Materials
ICILSM 2022

Determination of mechanical property profiles for improved crash performance of a dual phase automotive steel

Sarath Chandran^{a*}, Patricia Verleysen^a

^a*MST-DyMa Lab, Department of Electromechanical, Systems and Metal Engineering, Ghent University, Technologiepark 46, 9052, Zwijnaarde, Belgium*

Abstract

The most important objective of the automotive industry in the current decade is to design light weight vehicles in order to be environmental friendly. However, in the meantime, also safety requirements during collisions have to be met. Crashworthiness is mainly concerned with the controlled absorption of crash energy. Parameters such as internal energy absorption and crush force efficiency are key constants in evaluating a component's crash worthiness and its safety. In the design of automotive structures for crashworthiness, there is a strict requirement for null strain sub modules that provides a rigid space of survival area for the occupants and deformable sub modules which can dematerialize the kinetic energy effectively. The front crash box of a car is the one of the most important deformable components which dissipates kinetic energy during frontal crash, which is the most pronounced crash situation that affects the entire automotive structural behavior.

A comprehensive experimental program considering the material plasticity and fracture behavior under various loading conditions experienced in automotive crash situations are designed and carried out. A commercial dual phase automotive steel, DP-K1000, with a martensite phase fraction of 45% is considered for the study. The material is available in the form of rolled sheets with a final thickness of 1.5 mm. To determine the intrinsic mechanical properties of the dual phase steel under consideration, tests are performed at wide range of loading speeds, thereby covering the quasi-static, intermediate and dynamic strain rates (0.0001 to 1000 s^{-1}) and temperatures (-40 to 400°C). An Instron material testing machine is used to perform experiments at static and medium strain rates whereas the dynamic loading rates are achieved with the aid of split-Hopkinson tensile bar setup. A set of specially designed and optimised fracture specimen geometries are employed for damage and fracture characterization of DP1000 steel. Each specimen thus designed help in achieving a characteristic stress state (for example a central hole specimen for uniaxial tension, three notched dogbone samples R4.5, R1.8 and R0.4, a plane strain and shear specimen) and reveal a wide range of damage mechanisms exhibited by these kinds of advanced high strength steels.

A hybrid extended modified Bai-Wierzbicki (eMBW) damage plasticity model is then implemented to properly describe the non-negligible impact of damage in strength and ductility and dependence of stress state on damage accumulation. The material model constitutes a plasticity formulation to characterize the material behavior before the initiation of damage followed by a phenomenological criterion to indicate the damage initiation. A phenomenological formulation of ductile damage is used for a user friendly and simplified input of material parameters. Finally, a damage induced softening part incorporating a damage mechanics approach is adopted to characterize the post damage behavior. The performed experimental campaign provide a reliable data set to derive the material model parameters of the adopted damage plasticity model. The calibrated material model is thus used to investigate the crash response of this dual phase automotive steel both qualitatively and quantitatively. The constitutive model is imposed on the analysis for the dynamic response of auto-body crash box utilizing the explicit finite element scheme Abaqus.

* Corresponding author.

E-mail address: Sarath.Chandran@UGent.be

The proposed eMBW material model is implemented into Abaqus Explicit via a user material subroutine (VUMAT). A full scale model with 3D solid elements and sufficient mesh refinement is adopted to accurately predict the localization and damage phenomena within the crash box. The concurrence of the derived crashworthiness experimental results and deformation behavior from finite element scheme is thus evaluated.

Total energy absorption of the crash box can be due to the coupled effects of geometry and material property. The effect of geometry is decoupled from the material effects so that the energy absorption contribution from the material effects as a function of plastic deformation and damage properties of the material can be solely investigated. The study aims at the identification of relevant mechanical properties of the automotive material which are important to evaluate and improve its crash performance, as well as in-depth understanding of the influence of the material behavior on the component performance. The component performance is quantified by the energy absorption during a crash test on a crash box made of DP-K1000 steel. A Taguchi optimization procedure based on a concrete design of experiments was performed to assess the individual contribution of the material mechanical properties to the overall component performance. This technique is adopted on the component scale crash box model with the optimized set of material parameters. Material mechanical property sets are then varied within a predefined range in accordance with the strategy for design of experiments such that all possible combinations of material properties linked to the crash performance can be systematically analyzed. Yield strength, ultimate stress, hardening coefficient, damage initiation strain and failure strain were some of the parameters considered in the optimization routine. Additionally, relative contribution of each of the mechanical properties were addressed. The outcome of this optimization approach was a sorted list of relevant mechanical property profiles in order of their significance of contribution towards higher energy absorption.

The interaction between the contributing mechanical material properties is quantified for different strain rates, stress states and temperatures. Peak crushing forces will result in increased accelerations transmitted from the frame to the passenger compartment. Various material property sets were evaluated based on the common crashworthiness criteria to identify the effective design (combination of material mechanical parameter set) which provide low peak force and trigger the regular collapse behavior. Force versus displacement curves were plotted in each case, providing detailed insight into the force variation during deformation. Results from the analysis suggests that the material yield stress has the most significant contribution in bringing about a change in the energy absorption characteristics, followed closely by ultimate tensile strength ratio. Yield stress, ultimate strength and hardening rate together have a strong positive effect on the energy absorption characteristic while failure strain has a weak contribution. Crush efficiency increases with increase in yield strength primarily when the hardening capability of the material is higher. By the use of a material with optimized mechanical property profile, a performance improvement in the component level can be aimed at, using the same geometry and material thickness as in the original automotive crash box design.

Keywords: Crashworthiness, energy absorption, crush force efficiency, mechanical property profiles, Taguchi optimization

Acknowledgement: The authors would like to acknowledge the financial support of Research Fund for Coal and Steel (RFCS) of the European Commission and the partners of the ‘Toolkit’ project for the fruitful collaboration. Also Ghent University is acknowledged for the support of the study into damage and plasticity of AHSS by providing funding for the research-assistant mandate of the first author.

3rd International Conference on Impact Loading of Structures and Materials
ICILSM 2022

Experimental study for water impact of composite panels

Yuqian Tu^{a,*}, Mauro Zanella^b, Paolo Astori^b, Chiara Bisagni^a

^a*Delft University of Technology, Faculty of Aerospace Engineering, Delft, The Netherlands*

^b*Politecnico di Milano, Dipartimento di Scienze e Tecnologie Aerospaziali, Milan, Italy*

Abstract

To improve aircraft safety during an emergency landing on water, it is important to have a good knowledge of the structural behavior. However, the structural analysis during water impact is always challenging as the complex fluid-structure interaction phenomenon is involved.

This research aims to analyze composite panels during water impact and to evaluate the damage, if any. The presented work focuses on the test setup and test results for water impact of the composite panels.

The panels, manufactured at the Delft University of Technology, are made of AS4/8552 carbon epoxy composite material. They have a stacking sequence of $[45,0,-45,90]_{4s}$, resulting in a total thickness of 5.94 mm. The length and width are both 400 mm. A steel frame of 16 kg is added on the top of the panels.

During the water impact tests, conducted at Politecnico di Milano, the composite panels were released from different drop heights and impacted into a water basin. Two high-speed cameras were set on two sides to capture the impact moment and the panel's deformation. The structural response of the composite panels was sampled in terms of accelerations, strains and pressures measured at selected locations. The test setup and the test structure with instrumentation are shown in Figure 1.

The acceleration curves of a test from a 3-meter height impact are shown in Figure 2. The three acceleration curves are from the three accelerometers located on the steel frame. The panel resulted slightly tilted during the drop, since two accelerometers have higher peak values than the third accelerometer. The strain curves measured from the strain gauge installed in the center of the panel are shown in Figure 3. The x-direction and y-direction strains are slightly different due to the layups of the panel.

The complete test results will be presented at the conference.

* Corresponding author. E-mail address: y.tu@tudelft.nl

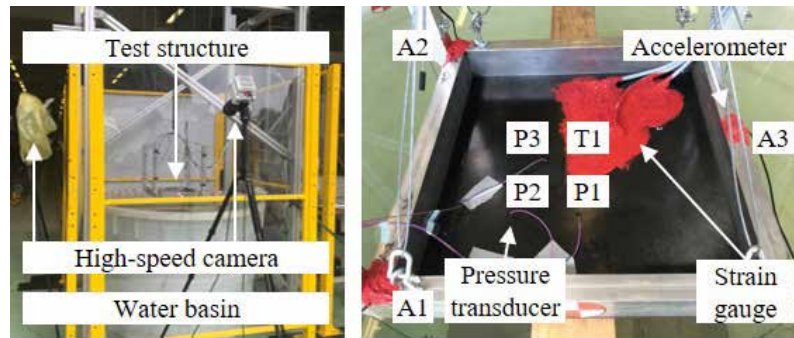


Figure 1: Test setup and test structure with instrumentations.

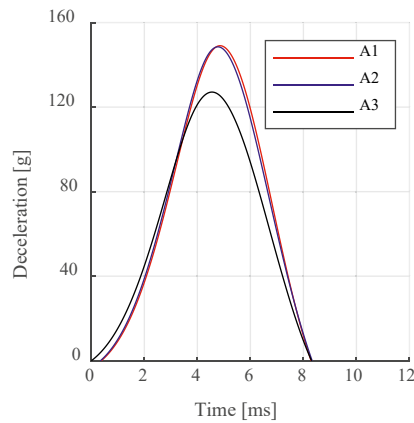


Figure 2: Deceleration curves measured during a 3-meter height water impact.

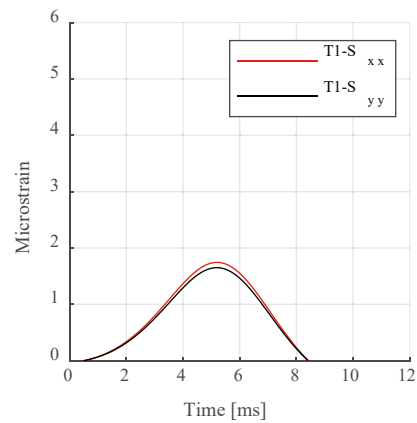


Figure 3: Strain curves measured during a 3-meter height water impact.

References

- Bisagni C, Pigazzini MS. Modelling strategies for numerical simulation of aircraft ditching. *Int J Crashworthiness* 2018;23:377–94.
- Anghileri M, Castelletti L-ML, Francesconi E, Milanese A, Pittofrati M. Survey of numerical approaches to analyse the behavior of a composite skin panel during a water impact. *Int J Impact Eng* 2014;63:43–51.
- Siemann MH, Langrand B. Coupled fluid-structure computational methods for aircraft ditching simulations: Comparison of ALE-FE and SPH-FE approaches. *Comput Struct* 2017;188:95–108.
- Climont H, Pastor G, Viana JT. Experimental ditching loads on aeronautical flexible structures. *Proceedings of the International Forum of 2017; IFASD–2017–45*.
- Spinosa E, Iafrati A. Experimental investigation of the fluid-structure interaction during the water impact of thin aluminium plates at high horizontal speed. *Int J Impact Eng* 2021;147:103673.

3rd International Conference on Impact Loading of Structures and Materials
ICILSM 2022

Using machine learning to analyze and design low-density foam for impact energy absorption

Feng Zhu^{a, b, *}, Runzhou Zhou^a, Zaihan Yang^c

^aHopkins Extreme Materials Institute, Johns Hopkins University, 3400 N Charles St, Baltimore, MD 21218, USA

^bDepartment of Mechanical Engineering, Johns Hopkins University, 3400 N Charles St, Baltimore, MD 21218, USA

^cDepartment of Mathematics and Computer Science, Suffolk University, 73 Tremont St, Boston, MA 02108, USA

Abstract

Low-density cellular solids such as metallic or polymeric foams are excellent energy absorbers and have been widely applied as impact energy absorbing devices. Their microstructures offer the ability to undergo large plastic deformation at nearly constant stress and thus can absorb large amounts of kinetic energy before collapsing to a more stable configuration or fracture. To further improve their performance, it is imperative to develop a systematic design method, to control the behavior of microstructures by tuning their geometric parameters, especially for those with irregular, random shapes.

In this work, a machine learning algorithm is combined with the finite element (FE) modeling to analyze and design open cell foams for absorbing impact energy. The foam geometry is constructed based on a large number of core points and convex polygons, known as the Voronoi diagram. In this work, 400 core points are generated in a $100 \times 100 \text{ mm}^2$ space to determine the location and shape of each individual cell. 20 design instances are created by adjusting the positions of these core points and then their corresponding Voronoi polygons to represent the 2D geometry of open cell foam. If all these core points are used as design variables, there are 800 ($= 400 \times 2$) dimensions for one design instance. It is not practical to design such a high dimensional system using either analytical solutions or traditional numerical optimizations. To address this issue, a machine learning approach, namely Principal Component Analysis (PCA) is used to significantly reduce the dimension of design space. PCA is a statistical technique used in many areas for data compression and recently has been successfully applied to design thin-walled energy absorbing structures with high dimensional design variables. In this method, when many data dimensions in the original data set are correlated, the first few principal components (PC) can contain the most variance of the entire dataset, so the data dimensions with less variance can be eliminated with minimal loss of information. In the present study, the geometry vector for each foam design instance is represented by a 20×800 geometry matrix $\mathbf{D}_{n \times m}$. Here, $n=20$ and $m=800$. In a general form, $\mathbf{D}_{n \times m}$ can be decomposed as

$$\mathbf{D}_{n \times m} = \bar{\mathbf{D}}_{n \times m} + \mathbf{S}_{n \times m} \mathbf{P}_{m \times m} \quad (1)$$

where each row of $\bar{\mathbf{D}}_{n \times m}$ is the mean vector of matrix $\mathbf{D}_{n \times m}$. $\mathbf{S}_{n \times m}$ is termed as PC scores (PCS) matrix and $\mathbf{P}_{m \times m}$ is the PC matrix representing the eigenvectors of $\mathbf{D}_{n \times m}$. Each unit eigenvector is orthogonal to each other and the sequence of eigenvectors in $\mathbf{P}_{m \times m}$ represents the order of deviation in that direction, which means that the first unit eigenvector defines the direction with the largest deviation from the mean of the original dataset. Using a small number of eigenvectors, for example, the first k ($k < n$), the original dataset can be represented with lower dimensional variables as

* Corresponding author. Tel.: +1-410 516 6785; fax: +1-410 516 7254
E-mail address: fzh8@jhu.edu

$$\mathbf{D}_{n \times m}^* = \bar{\mathbf{D}}_{n \times m} + \mathbf{S}_{n \times k} \mathbf{P}_{k \times m} \quad (2)$$

where $\mathbf{D}_{n \times m}^*$ is the approximation of the initial geometry dataset of the foam by its first k principal components. $\mathbf{S}_{n \times k}$ and $\mathbf{P}_{k \times m}$ are the first k columns and rows of PCS and PC matrices, respectively. The geometric differences between each sample in the initial geometry dataset can be presented by the different values in $\mathbf{S}_{n \times k}$. So changing the value of each PCS will move the locations of core points and then change the geometry of cells. Therefore, these PCSs can be used as the design variables to replace core points in the microstructure shape design to achieve the dimension reduction. The modified geometric model can be reconstructed by the inverse process of PCA with the selected k PCS and PCs. In the current case, the results show that the first 16 PCSs represent more than 90% of the cumulative variance of geometry. Then k is taken as 16. In this way, the dimension of design variables has been reduced from 800 to 16. The reconstructed core points and cells are compared with the original in Figure 1a and 1b, respectively. A high degree of agreement before and after PCA verifies this method.

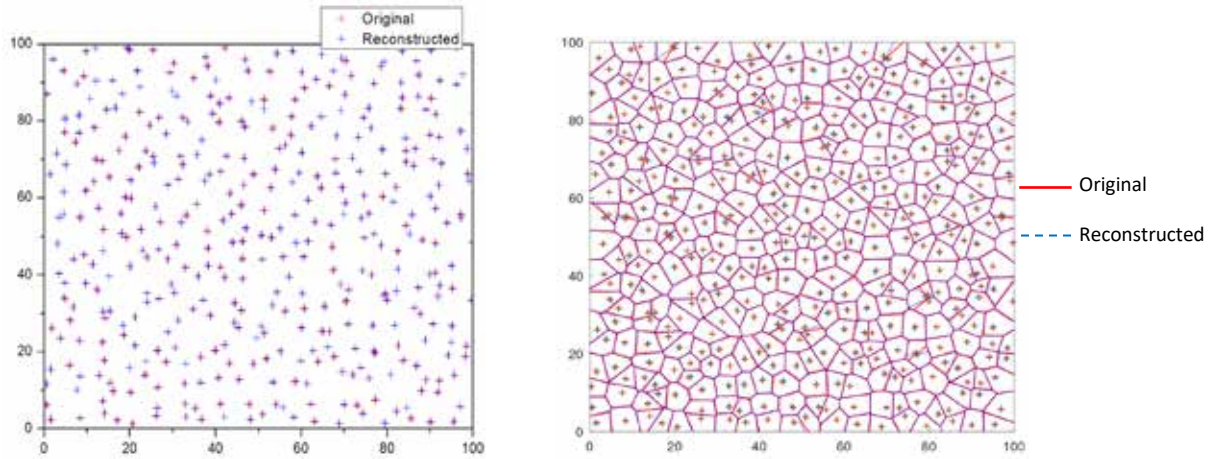


Figure 1. Comparison of the original foam design and the reconstructed after PCA: (Left) Core points; (Right) Voronoi diagram for foam geometry

Next, the Voronoi diagram for each of the 20 foam design instance is converted to a 2D finite element model (Figure 2), to simulate the crush loading response and calculate the corresponding plateau stress. The original and new design variables (i.e. core points and PCSs) as well as the simulation results form a simulation dataset.

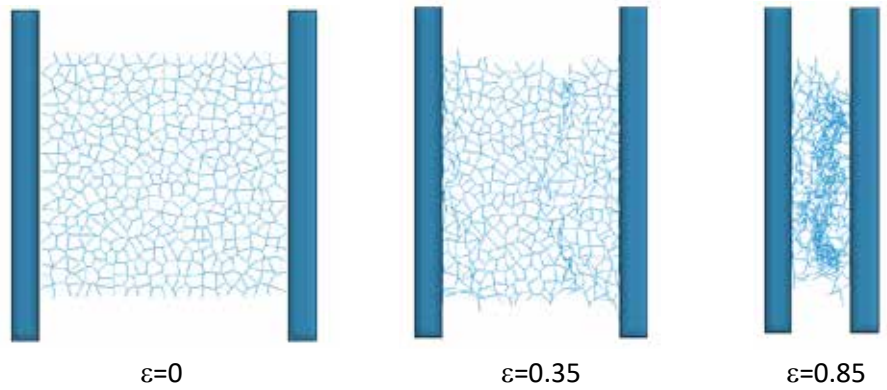


Figure 2. Model simulated deformation process of a 2D open cell foam subject to uniaxial crush loading

With the simulation dataset, a liner regression function is used to establish the relationship between the structural response (i.e. plateau stress) and reduced design variables (i.e. PCSs). Using this equation, for any given plateau stress value, the corresponding PCSs can be predicted, and the corresponding geometry of the open cell foam can be constructed. The results of case study in this work demonstrated that proposed method is able to significantly reduce the dimension of design variables for complex structures. It may be used as a general approach to effectively and efficiently design the cellular energy absorbers with stochastic, truss-type microstructures (such as open cell foams) at relatively low computational cost.

3rd International Conference on Impact Loading of Structures and Materials
ICILSM 2022

The effective width and fold size of thick square tubes under axial loading

Nima Jafarzadeh Aghdam^{a,*}, Kai-Uwe Schroeder^a

^a*Institute of Structural Mechanics and Lightweight Design, RWTH Aachen University, Wüllnerstr. 7, 52062 Aachen, Germany*

Abstract

The effective width of the plates is used widely for designing plates under compression loading. Even though there are some papers in the literature on this topic, there are just a few papers about the effective width of thick plates that undergo plastic buckling. In this study, experimental and numerical tests have been done on aluminum (Al) square tubes. Square tubes can be considered as four connected plates. It is shown that the fold length of the plate is directly related to the effective width of the plate. It is revealed numerically and experimentally that the fold length to width ratio of the thick plates is almost constant. Then it is proved analytically that the ratio should be between 0.5 and 0.63 for the progressively-buckled tubes.

Introduction

By initiation of the buckling in plates, stress decreases at the mid-side of the plate and increases at the sides of the plate. The width of the plate that still bears the stress is named the effective width of the plate. The effective width concept proposed by Von Karman et al. is the most famous method to resolve plate buckling problems theoretically [1]. Some methods to calculate the effective width are introduced by several researchers, however, these methods mostly are for elastic buckling of the plates and they cannot be used for precise calculation of the effective width of plates buckling plastically. Square tube is considered as four connected plates. In this research buckling of thick square tubes under impact load is studied and equations for calculating fold length and effective width of the tube have been extracted.

Finite Element simulation and experimental testing

A square, 40 mm x 40 mm, tube made of aluminum 6060 is used for the drop tower test. The height and thickness of the tube are 250 mm and 2 mm respectively. A drop mass of 162 kg is released from 3.3 m on the tube. Using two piezoelectric accelerometers and a laser sensor for extracting the force-displacement diagram. Finite element (FE) simulation of the tube is performed by the Explicit solver of ABAQUS. By mesh convergence analysis, the mesh size of 1.25 mm was chosen for shell elements of the model. A good agreement between the numerical and experimental test results could be obtained (Fig.1). The average fold length of a tube can be extracted by dividing the length of the tube by the number of folds. Therefore, after validation of the FE model, to have a better estimation of the fold size 400 mm long tube was considered for the simulations. It should be noted that the tube length does affect the fold size of a progressively buckled tube [2]. All other parameters of the tubes are kept as before. To study the effects of the material on the effective width and fold size of the tube different material cards have been defined.

Result and discussion

In the conducted experiment, the tube has 11 folds (Fig.1) which results in a 0.58 fold length to width ratio. In inextensional folds, the crests and the valleys of the buckles appear alternately in the adjacent side planes of the tube [1]. Performing parametric studies on the tube showed that the thickness and length of the tube do not play any significant role in its fold length [2]. However, the width showed a high effect on the fold length. By conducting a parametric study, it was observed that even though the width affects the fold length significantly, the extracted fold length to tube width ratio was constant, i.e. 0.58, for a wide range of the tube widths. The material effect was also studied on the

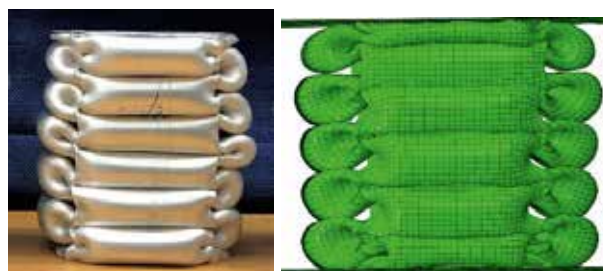


Figure 1. Experiential test result and FE simulation of Al tube

* Tel: +49 241 80 96651 ; fax: +49 241 80 92230
Email: nima.aghdam@sla.rwth-aachen.de

extracted ratio. Three new elastic-ideal plastic materials with the same elastic modulus of Al and different yield stresses of 70, 150 and 201.5 MPa were considered. The extracted fold length to width ratio of the tubes was 0.58. This is an interesting outcome and it can provide useful information for analyzing the crush behavior of the tubes.

(Fig.2) shows longitudinal stress distribution on the first fold, along the width of the tube's plate, at different time steps. The effective width region at two sides of the plate is obvious by the initiation of the folding. The region at the middle of the plate is named mid-plate. It is revealed by the initiation of the buckling the mid-plate of the tube is buckled with a width to length ratio of one, which belongs to minimum plate buckling coefficient, K , in Eq.1 [3] for plates with simply supported boundary condition (BC)! E , ν , t and b are Young's modulus, Poisson's ratio, thickness and width of the plate respectively.

The explanation of the phenomenon is related to the plastic buckling of the plate. In plastic buckling due to a severe decrease of the tangent modulus, the BC of the plates are changed, which can be the key for analyzing and extracting the effective width of the plate. The high effect of not loaded edges of the plate under axial impact load has been reported by many researchers. BC of the tube's plates cannot be considered clamped even though some moments are transferred at the sides of the plate. On the other hand, BC of these plates cannot be considered completely simply supported either. By increase of the stress beyond the yield point the plate losses its capacity in transferring moment from sides to the mid part of it. Consequently, this mid-plate part behaves separately than the side-plates (the effective width region), which have stiffer BC. It can be considered by removing moment transferring capacity, the clamped BC is changed to simply supported BC at mid-plate. That is the reason why the width to fold length ratio of the mid-plate is always one. Even though neither simply supported nor clamped BC is not a precise assumption for the plates of the tube, buckling-load-shift of the plates due to the transition of the BCs provides useful information. By considering a four-side clamped plate K value can be calculated [3]. Later the equivalent width, b_{eq} , of a four-side simply supported plate in order to have the same buckling stress can be calculated (Eq.2).

$$\sigma = K \frac{\pi^2 E}{12(1-\nu^2)} \left(\frac{t}{b}\right)^2 = \frac{K}{b^2} \cdot A \quad (1)$$

$$\frac{K_{cl}}{b_{cl}^2} = \frac{K_{ss}}{b_{eq}^2} \rightarrow \frac{K_{ss}}{K_{cl}} = \left(\frac{b_{eq}}{b_{cl}}\right)^2 \quad (2)$$

By considering the width to length ratio of the fold between 0.5 and 1, since fold length more than width length of the tube is not possible in plastic buckling, b_{eq}/b_{cl} can be calculated (Eq.3). Which fits very well by experimental and numerical results i.e. $b_{eq}/b_{cl} = 0.58$.

$$0.5 < \frac{b_{eq}}{b_{cl}} < 0.63 \quad (3)$$

It should be noted that the calculated ratio is for the plastic buckling of tubes with the inextensional folding pattern.

Conclusion

The results of this study show that by the increase of stress beyond the yield point, the moment cannot be transferred to the mid-side of the plates from the sides anymore, which results in a transition to simply supported BC for the mid-side of the plate and sudden buckling of it. It was revealed that the effective width of the tube has an important effect on defining the fold length of the tube that buckles plastically. By the provided information, the fold length of a tube that buckles plastically can be calculated with good accuracy, and the fold length to the tube's width ratio is between 0.5 and 0.63. Furthermore, it was shown that the effective-width to width ratio of thick plates is between 0.37 and 0.5.

References

1. Chen D-h. Crush mechanics of thin-walled tubes. CRC Press. 2015.
2. Aghdam NJ, Tatikonda UBC, Bühring J, Mekala NR, Schröder K-U. Impact of thin-walled square aluminum tubes. Proc. Appl. Math. Mech. 2019. doi:10.1002/pamm.201900395.
3. Schulz, Handbuch Struktur Berechnung(HSB)(IASB, 2015), 45111–04.

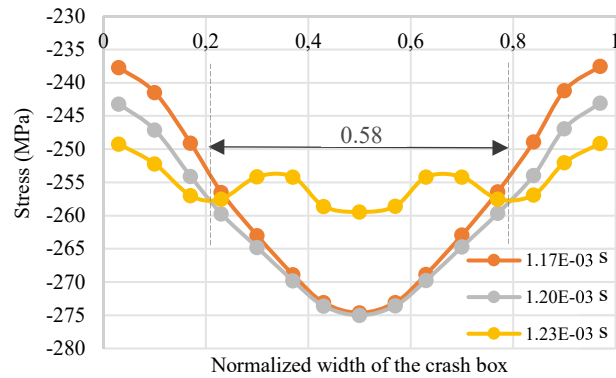


Figure 2. Longitudinal stress distribution along the width

3rd International Conference on Impact Loading of Structures and Materials
ICILSM 2022

Characterization and modelling of the fast dynamics strength of a Pa66/Aluminum SPR assembly

N. Leconte^{a,*}, B. Bourel^a, F. Lauro^a, E. Markiewicz^a

^aUniv. Polytechnique Hauts-de-France, CNRS, UMR 8201 - LAMIH, Valenciennes F-59313, France

Abstract

The self piercing riveting (SPR) process is increasingly used in the automotive industry due to its ability to connect multi-materials for weight reduction considerations. The strength and failure of such multi-material assemblies need to be characterized and modelled for full-scale structural computations.

An aluminum/PA66 2-sheet SPR assembly is characterized in pure and mixed tensile/shear single connection Arcan experiments.

The evolution of the peak force and dissipated energy with the loading angle are evaluated. Loading velocities in the range 0.016 mm/s - 100mm/s are tested. The failure modes of aluminum-Pa66 SPR assembly are compared to that of metallic SPR assemblies.

Experiments are also carried out on a single hat component with multiple connections for two loading rates: 5mm/s and 1500 mm/s. The evolution of the peak force and dissipated energy with the loading angle are evaluated. The loading experienced by the connections is checked.

A connector model for the aluminum-Pa66 SPR assembly is proposed. The parameters are identified based on the Arcan tests and validated on the component experiments. The overall comparison between computations and experiments show satisfactory results.



* Corresponding author. Tel.: + 33 3 27 51 14 08
E-mail address: nicolas.leconte@uphf.fr

3rd International Conference on Impact Loading of Structures and Materials
ICILSM 2022

Development of a numerical model of a motorcycle helmet for the investigation of road traffic accidents

Henrique Ramos^{a,b,*}, Rafael Santiago^{a,b}, Marcilio Alves^a

^aDepartment of Mechatronics and Mechanical Systems Engineering, Group of Solid Mechanics and Structural Impact, University of Sao Paulo, Brazil

^bTechnology Innovation Institute, Advanced Materials Research Center, Abu Dhabi, United Arab Emirates

Abstract

The most vulnerable part of a motorcyclist during a road traffic accident is the head, being the helmet considerably effective to mitigate brain injuries. This research aims to develop a finite element (FE) model of a helmet impact test, to be used for further investigations based on user-centred protective helmets designs. A commercial helmet was tested in a helmet testing rig and used to develop a representative full-face helmet design. The helmet geometry was imported into LS-Dyna and coupled with a standardized human headform to obtain the resulting acceleration transmitted to the head. Helmet impact simulations were developed under similar conditions to the experimental procedure. Peak linear acceleration and impact duration of the headform were recorded and compared. A good correlation between the numerical model and experimental data was observed. The proposed method and procedure could be used in further evaluation to optimize motorcyclist helmets impact performance towards diminishing brain injuries caused by accidents.

Introduction

Traumatic Brain Injury (TBI) is the leading cause of severe and fatal injuries to a motorcyclist [1,2]. The primary protective and the most effective element for reducing TBI severity is the standard certified helmet [3]. A commercial motorcycle helmet is formed by a rigid outer shell, protective padding, comfort padding, and the retention system, as shown in Figure 1a. The inner protective padding and outer shell are responsible for absorbing the impact energy in a crash condition. Commercial helmets use a rigid expanded polystyrene foam (EPS) as inner padding to absorb the impact energy by reducing the linear head acceleration. In combination with an outer shell, this standard EPS helmet is highly effective in minimizing risks of skull fracture, penetration injuries, and TBI. Although, recent studies highlighted that concussions and TBI could readily be caused by rotational head acceleration, which subjects brain tissues to shear forces and results in diffuse axonal injury [4]. Many types of helmets are available in the market, whereas the development of protective helmets for linear and rotational acceleration demands further investigations, given the current paucity of information.

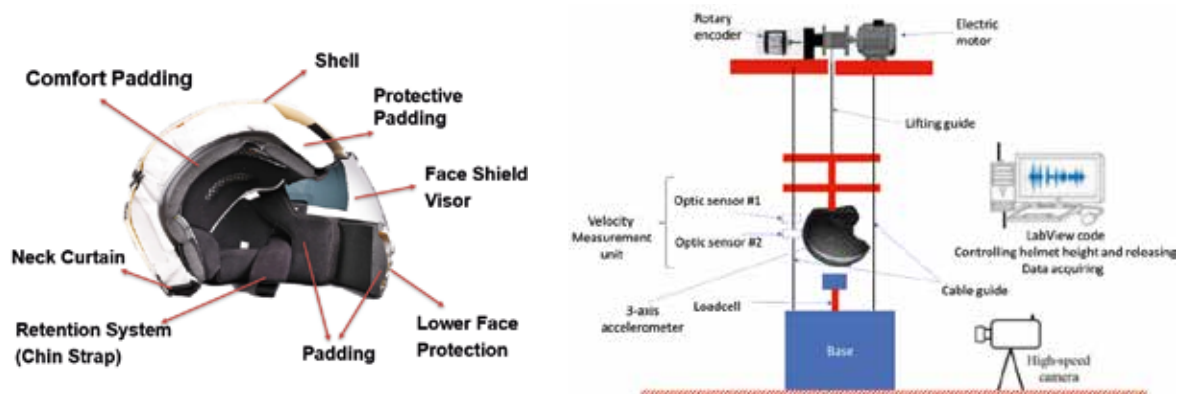


Figure 1 – (a) The Anatomy of a Motorcycle Helmet and (b) the schematic presentation of the Helmet testing Machine.

Materials and Methods

Tests were conducted according to the NBR-7471 standard at the Helmet Impact Machine (HIM), developed by the Group of Solid Mechanics and Structural Impact (GMSIE) from the University of Sao Paulo. A tri-axis accelerometer, Kistler 8763B, was instrumented at the centre of gravity of the headform to record the acceleration history at a sample rate of 20 kHz in a data acquisition system (NI- PCI-6110, National Instruments, US). A Photron SA5 (Imagina Group Inc., Japan) high-speed camera

* Corresponding author. Tel.: +971 55 193 9133.
E-mail address: henriqueros@usp.br

was also used at the rate of 3k frames per second. Figure 1b shows the experimental setup at the HIM. The experimental tests were conducted in an EBF-E8 helmet fitted in a metallic headform. The coupled system was impacted in two impact locations (i.e., Superior and Lateral left, being released from the HIM system at the height of 2.5 m, leading to an initial velocity of 7 m/s impacts against a rigid flat anvil. A representative full-face motorcycle helmet was designed, Figure 2a, and pre-processed on HyperMesh (Altair HyperWorks, U.S) and then imported in LS-DYNA (Ansys, U.S.) explicit simulation code (Figure 2b). The helmet outer shell was made with a thickness of 3 mm ABS and EPS protective paddings. The elastoplastic material model (MAT_24: MAT_PIECEWISE_LINEAR_PLASTICITY) and foam material model (MAT_63: CRUSHABLE_FOAM) were adopted for the outer shell and the inner padding of the helmet, respectively [5,6].

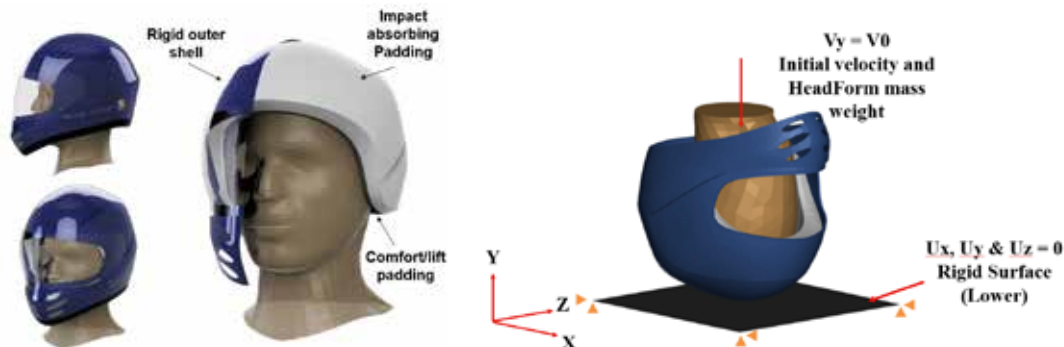


Figure 2 – (a) A representative full-face motorcycle helmet and (b) a full finite element model of a commercial helmet.

Results and Discussions

The comparative numerical-experimental results response are shown in Figures 3a and 3b. The peak linear acceleration recorded by numerical simulation was slightly similar for both impact conditions. However, it was also noticeable that the slope of the numerical simulation drop was steeper than those of experimental tests, which is more evident on the left lateral impact. It may be related to the simplified model of the helmet regarding the lack of the comfort padding not considered in the model and the surface contact definition between the helmet and the rigid headform. However, the peak acceleration presented a good correlation with experimental results, being able to predict the overall behaviour of the helmet impact response.

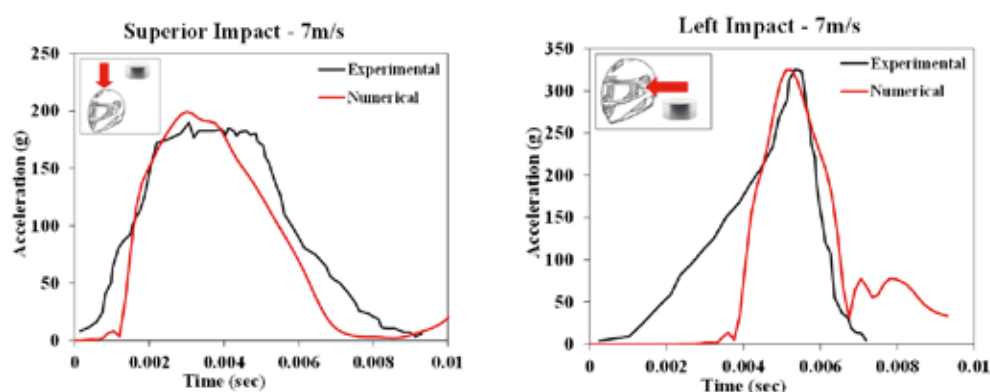


Figure 3 – Linear acceleration comparison of numerical simulation and experimental for (a) superior and (b) lateral left impact.

Conclusions

Numerical simulation and experimental drop test were conducted in a commercial helmet. The designed helmet and headform were evaluated numerically by simulating a drop helmet test into a flat anvil. Acceleration histories comparisons were carried out, showing a good correlation between the experimental and numerical. The numerical model could be used for further analysis in biomechanics analysis of traumatic brain injuries over a wide range of realistic road accident or into novel designs of motorcycle helmets to prevent linear and rotational acceleration.

Acknowledgement

The authors acknowledge the FAPESP project 2019/05444-0 for the financial support.

References

- [1] B. Chinn, B. Canaple, S. Derler, D. Doyle, D. Otte, E. Schuller, R. Willinger, COST 327 Motorcycle safety helmets, Eur. Comm. Dir. Gen. Energy Transp. (2001).
- [2] T. Gibson, K. Thai, Helmet protection against basilar skull fracture, ATSB Res. Anal. Rep. (2007).

- [3] H.H. Hurt, Motorcycle accident cause factors and identification of countermeasures, The Administration, 1981.
- [4] E. Bliven, A. Rouhier, S. Tsai, R. Willinger, N. Bourdet, C. Deck, S.M. Madey, M. Bottlang, Evaluation of a novel bicycle helmet concept in oblique impact testing, *Accid. Anal. Prev.* 124 (2019) 58–65.
- [5] L. Jiang, H. Hu, Finite element modeling of multilayer orthogonal auxetic composites under low-velocity impact, *Materials (Basel)*. 10 (2017) 908.
- [6] C. Ling, P. Cardiff, M.D. Gilchrist, Mechanical behaviour of EPS foam under combined compression-shear loading, *Mater. Today Commun.* 16 (2018) 339–352.

3rd International Conference on Impact Loading of Structures and Materials
ICILSM 2022

Simulation of a 1000 MPa Front Side Frame

Suh Ho Lee^a, Matt Tummers^a, Michael Worswick^a, Skye Malcolm^b

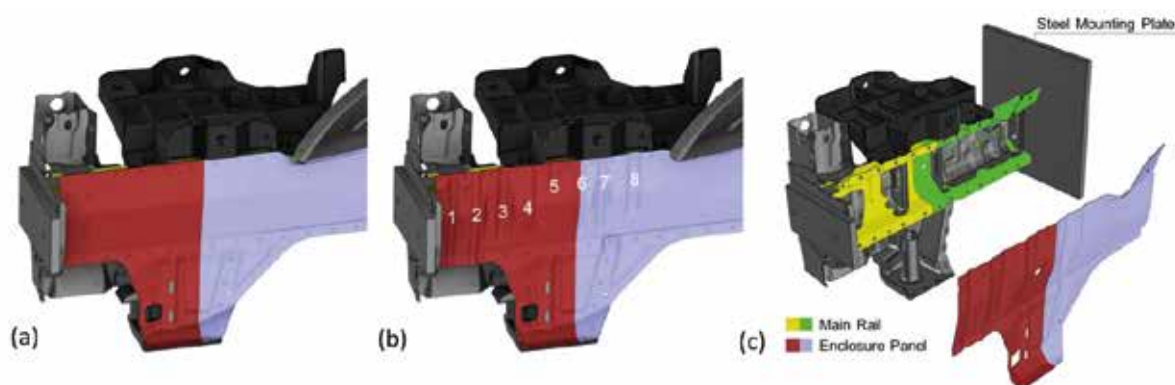
^aUniversity of Waterloo, Waterloo, Ontario, N2L 3G1, Canada

^bHonda Development & Manufacturing of America, Raymond, Ohio, USA

Abstract

Numerical simulation has been undertaken of the axial crush response of a side frame member fabricated utilizing a hot stamped steel, Ductibor® 1000-AS. This alloy has a tensile strength in excess of 1,000 MPa and good ductility [1]. Of particular interest was the potential reduction of the component weight, relative to the current JAC590R commercial build, while ensuring good crush and energy absorption characteristics without cracking or spot weld failure.

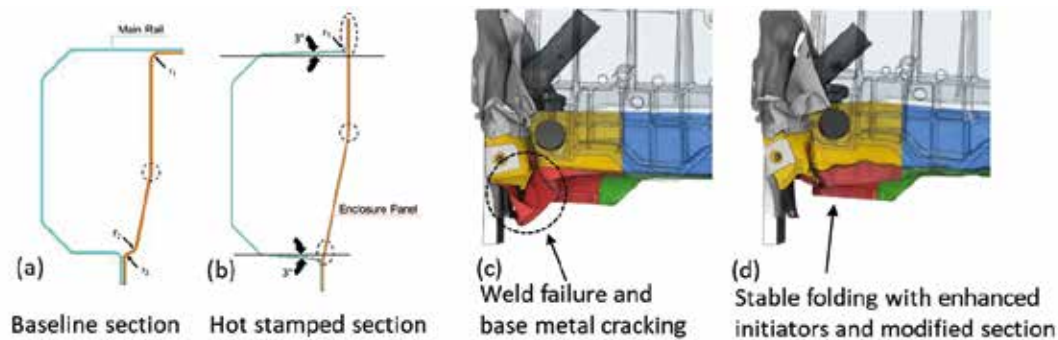
The figure below (a) shows the initial geometry of the side frame member assembly [2]. Two hot stamped components, referred to as the main rail and enclosure panel, as shown in the exploded view (c) were introduced into the assembly and replaced the existing cold formed JAC590R components. Tailor welded blanks (TWBs) were used with thicknesses of 1.0 and 1.2 mm at the front and rear sections. These values were selected based on initial analytical estimates and resulted in a weight reduction of 28% relative to the JAC590R build. A number of internal bulkheads, brackets and the battery tray were considered, that are part of the current commercial side frame assembly. In addition to the current simulation effort, the assembly shown in (c) was fabricated and tested, as described in [2].



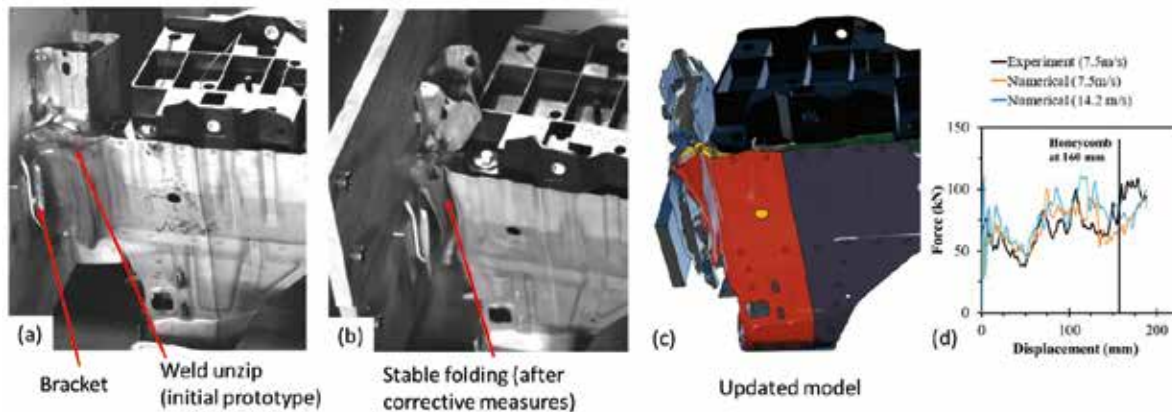
The numerical simulations of the crush response were performed using LS-DYNA with a rate-sensitive constitutive response and a GISSMO damage model utilizing a triaxiality-dependent fracture *locus* [1]. The impact mass and initial velocity were 7.5 m/s and 855.5 kg, respectively. A *MAT_Spotweld_Damage_Failure spot weld treatment was considered.

Initial simulations revealed that a simple material substitution of the hot stamped Ductibor® 1000-AS sheet resulted in excessive spot weld failure and parent metal failure, as can be seen in the figure below (c). In order to address this issue, the original cross section (a) was modified to better approximate a single hat section (b), since this profile is better able to fold in a stable fashion. In addition, a large number of simulations were performed in which fold initiators were added (figure above,

b) to promote stable, serpentine folding of the lower and upper flange (d), that served to suppress the predicted extent of weld and parent metal cracking. Based upon these predictions, prototype versions of the crush tip were fabricated and tested.



Unfortunately, the initial tested prototypes exhibited excessive levels of spot weld failure (figure below, a). The root cause of the issue was the rather strong front bracket (labeled in a) that did not fold as predicted and acted as wedge, causing the spot weld flanges to unzip. Modifications to the bracket and improvements to the spot welding procedures (increased nugget size) and weld strength were shown to result in stable folding (b), as described in [2]. This improved behavior was also captured in updated models (c) incorporating the modified bracket geometry and increased spot weld strength. The predictions of force-displacement during crush (d) are also seen to agree reasonably well with experiment.



The current study and results in [2] serve to demonstrate the strong potential for use of 1,000 MPa hot stamped steels within frontal crash safety structures. As discussed in [2], the energy absorption of the tailor-welded hot stamped side frame member dropped below that of the current production JAC590R side frame, likely due to the cross section changes, shown above, that were introduced after the initial thickness selections. Future work should address improved final thickness selections such that the prototype energy absorption more closely matches the production component. The extent of fracture and spot weld failure in this high strength alloy highlights the importance of accurate CAE predictions to support optimization and validation prior to deployment in safety-critical applications. To this end, the current study comprised a successful material substitution exercise in which modifications to the topology of the production parts were limited by the need to maintain assembly compatibility. Design of a hot stamped side frame as part of a “clean slate”, new build may offer further opportunity for weight reduction, while reducing tendency towards weld and base metal failures.

References

1. Lee, S.H., On the Development of Fold Initiator Patterns to Promote Progressive Folding of Hot Stamped Ultra-High Strength Axial Crush Structures, MASc thesis, University of Waterloo, 2021, <http://hdl.handle.net/10012/17114>.
2. Lee, S.H., *et al.*, Development of a 1000 MPa Hot Stamped Crush Tip, Proceedings CHS2, Barcelona, Spain, May 30-June 2, 2022.

3rd International Conference on Impact Loading of Structures and Materials
ICILSM 2022

Novel test for characterizing resistance spot weld group assemblies under shear loading

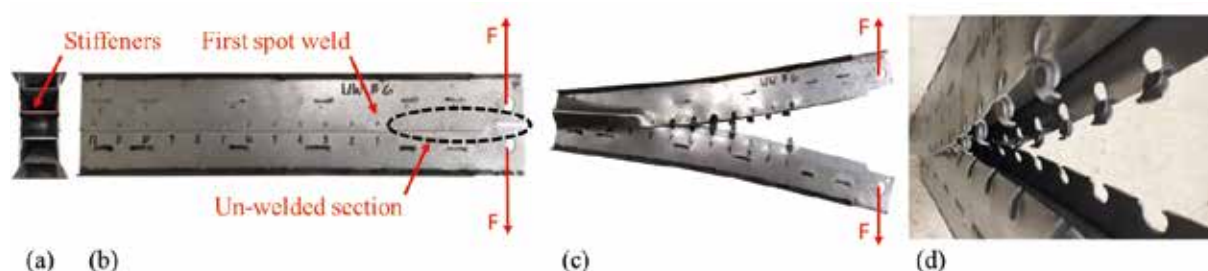
Cameron Tolton^{a,*}, Jose Imbert-Boyd^a, Michael Worswick^a, Skye Malcolm^b

^aUniversity of Waterloo, 200 University Ave W, Waterloo, Ontario, N2L 3G1, Canada

^bHonda Development & Manufacturing of America, Raymond, Ohio, USA

Abstract

Significant interest exists within the automotive crash safety community in developing accurate models of spot weld failure, particularly within welded connections comprising groups of welds. Published work that considers failure of groups of welds includes the T-connection experiments by Yang *et al.* [1] and the recent mode I Caiman experiments by O’Keeffe [2]. In this work, the failure behaviour of spot welded connections is investigated in components fabricated using two different 1.2 mm Al-Si hot stamped steels, Ductibor[®] 500-AS and Usibor[®] 1500-AS, with tensile strengths of 600 and 1500 MPa, respectively. A novel experiment, termed the Mode III Caiman test, was developed to characterize the propagation of weld failure within groups of welds under *predominantly shear loading conditions*. The Mode III Caiman specimen, seen in the figure below (a and b), comprises two overlapping U-channel assemblies, incorporating inner stiffeners to maintain stability [3]. For quasi-static testing, the channels are spot welded together and one end of the specimen is left un-welded (b). The channels are pulled apart in a tensile frame (c) resulting in shear failure that propagates along the line of spot welds (d). For dynamic testing, a fixture has been developed using a crash sled to examine weld failure under rates that are representative of impact loading during a vehicle crash scenario. This new test has proven useful to promote progressive weld failure and characterize the loads and absorbed energy, while accounting for load sharing within weld groups, under shear loading for quasi-static and high-rate dynamic test conditions.

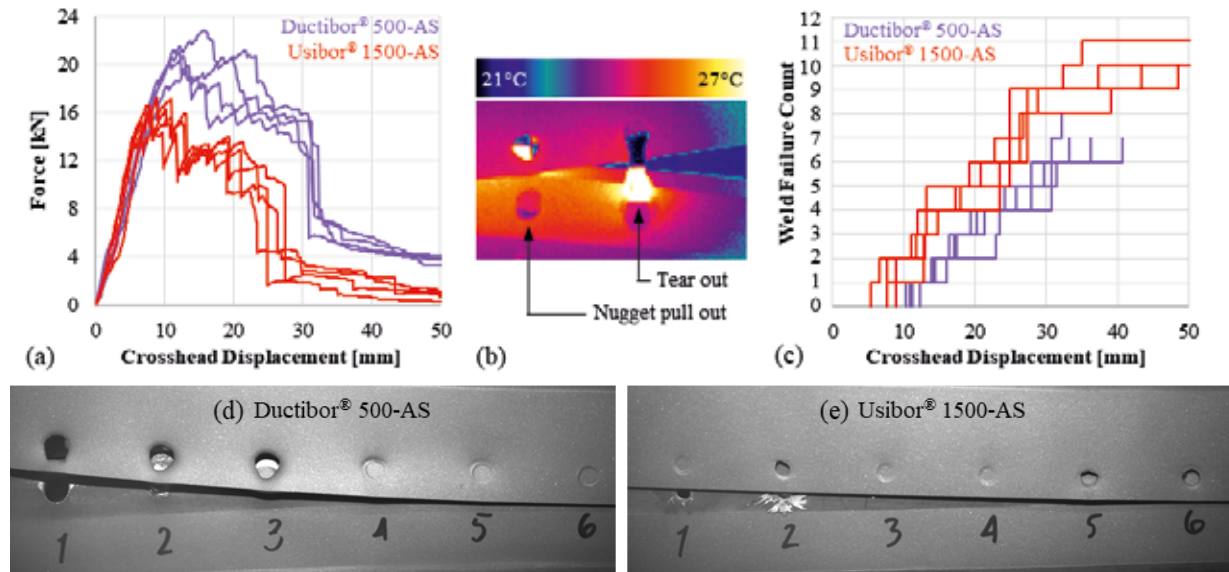


Mode III Caiman experiments were performed under quasi-static and dynamic loading conditions to examine the mechanical properties of spot welds in a structure in which the applied load can be shared across multiple spot welds. The quasi-static force *versus* displacement curves for the two alloys, shown in the figure below (a), show a similar response but with the Ductibor[®] 500-AS material having consistently higher loads throughout the tests, in contrast to the relative ranking of the base metal strengths. The sudden drops in load correspond to the failure of individual spot welds which were detected using high speed thermal imagery (b) to capture the heat associated with the intense local plastic work during failure in both the quasi-

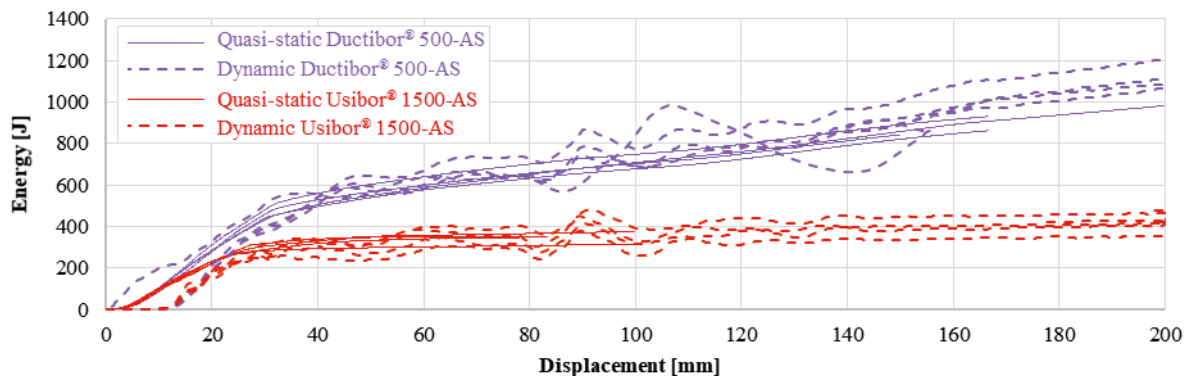
* Corresponding author.

E-mail address: cjtolt@uwaterloo.ca

static (c) and the dynamic Mode III Caiman experiments. Spot weld failure timing was recorded to characterize the extent and rate of spot weld failure propagation in the Mode III Caiman experiments. The Ductibor® 500-AS (d) exhibited a slower rate of failure propagation through the weld group (for a given cross head displacement) compared to Usibor® 1500-AS (e), which is attributed to the increased parent metal ductility, differences in spot weld failure mode and toughness, and presence of expulsion [4].



The measured absorbed energy versus displacement from the dynamic (and static) Mode III Caiman experiments are shown in the figure, below. The higher energy absorption of the Ductibor® 500-AS samples is evident in the figure and is attributed to the higher strength and toughness of the Ductibor® 500-AS spot welds, consistent with single spot weld testing by Tolton [3]. The higher toughness of the Ductibor® 500-AS spot welds delayed propagation of failure along the weld line, dramatically increasing the energy absorption. Interestingly, the absorbed energy in the static and dynamic tests is similar for each alloy, as is the rate of weld failure propagation with respect to cross head displacement (not shown for brevity).



The current work has demonstrated that the Mode III Caiman shear experiment provides a useful approach to study the propagation of spot weld failure within weld groups. The current results are interesting in that the ranking of the mechanical performance of the Caiman samples, in terms of both strength and energy absorption, was the opposite of the ranking of the parent metal strengths. On-going work addresses the use of the Mode III (and Mode I) Caiman test for CAE validation of spot weld models.

References

- [1] Y. P. Yang, J. Gould, W. Peterson, F. Orth, P. Zelenak, and W. Al-Fakir, "Development of spot weld failure parameters for full vehicle crash modelling," *Sci. Technol. Weld. Join.*, vol. 18, no. 3, pp. 222–231, Apr. 2013, doi: 10.1179/1362171812Y.0000000082.
- [2] C. O'Keeffe *et al.*, "Examination of mode 1 loading on resistance spot weld groups in tailored hot stampings," in *Procedia Engineering*, 2017, vol. 197, pp. 294–303, doi: 10.1016/j.proeng.2017.08.107.
- [3] C. Tolton, "Characterization of Spot Weld Failure within Weld Groups under Predominantly Shear Loading," MASC thesis, University of Waterloo, 2020, <http://hdl.handle.net/10012/16487>.
- [4] A. Mohamadizadeh *et al.*, "Spot weld strength modeling and processing maps for hot-stamping steels," *Weld. J.*, vol. 98, no. 8, pp. 241S–249S, 2019, doi: 10.29391/2019.98.021.

3rd International Conference on Impact Loading of Structures and Materials
ICILSM 2022

The Virtual Fields Method for Reconstruction of Impact and Blast Loading

Rene Kaufmann^{a*}, Sindre Nordmark Olufsen^{a,b}, Egil Fagerholt^{a,b}, Vegard Aune^{a,b}

^aStructural Impact Laboratory (SIMLab), Department of Structural Engineering, NTNU - Norwegian University of Science and Technology, NO-7491 Trondheim, NORWAY

^bCentre for Advanced Structural Analysis (CASA), NTNU, NO-7491 Trondheim, NORWAY

Abstract

The development of blast-resistant structures requires detailed knowledge of the blast-structure interactions that occur during impact (Kambouchev, Noels, & Radovitzky, 2007) (Rigby, Tyas, & Clarke, 2015) (Rigby, et al., 2016). Experimental techniques like 3D-DIC allow time-resolved, full-field measurements of deformations on structures both in experimental settings and *in situ*. The measurement of surface loads however usually relies on pointwise approaches on nearly non-deformable structures using pressure transducers or load cells. These allow validations of numerical or analytic models, but they only provide low spatial resolution and are intrusive. Therefore, they are not well suited for the investigation of blast-structure interaction problems. Available full-field techniques on the other hand are generally limited in terms of their applicability. Particle image velocimetry (PIV) and particle tracking velocimetry (PTV) are well established techniques that allow pressure reconstructions from velocity fields but require optical access to the flow field (de Kat & van Oudheusden, 2012) (Schneiders, Caridi G.C.A., & Scarano, 2016). For blast environments, and particularly when investigating fluid-structure interaction (FSI), this is challenging for the flow close to the surface of a flexible structure. Pressure sensitive paints (Beverley & McKeon, 2007) can be used for surface pressure measurement, but they require optical access to the pressure side of the surface, which is often difficult in blast environments.

Obtaining full-field loading information from non-contact measurements on the surface side that is not exposed to the blast would provide new insights into the dynamic interaction between structure and fluid during blast impact. The present study addresses this opportunity by using the mechanical equilibrium equations to reconstruct surface loads from deformation measurements on a thin, flat steel plate impacted by blast waves. Restricting experimental conditions to yield limited deflections such that the investigated steel plates behave as thin plates in pure bending allows employing the Kirchhoff-Love theory which yields a simplified description of the plate equilibrium. The key challenge in this approach is that it involves fourth order spatial derivatives and second order temporal derivatives of the deflections, which make it susceptible to the influence of experimental noise. The virtual fields method (VFM) was demonstrated to be a promising technique to address this issue. The VFM is an application of the principle of virtual work and utilizes full-field deformations and material constitutive mechanical parameters to extract load information or *vice versa* (Pierron & G  diac, 2012). The present study utilizes a piecewise VFM approach to obtain spatially resolved load information. Optical deformation measurements were realised using a deflectometry setup. Deflectometry is a highly sensitive optical technique that allows slope measurements on reflective surfaces. Deflectometry and the VFM were previously combined to reconstruct dynamic mechanical point loads problem (O'Donoghue, Robin, & A Berry, 2017) and pressure from air jets impinging on a thin, glass mirrors (Kaufmann, Pierron, & Ganapathisubramani, 2019-1) (Kaufmann, Ganapathisubramani, & Pierron, 2019-2), (Kaufmann, Pierron, & Ganapathisubramani, 2020). These previous studies found that the spatial features of the investigated events were captured accurately, but that the accuracy of pressure amplitudes depended significantly on the chosen virtual fields and the noise levels in experimental data. A general approach for assessing the accuracy of reconstructions using virtual experiments is proposed in (Kaufmann, Pierron, & Ganapathisubramani, 2019-1). The present study applies a similar approach as (Kaufmann, Pierron, & Ganapathisubramani, 2019-1) for surface pressure reconstruction of blast-like loading generated in shock tube experiments. The shocktube experiments are also used to address measurement uncertainty and to investigate the performance of the VFM for different levels of random noise and bias.

The deflectometry setup consisted of a Phantom v2511 camera recording at 75 kHz, a printed, cross-hatched grid with 5.9 mm pitch and a thin steel plate sample with one surface polished to a mirror-finish. The setup was placed in the dump tank of the SIMLab shock tube facility (SSTF) (Aune, Fagerholt, Langseth, & B  rvik, 2016). Using several exit blockages, different shockwave symmetries were generated to demonstrate the performance of the technique in capturing dynamic, spatially distributed loading events. The results were compared to pressure transducer measurements to evaluate the accuracy in pressure amplitude. Figures 1 and 2 show full-field pressure reconstructions of the blast impact at different instances. Figures 3 and 4 show a comparison of pressure reconstruction results and transducer measurements along a vertical line at the center of the plate. The

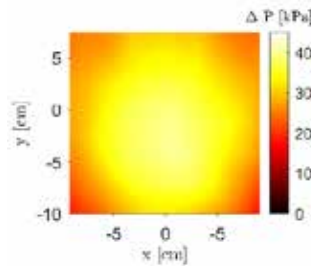


Figure 1: VFM reconstruction of pressure field at instance of peak pressure.

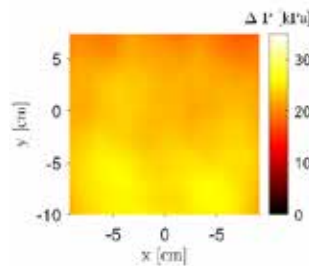


Figure 2: VFM reconstruction of pressure field 50 μ s after peak pressure instance.

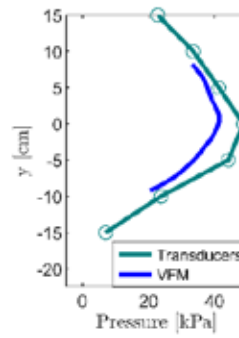


Figure 3: Comparison of VFM pressure reconstructions and transducer measurements at peak pressure instance.

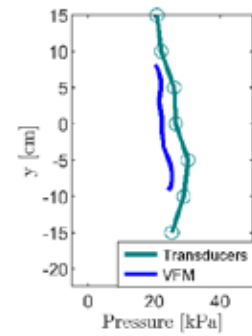


Figure 4: Comparison of VFM pressure reconstructions and transducer measurements 50 μ s after peak pressure instance.

pressure reconstructions agree well with the spatial distribution and dynamic behaviour of the pressure data obtained from transducer measurements. However, the amplitudes from reconstruction results are 10% - 20% lower than those from transducer measurements. Experimental bias originating in restricted capabilities of the deflectometry setup to obtain acceleration information from slope maps was identified as likely reason. Future research will be directed towards improving the experimental approach and to extend the reconstruction framework towards scenarios with large mechanical deformations of the investigated specimen to improve both the accuracy of the method and the application range. The presented results show that the new approach is a promising and powerful addition to existing measurement techniques in the field of blast wave research due to its capability of capturing full-field, time-resolved pressure distributions.

References

- Aune, V., Fagerholt, E., Langseth, M., & Børvik, T. (2016). A shock tube facility to generate blast loading on structures. *7(3)* 340-366.
- Berry, A., & Pierron, F. (2014). Identification of dynamic loading on a bending plate using the virtual fields method. *Journal of Sound and Vibration*, 333(26):7151 – 7164.
- Beverley, J., & McKeon, R. (2007). *Springer handbook of experimental fluid mechanics, chap 4.4, pp 188 – 208*. Springer-Verlag Berlin Heidelberg.
- de Kat, R., & van Oudheusden, B. (2012). Instantaneous planar pressure determination from PIV in turbulent flow. *Experiments in Fluids* 52(5):1089–1106.
- Kambouchev, N., Noels, L., & Radovitzky, R. (2007). Numerical simulation of the fluid–structure interaction between air blast waves and free-standing plates. *Volume 85, Issues 11–14, pp 923-931*.
- Kaufmann, R., Ganapathisubramani, B., & Pierron, F. (2019-1). Surface Pressure Reconstruction from Phase Averaged Deflectometry Measurements Using the Virtual Fields Method. *e1741-2765*.
- Kaufmann, R., Pierron, F., & Ganapathisubramani, B. (2019-2). Full-field surface pressure reconstruction using the Virtual Fields Method. *Experimental Mechanics*, 59(8), 1203–1221.
- Kaufmann, R., Ganapathisubramani, B., & Pierron, F. (2020). Reconstruction of surface-pressure fluctuations using deflectometry and the virtual fields method.
- Lagran-Wheeler, C., Rigby, S., Clarke, S., Tyas, A., Stephens, C., & Walker, R. (2021). Near-field spatial and temporal blast pressure distributions from non-spherical charges: Horizontally-aligned cylinders. *International Journal of Protective Structures (published online)*.
- O'Donoghue, P., Robin, O., & Berry, A. (2017). Time-resolved identification of mechanical loadings on plates using the virtual fields method and deflectometry measurements. *54(3):e12,258*.
- Pierron, F., & Gédiaç, M. (2012). *The virtual fields method. Extracting constitutive mechanical parameters from full-field deformation measurements*. Springer New York.
- Rigby, S., Fay, S., Clarke, S., Tyas, A., Reay, J., Warren, J., . . . Elgy, I. (2016). Measuring spatial pressure distribution from explosives buried in dry leighton buzzard sand. *International Journal of Impact Engineering* 96 (89-104).
- Rigby, S., Tyas, A., & Clarke, S. (2015). Observations from preliminary experiments on spatial and temporal pressure measurements from near-field free air explosion. *6(2): 175-190*.
- Schneiders, J., Caridi G.C.A., S., & Scarano, F. (2016). Large-scale volumetric pressure from tomographic PTV with HFSB tracers. *Experiments in Fluids* 57(11):164.

3rd International Conference on Impact Loading of Structures and Materials
ICILSM 2022

Suppression of Extra Oscillations on Impact Force Wave in Instrumented Taylor Impact Test by Pulse-shaping Technique

Chong Gao^a, Takeshi Iwamoto^{b, *}, Yoshikazu Tanaka^c, Takayuki Kusaka^d

^aGraduate School of Engineering, Hiroshima University, 1-4-1 Kagamiyama, Higashi-Hiroshima, 739-8527, Japan

^bAcademy of Science and Technology, Hiroshima University, 1-4-1 Kagamiyama, Higashi-Hiroshima, 739-8527, Japan

^cGraduate School of Advanced Science and Engineering, Hiroshima University, 1-4-1 Kagamiyama, Higashi-Hiroshima, 739-8527, Japan

^dDepartment of Mechanical Engineering, Ritsumeikan University, Kusatsu 525-8577, Japan

Abstract

1. Introduction

In Taylor impact test, linearly-changing regions of the internal force in a specimen are newly assumed in our previous work and a method for calculating the distribution of stress is established [1, 2]. From the viewpoint of nonuniform deformation, the stress-strain curve is possibly obtained by a spatial synchronization of distribution of strain and stress. So that, the stress-strain curve is measured from an instrumented Taylor impact test which the high-speed camera and Hopkinson pressure bar are introduced into the apparatus to measure the deformation profile and impact force of the specimen [1,2].

According to the measured stress-strain curve, only the result in low strain range is reliable because the excessive local deformation found near the impact surface during the high-speed impact leads our important assumption of linearly distribution of internal force become unavailable. Another reason affected the accuracy of measured results is the extra oscillations on the impact force wave due to Pochhammer [3] and Chree [4] effect. These extra oscillations propagate into the specimen and reciprocate for many times. As a result, the deformation behavior of specimen is strongly affected.

Additionally, the pulse-shaping technique is widely used in split Hopkinson pressure bar test for suppressing the extra oscillations on impact force wave and obtaining a stress-strain curve with a high accuracy [5]. Simultaneously, accompanying the suppression of extra oscillations, the decrease in the rise time of the impact force wave is inevitable [6]. Hence, challenges on a control of the rise time using pulse-shaping technique are well done [7].

In this work, a specimen with a pulse-shaper is newly designed to suppress the extra oscillations. The influence of size for pulse-shaper on suppressing the extra oscillations is discussed based on finite element simulation. Finally, the actual specimen with the designed pulse-shaper is manufactured and tested.

2. Results

Fig. 1 shows the specimen designed in this work. A tiny cylindrical pulse-shaper is established on the impact surface of specimen. In this figure, a and b show the length and diameter of pulse-shaper. b and d_0 denote the length and diameter of body for specimen, respectively. The mass and d_0 is set as the same to our previous work [1, 2]. So that, the parameters needed to be determined only remain a and b .

* Corresponding author. Tel.: +81-82-424-7576; fax: +81-82-422-7193.

E-mail address: iwamoto@mec.hiroshima-u.ac.jp

After performing the finite element simulation, external force waves impacted at 140 m/s in velocity captured by the Hopkinson pressure bar are present in Fig. 2. The time period circled by dashed lines shows the Phase 2 which can be employed to calculate the stress-strain curve as mentioned in the work by authors [1, 2]. The figures (a) and (b) show the results from the specimens with various a/d and constant d/d_0 as well as constant a/d and various d/d_0 , respectively. From Fig. 2(a) and (b), it can be observed that the amplitude of oscillations decreases with an increase of a/d and decrease of d/d_0 . So, a larger value of a/d and smaller value of d/d_0 should be selected. Nevertheless, as time advances, oscillations of the wave for 0.65 in d/d_0 becomes larger abruptly than that for other d/d_0 at a time over 25 μs . Considering the time for calculating the stress-strain curve mentioned in our previous work [1, 2], oscillations in the time period from 26 to 51 μs were requested to be suppressed. Thereupon, 0.75 of d/d_0 is the best result. An inset in Fig. 2 shows a magnified view in the initial part of waves. A larger value of a/d and smaller value of d/d_0 induces a longer rise time of waves.

From the results mentioned above, larger a/d and smaller d/d_0 shows a better effect for suppression of extra oscillations. So that, 0.27 of a/d and 0.75 of d/d_0 is determined. It can be predicted that the stress-strain curve with a high accuracy can be measured from the newly designed specimen. However, the relationship between the rise time shown in the upper right side of Fig. 2(a), (b) and the accuracy of stress-strain curve is unknown. Besides, the suppression method for excessive local deformation is not discussed. The mentioned problems will be discussed in future plan.

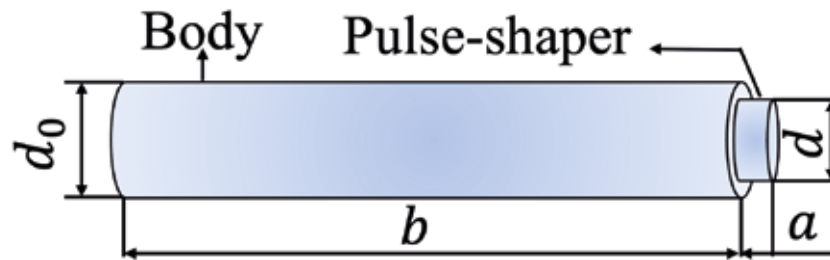


Fig. 1. Schematic illustration of the designed specimen with a pulse-shaper.

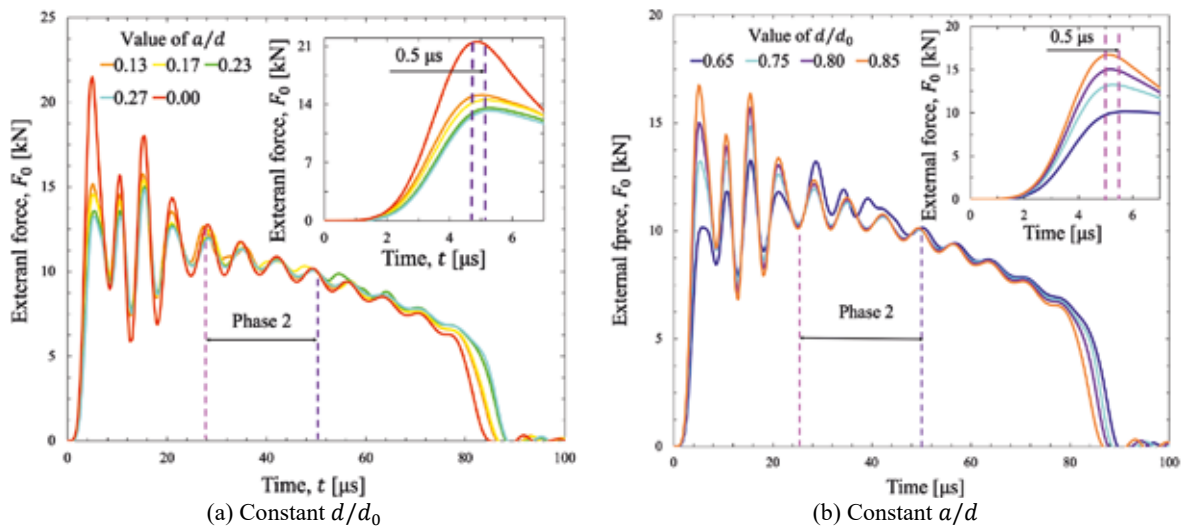


Fig. 2. Impact force waves for specimens with various values of a/d and d/d_0 .

Reference

- [1] Gao C, Iwamoto T. Finite element analysis on a newly-modified method for the Taylor impact test to measure the stress-strain curve by the only single test using pure aluminum. *Metals* 2018; 8: 642-657. <https://doi.org/10.3390/met8080642>
- [2] Gao C, Iwamoto T. Instrumented Taylor impact test for measuring stress-strain curve through single trial. *Int J Impact Eng* 2021; 157: 103980. <https://doi.org/10.1016/j.ijimpeng.2021.103980>
- [3] Pochhammer L. Über die fortpflanzungsgeschwindigkeiten kleiner schwingungen ineinem unbegrenzten isotropen kreiszylinder. *J Reine Angew Math* 1876; 81: 324-336. <https://doi.org/10.1515/crll.1876.81.324>
- [4] Chree C. Longitudinal vibrations of a circular bar. *Quart J Pure Appl Math* 1886; 21: 287-298.
- [5] Rigby SE, Barr AD, Clayton M. A review of Pochhammer-Chree dispersion in the Hopkinson bar. *Eng Comput Mech* 2018; 171: 3-13. <https://doi.org/10.1680/jenclm.16.00027>
- [6] Wang JB, Li WF, Xu LZ, Du ZH, Gao GF. Experimental study on pulse shaping techniques of large diameter SHPB apparatus for concrete. *Lat Am J Solid Struct* 2021; 18. <https://doi.org/10.1590/1679-78256268>
- [7] Chen XD, Asce AM, Ge LM, Zhou JK, Wu SX. Experimental Study on Split Hopkinson Pressure Bar Pulse-Shaping Techniques for Concrete. *J Mater Civ Eng* 2016; 28: 04015196. [https://doi.org/10.1061/\(ASCE\)MT.1943-5533.0001494](https://doi.org/10.1061/(ASCE)MT.1943-5533.0001494)

3rd International Conference on Impact Loading of Structures and Materials
ICILSM 2022

A Measurement of Impact Force by PVDF for Instrumented Taylor Impact Test

Naoko Sakata^a, Gao Chong^b, Takeshi Iwamoto^{c,*}, Yoshikazu Tanaka^d

^aNaoko SAKATA, Hiroshima University, 1-4-1 Kagamiyama, Higashi-Hiroshima, Hiroshima, 739-8527, Japan

^bChong GAO, Hiroshima University, 1-4-1 Kagamiyama, Higashi-Hiroshima, Hiroshima, 739-8527, Japan

^{c,*}Takeshi IWAMOTO, Hiroshima University, 1-4-1 Kagamiyama, Higashi-Hiroshima, Hiroshima, 739-8527, Japan

^dYoshikazu TANAKA, Hiroshima University, 1-4-1 Kagamiyama, Higashi-Hiroshima, Hiroshima, 739-8527, Japan

Abstract

1. Introduction

In the field of aerospace industries, problems of the impact by space debris to spacecrafts are inevitable. So that, understanding the mechanical behavior of structural materials used for the field under high-speed deformation becomes important. From the viewpoint, to measure the deformation behavior under an extremely-high deformation speed, an instrumented Taylor impact test [1], [2] is newly proposed. In this test, a high-speed camera and a Hopkinson pressure bar made of bearing steel with strain gauges are introduced. Additionally, an improvement is done, by an introduction of a harder pressure bar made of a tungsten carbide (WC) instead of the steel into apparatus to suppress the indentation on the impact surface. However, in such a case, unavoidable oscillations on the impact force wave due to Pochhammer-Chree effect [3] and reflections of the wave back into the specimen are hardly observed. The reason can be considered as the limitation of the bandwidth of the amplifier for strain gauge used for measuring the wave.

On the other hand, the strain can be measured from the piezoelectric films based on the piezoelectricity effect. The advantage of the film is a quite high flexibility and a high capability as same as the strain gauge. Because of its higher output level, any amplifiers are not required. Besides, the measurement in a higher frequency band with a high accuracy is expected. By employing the piezoelectric films as a sensor, challenges on measuring the guided waves [4] and the impact force [5] are focused on. Furthermore, its durability and the effect of temperature gradients are widely discussed [6].

However, the application of the piezoelectric films at a strain rate over 10^5 s^{-1} has not been challenged because of the limitation for the experimental method used for achieving the high-speed impact. Additionally, to measure the impact force, the plane of the film is employed directly as the impact surface as similar to the solid quartz[7], which is one of the piezoelectric material and a commercially-provided sensor [7]. Even though it has the thin sheet with the huge flexibility, its attachment is not the same as the strain gauge. Besides, the validity of the piezometric films at 2 MHz in frequency is still questionable.

In this study, a piezoelectric film made of polyvinylidene fluoride (PVDF) with double-sided aluminum electrodes is employed. Before performing the Taylor impact test, two PVDF films are attached on aluminum and acryl sheets to perform the preliminary test. In this case, a signal with 2 MHz is inputted into one PVDF film as an actuator and the other PVDF film as a sensor measures the vibrations generated by inverse piezoelectric effects on the specimen. The validity of PVDF at 2 MHz in measured frequency is discussed from the output signal of the PVDF film as a sensor. After that, the PVDF films are newly introduced into the instrumented Taylor impact test, and the validity is evaluated by comparing the output result from the strain gauge.

2. Results

Fig. 1 shows the normalized output signal from a PVDF film sensor when the input signal to the actuator is 2 MHz in the frequency. The red line is the input voltage, and the blue and yellow lines are the output voltage when the specimen is acryl and aluminum, respectively. From this figure, it is confirmed that the periods measured on the acryl and aluminum is the same as the input voltage. Therefore, the film is useful to measure the result at a higher frequency of the output signal with the same frequency of the input signal. However, the maximum output voltage from a sensor is 0.005 V for aluminum and 0.03 V for acryl, respectively. Although the amplitude of the input signal supplied is 10 V, the output level is quite small. This means that the performance of PVDF as an actuator is insufficient.

Fig. 2 shows the output voltage from PVDF film and strain gauge measured in the Taylor impact test. The blue and orange lines denote the results measured by strain gauge and PVDF, respectively. From the figure, the output voltage of PVDF is much higher than the strain gauge. This result supports the insufficient performance as the actuator. Oppositely, the electromagnetic noises from the environment detected by PVDF is smaller. However, the output voltage for PVDF is not zero before the impact. Hence, it is predicted that some other unknown factors exist the output signal before rising the impact force wave. In addition, even though the position for attaching the strain gauge and PVDF is different, time delay for rising point of stress wave is hardly observed. This is because of the effect of electromagnetic noises containing in the measurement system. So, it is necessary to improve the measurement system to remove the noises or to reconsider the attachment position of PVDF. On the other hand, on the orange curve, the vibration which is not observed before the impact appears after impact. That means that the output voltage from PVDF contains vibrations at the high frequency in the external force wave which could not be measured by strain gauge. Different from the previous study, PVDF does not need to attach on the impact surface in this method. So, it can be considered the measurement errors due to impact such as frictions and slip are smaller.

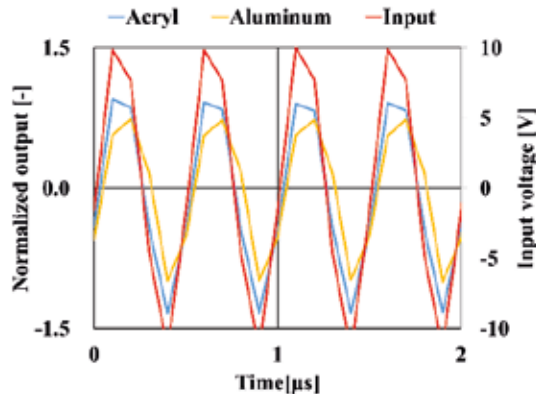


Fig.1 Validity of the sensor of PVDF in input frequency of 2 MHz

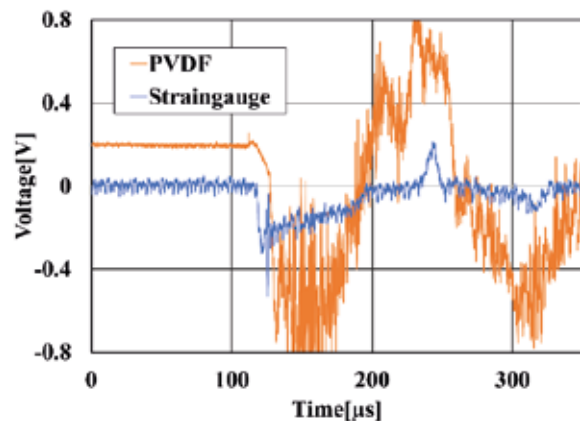


Fig.2 Time histories of output voltage from PVDF and strain gauge

- [1] Taylor, G.I., 1947, "The use of flat-ended projectiles for determining dynamic yield stress Theoretical considerations", Proceedings of the Royal Society A, Vol. 194, pp. 289-299.
- [2] Gao, C., and Iwamoto, T., 2021, "Instrumented Taylor impact test for measuring stress-strain curve through single trial", International Journal of Impact Engineering, Vol. 157, 103980
- [3] Pochhammer, L., 1876, "Ueber die fortpflanzungsgeschwindigkeiten kleiner schwingungen in einem unbegrenzten isotropen kreiscylinder", Journal für die reine und angewandte Mathematik, Vol. 81, pp. 324-336
- [4] Tanaka, Y., Tamoto, E., Fujimoto, Y., 2010, "Development of contact-type sensor using piezoelectric film for guided wave measurement", International Journal of Applied Electromagnetics and Mechanics, Vol. 33, pp. 1237-1244
- [5] Fujimoto, Y., Shintaku, E., Tanaka, Y., and Fujiyoshi, J., 2011, "Pad Type Compressive Force Sensor Suitable for High-Speed Impact Force Measurement", Transactions of the Japan Society Mechanical Engineering, Vol. 78, No. 791, pp. 84-95 (in Japanese)
- [6] Shirinov, A.V., Schomburg, W.K., 2008, "Pressure sensor from a PVDF film", Sensors and Actuators A: Physical, Vol. 412, Issue 1, pp. 48-55
- [7] Yahaya, M.A., Ruan, D., Lu, G., Dargusch, M.S., and Yu, T.X., 2005, "Selection of Densification Strain to Predict Dynamic Crushing Stress at High Impact Velocity of ALPORAS Aluminum Foam", Key Engineering Materials, Vol. 626, pp. 383-388

3rd International Conference on Impact Loading of Structures and Materials
ICILSM 2022

Impact of PU Foam Projectiles to Assess the Performance of Aluminum Panels Against Blast Loading

Dhruv Narayan^a, Naresh Bhatnagar^a

^a*Indian Institute of Technology, Delhi, India*

Abstract

The performance of a target panel against blast waves can be tested through actual blast experiments. However, these experiments are expensive and require special safety considerations. Moreover, in academic institutions, where the land law prohibits explosives, these tests could not be conducted. In such cases, a testing methodology is required to imitate the blast loading. The loading on a target panel due to the impact of foam projectiles bears a significant resemblance to the blast loading. The amplitude and duration of the shock wave depend upon the mechanical properties and dimensions of the foam projectile[1].

Projectiles of PU foam of specific gravity 0.5 are fabricated. Alongside, the quasi-static compression test of the same PU foam was conducted following ASTM D1621-94 standard[2]. With the help of a single stage gas gun, these foam projectiles were made to impact on Aluminium target panels and the force time history was measured using Kistler force sensor. The target panel assembly including the clamping mechanism was hung above ground to eliminate the interference of friction force in measurement of the force time history. Upon impact, the force is directly transferred to the sensor and force time history was measured. Finally the force time history of foam impact test was correlated with the force time history of a blast event obtained using Kinney and Graham approach.

3rd International Conference on Impact Loading of Structures and Materials
ICILSM 2022

Optimization of the electromechanical behavior of a piezoresistive polyurethane based foam during quasi-static and dynamic solicitations

Antoine Poirot^{a,b}, Michel Arrigoni^b, Nacera Bedrici^a, Jean-Christophe Walrick^{a*}

^a ESTACALAB[†], ESTACA Campus Ouest, Parc universitaire Laval-Changé, Rue Georges Charpak -BP 76121, 53061 Laval Cedex 9, France.

^b IRDL, ENSTA Bretagne, 2, rue François Verny, 29806 Brest Cedex 09, France.

Abstract

From transportation to space including defense applications, engineered systems are likely to face dynamic loads such as impact, drop or blast loadings. In order to assess the residual strength or the survivability of the target, it is necessary to bring models when experiments turn to be destructive and thus expensive. The modelling also meets some limits because it cannot be relevant regarding the too large variety of material behavior or loading. At such a point it is then important to implement Structural Health Monitoring (SHM) techniques in systems in service, especially able to monitor dynamic events. From this fact, implementation of physical sensors in structures are needed.

The presented work aims at implementing a sensor within a structural assembly and then to observe its response to a dynamic loading. A first suggestion is the use of an electrically conductive foam. As a first step, it is necessary to know about its constitutive law and the relation between stress and conductivity. An open-cell foam with a low density (20 kg/m³) coated with a conductive solution is thus studied. The work describes the elaboration of the sample and its electrical response when subjected to compression tests in order to assess its piezoresistive response. In that purpose, the foam is characterized with quasi-static tests (cyclic uniaxial compressions at low velocity) conducted with a press, in free and confined (oedometric) configurations. These tests are performed in the same humidity and temperature conditions. It is observed that the electrical response (sensitivity, signal stability) of the conductive foam depends on its mechanical behavior which depends on its physical parameters. Thereby, the morphology (geometry, size and repartition of cells, density...) of the conductive foam and its electrical conductivity are key parameters to be considered in the characterization. To optimize the deformation and pressure sensitivity of the foam, it is coated with a conductive ink based on PEDOT:PSS copolymers at various concentration ratios.

Finally, a calibration of studied samples could be achieved in quasi static regime and its dependency to key parameters was assessed.

As a second step, the dynamic characterization of the foam is studied. The objective is to evaluate the performance of the foam as a shock sensor by identifying the key parameters. Initially, it consists of subjecting low energy impacts on a sandwich structure with integrated foam sample. From the results, the sensing performance depends on various parameters such as foam calibration, conductivity and sandwich constitution (materials, dimensions...). Supplementary tests could be performed with Hopkinson bars for obtaining high rate foam behavior and defining its pressure sensing range. The dynamic behavior of the conductive foam is compared to that in quasi static regime. The role played by viscoelasticity in the electrical response is then evidenced.

* Antoine Poirot. Tel.: +33 6 29 71 40 50

E-mail address: antoine.poirot@estaca.fr

Michel Arrigoni. Tel.: +33 2 98 34 89 78

E-mail address: michel.arrigoni@ensta-bretagne.fr

3rd International Conference on Impact Loading of Structures and Materials
ICILSM 2022

Design of a high strain rate in-plane torsion test

Vincent Grolleau^{a,b*}, Christian C. Roth^a, Bertrand Galpin^{b,c} and Dirk Mohr^{a*}

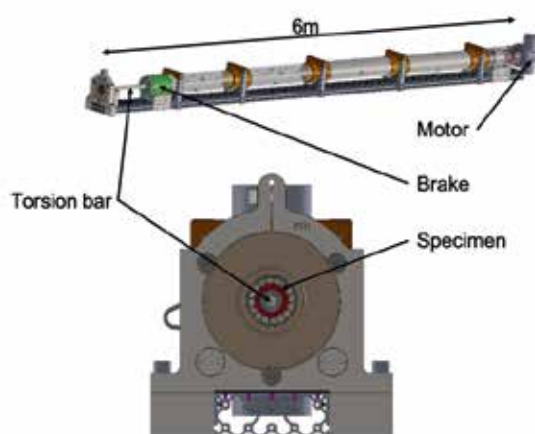
^aDepartment of Mechanical and Process Engineering, ETH Zurich, Tannenstrasse 3, 8092, Zurich, Switzerland

^bIRDL, Univ. Bretagne Sud, CNRS UMR 6027, F-56100 Lorient, France

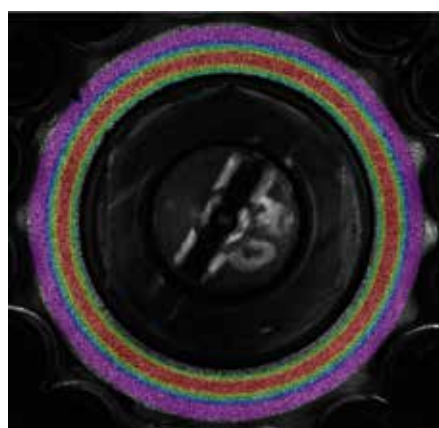
^cEcoles Saint-Cyr Coetquidan, CREC, F-56380 Guer, France

Abstract

While a variety of tests exist to perform tensile tests at high strain rates on sheet metals, experiments in a shear stress state are usually limited to one material orientation. At the same time these geometries need to be chosen carefully as fracture might initiate from a free boundary. In-plane torsion testing of a disc specimen however offer a significant advantage: they do not feature any free boundaries. In the present work a novel in-plane torsion test is presented in which the specimen is clamped on its outer diameter, while a Split-Hopkinson torsion bar is used to apply the loading to the inner clamping. A circular groove, i.e. a local thickness reduction, is introduced to ensure a strain localization away from the clamped specimen shoulders. The setup grants full optical access to the sheared gauge section, allowing DIC measurements. The experimental campaign includes experiments at low (0.001/s), intermediate (1/s) and high strain rates (>100/s) on advanced high strength steels and aluminum alloys.



View of the experimental set-up



Circumferential strain field
(quasi-static and intermediate strain rates)

* Corresponding author. Tel.: +41-44-632-2612

E-mail address: vgrolleau@ethz.ch, dmohr@ethz.ch

3rd International Conference on Impact Loading of Structures and Materials
ICILSM 2022

High strain-rate tests at high temperature in controlled atmosphere

Alberto Morena*, Martina Scapin, Lorenzo Peroni

DYNLab, Department of Mechanical and Aerospace Engineering, Politecnico di Torino, Corso Duca degli Abruzzi 24, 10129, Turin (Italy)

Abstract

In many applications such as machining, metal forming, high velocity impact or high energy deposition on metals, materials are deformed at very high rates and in many cases also at high temperature. The stress-strain response of materials and structures will be a balance between the effects of hardening (due to strain and strain-rate) and thermal softening: temperature and strain-rate sensitivities are mutually related, and the thermal effects obtained from quasi-static tests cannot be used to predict material response under dynamic loading conditions. Hence, the need to investigate the mechanical response of materials in a properly defined range of interest: the development of testing methodologies and facilities able to completely explore is the starting point. This work analyzes an experimental technique applicable for high strain-rate tests at high temperature focusing the attention on a setup operating in a controlled atmosphere (insufflation of inert gas or vacuum) to avoid the specimen oxidation. The proposed setup was tested on several metallic dog-bone specimens.

The proposed methodology uses an induction heating system, which represents a fast and efficient method for increasing the temperature of electrically-conductive materials. It is a non-contact method able to guarantee a good level of repeatability and uniformity. It finds several applications, such as brazing, heating treatment, testing materials, bonding, forging, soldering and shrink fit. Moreover, it is a technique used in many industrial and production processes in different fields, such as automotive, aerospace, and medical industries. With respect to other heating systems the induction one has a series of advantages, among which the most important is that the energy is mainly focused and transferred to heat only the targeted area. With respect to a resistance oven, an induction system requires less energy and time: in an oven a great amount of energy is required to increase the temperature and to hold it into the entire chamber, if present. In addition, a common oven requires time for the process ramp-up, while with induction the heat is applied and stopped instantly. Finally, electrical resistance heating is less efficient since there is a big amount of heat which results to be lost to the surrounding.

The used induction system has a single turn coil which can be placed on the side of the specimen. The system is coupled with the Hopkinson Bar setup in direct impact configuration present at the DYNLab laboratory of the Politecnico di Torino. The setup, as reported in the scheme of Figure 1, consists of a gas-gun, a hollow striker, an input bar and an output one. An anvil is fixed at one end of the input bar and is hit by the striker, which is pneumatically accelerated. A tensile stress wave is then generated in the incident bar and propagates along it towards the specimen. The temperature measurement is performed with two multi-wavelength infrared pyrometers able to measure the maximum temperature reached in the gage length of the specimen (Williamson Pro MW-10-20-C in the range of temperatures 475-1750°C and Williamson Pro MW-20-5-C in the range of temperatures 150-475 °C) and with a high-speed infrared camera (FLIR X6900SC). The measurement coming from the infrared camera depends on the emissivity of the material which needs to be calibrated. Moreover, it depends on the temperature itself, hence it can vary during a dynamic test because of the adiabatic heating. In this study a high-speed infrared camera is adopted, which allows also to obtain the information on the adiabatic heating during the tests. The multi-wavelength infrared pyrometers can give the temperature measurement without knowing the emissivity of the material, but the spot over

* Corresponding author. Tel.: +39-0110903543.

E-mail address: alberto.morena@polito.it

which they measure the temperature is bigger than the sample, so the signal strength has to be adjusted to be able to perform the measure, but this procedure reduces the range of measurable temperature. By taking into account these considerations, the authors decided to use both the measuring systems and to check the consistency between the performed measurements. Each test is also video recorded to obtain the deformation of the specimen directly measured on the sample by using the high-speed camera PHOTRON SA5.

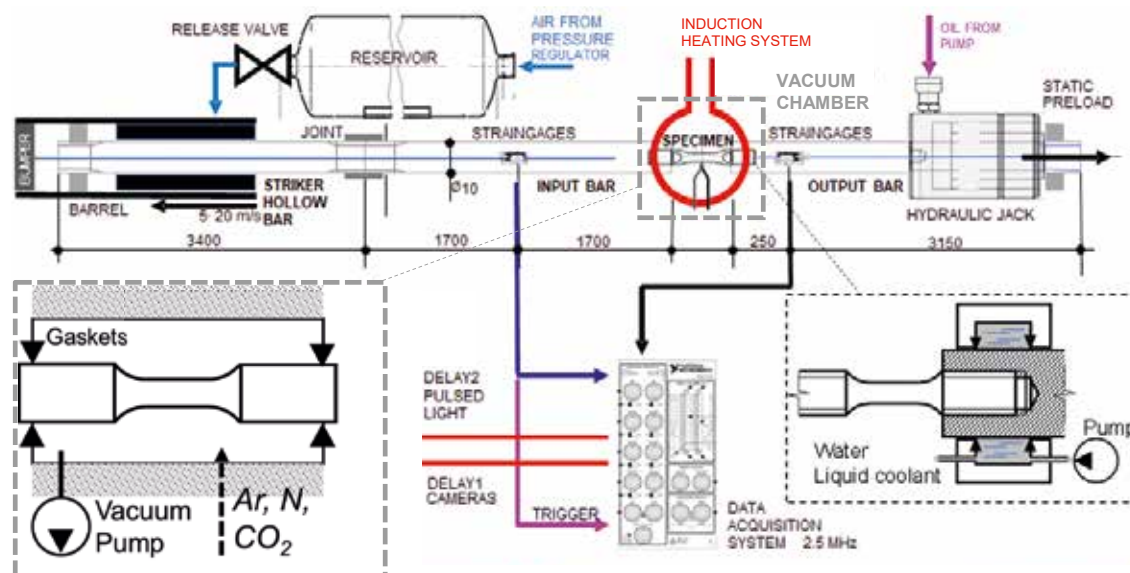


Figure 1: Scheme of the Hopkinson Bar setup used for tests at high temperature.

An aspect of fundamental importance to consider is related to the control of oxidation of the sample. The solution of the problem of oxidation is not strictly related to the testing of metals, but it represents an important issue also in case of composite materials when they are carbon-based. If the material to be heated is particularly reactive to the presence of oxygen, the oxidation can be critical: it can deteriorate the mechanical properties of the specimen in case the involved portion of material is extended. Since the oxidation is extremely rapid, especially at very high temperatures, to completely prevent the oxidation it is necessary to avoid any contact with air once the heating is started. This could be critical in some conditions, especially when the movement of the specimen is required between the heating phase and the testing one or the heating is not performed in a protective atmosphere. Moreover, the oxidation has to be limited as much as possible, because the oxidized layer can also compromise the quality of the video recording of the test. The oxide is brittle and suddenly fails under dynamic loads. The failure of the oxidized layer generates a cloud of particles which explodes from the specimen surface and limits the view of the specimen itself. In addition, the ejected hot particles could also damage some components of the setup. To avoid the problem of oxidation many researchers directed a jet of inert gas (e.g., argon or nitrogen) or of carbon dioxide on the specimen. Often this solution can only limit the oxidation, but it is not able to completely avoid it. As a matter of fact, the jet produces turbulence on the specimen surface, which allows the oxygen to mix with the protective gas making this method less effective. This method requires a big quantity of protective gas and has the other big disadvantage that the flow of gas directed on the specimen is responsible for the cooling down of the surface of the specimen: the surface temperature could no longer be uniform and above all a significant gradient of temperature could be induced between the surface and the core of the specimen. To create a non-oxidizing atmosphere is particularly easy when a closed chamber is adopted for the heating of the specimen. In this case, it is sufficient to use a vacuum pump before the heating and/or to fill the chamber with inert gas. The last important aspect to be considered is that, when the temperature of the sample is very high or the strength of the bars strongly decrease at high temperature, it is also necessary to cool down the gripping systems to prevent damage of the sensors used to measure loads and displacements in the test equipment (i.e., the strain gages on the bars). The cooling of the machine could be obtained in different ways: in this work an ad-hoc water-cooled supports are mounted both on input and output bars near the specimen interfaces and integrated with the vacuum chamber.

Walley, S.M. The Effect of Temperature Gradients on Elastic Wave Propagation in Split Hopkinson Pressure Bars. *J. dynamic behavior mater.* 6, 278–286 (2020), <https://doi.org/10.1007/s40870-020-00245-9>.

Song, B. *Advances in Experimental Impact Mechanics*, Elsevier, ISBN 978-0-12-823325-2 (2022), <https://doi.org/10.1016/C2019-0-05017-0>.

3rd International Conference on Impact Loading of Structures and Materials
ICILSM 2022

A simple methodology to perform dynamic triaxial tests using split-Hopkinson bars

D. Kumar^{a,b}, S. N. Khaderi^{a,*}, Dong Ruan^b

^aIndian Institute of Technology Hyderabad, Kandi, Sangareddy, Hyderabad, Telangana 502285, India.

^bDepartment of Mechanical and Product Design Engineering, School of Engineering, Swinburne University of Technology, Hawthorn, Victoria 3122, Australia

Abstract

A split-Hopkinson pressure bar (SHPB) is an experimentally facility used to characterize the stress-strain response of materials at high strain rates ($10^2 - 10^3 \text{ s}^{-1}$). Many variants of this facility have been proposed to perform material characterization in tension, torsion, high temperature, etc. A common feature in most of the set-ups is that the material being characterized is subjected to uniaxial stressing. For example, if a sample is being compressed in the z-direction, all the stress components except σ_{zz} vanish. This mode of loading is sufficient to characterize the response of metals, which are considered to be plastically incompressible even at the above-mentioned high strain rates. In metals, the yielding is governed by a single parameter – the yield stress, which can be easily obtained from SHPB experiments. On the other hand, if we consider pressure dependent materials, such as polymeric/metal foams, sand, concrete, and ceramics, the yield stress depends on the magnitude of lateral pressure.

Experiments in which we apply an axial load in addition to lateral pressure are usually carried out in a triaxial set-up under quasi-static conditions. Since these triaxial set-ups are not adaptable to high strain rate characterization, a compromise is made using the following two approaches in SHPB tests. In the first approach, the diameter of a cylindrical sample is chosen to be the same as the bar diameter. A sleeve is fitted over the circumference of the sample to constrain lateral expansion. During a typical test, the sample gets compressed along the axial direction, and its circumference expands, which is resisted by the sleeve. The axial stress is measured from the SHPB equations, and the confining pressure is calculated by measuring the circumferential strain in the sleeve. The axial pressure and lateral pressure increase at a high rate during these experiments. This approach can be used for materials which show a significant expansion during uniaxial compression. Thus, they are not suited for foams, which have a very low Poisson's ratio. In the second approach, again, the sample diameter is taken to be the same as the bar diameter. The sample, together with the incident and transmission bars, is enclosed in a custom-built hydraulic chamber using which an external pressure can be applied to the lateral surfaces of the sample. During testing, the axial stress is applied by the impact of the bars while the lateral pressure is maintained constant. This method suffers from the drawback that the lateral pressure is being applied in a quasi-static manner. Hence, although the axial stress increases at a high rate, the lateral pressure is maintained constant.

We propose a simple methodology to perform triaxial SHPB experiments in which (1) the axial and lateral stresses increase within the loading duration of a SHPB experiment and (2) the testing of materials of all Poisson's ratios is facilitated. The cylindrical sample is chosen to have a diameter smaller than the incident and transmission bars (see Fig. 1). A polymeric sleeve is placed over the incident and transmission bars so that a fluid can be filled between them. The sample is compressed between the bars to apply an axial loading. As the samples is compressed, the distance between the bars gets reduced, which pressurizes the fluid between them. This pressure leads to a lateral pressure on the sample, which is measured using the strain gauge bonded to the sleeve. Thus, the axial and lateral pressure increase simultaneously during the experiment. Since the pressure is controlled by the relative displacement of the bars, materials of all Poisson's ratio can be tested. The use of this methodology to experimentally characterize the yield behavior of polyurethane foams at high strain rates will be presented.

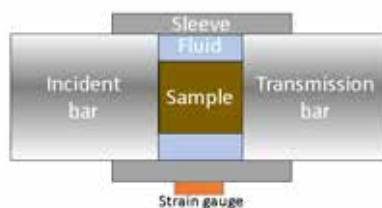


Figure 1: A schematic representation of the set-up used to perform triaxial experiments on split-Hopkinson pressure bar.

3rd International Conference on Impact Loading of Structures and Materials
ICILSM 2022

Testing and Modelling of Aluminium Rims under Quasi-static and Dynamic Loadings

D. Morin^a, O.S. Hopperstad^a, M. Langseth^a

^aSFI CASA, Department of Structural Engineering, NTNU, Norway

Abstract

Nowadays, crash requirements of automotive structures involve chassis parts in addition to the traditional body in white. Recently, the Insurance Institute for Highway Safety (IIHSS) in the U.S. has released new crash scenarios which solicitate the full front end of a car. For example, a new test (referred to as the small overlap frontal test), subjects only 25% of the front end of a vehicle to a 64 km/h impact. Under these circumstances, the suspension system of the vehicle, including the wheel and rim, becomes part of the solution to manage the energy from the impact.

Because of this new load case, accurate representations of aluminium rims in large-scale analyses are now mandatory in order to design bodies in white capable of fulfilling these new crash requirements. There are two main challenges linked to the numerical modelling of aluminium rims under these types of loads. Firstly, due to the casting process used to manufacture the rims, large scatter can be observed on the ductility of the aluminium alloy. Secondly, due to their complex shapes, it is difficult to carry out reliable component tests which are needed to validate numerical models.

In this work, we have investigated the material properties of an aluminium rim and its behaviour for different stress states and strain rates. A new test-setup was proposed to carry out dynamic crushing tests of aluminium rims. The component tests, both quasi-static and dynamic, were used to validate a numerical model applicable to large-scale analyses.

3rd International Conference on Impact Loading of Structures and Materials
ICILSM 2022

Effect of Diaphragm on Pressure Profiles Generated in Shocktube

Lekhani Gaur^{a*}, Rashmi Singh^b, Tanusree Chakaborty^c

^aPh.D. Scholar, School of Interdisciplinary Research, Indian Institute of Technology (IIT) Delhi, New Delhi 110016, India

^bPh.D. Scholar, Department of Civil Engineering, Indian Institute of Technology (IIT) Delhi, New Delhi 110016, India

^cProfessor, Department of Civil Engineering, Indian Institute of Technology (IIT) Delhi, New Delhi 110016, India

Abstract

The shock waves generated from an explosion may cause serious damage to the nearby public, residential or industrial structures. Therefore, the study of shock wave interaction with structures and geological media are of great interest to the engineers dealing with the analysis and design of underground and above ground structures. A shocktube is a laboratory scaled experimental facility for simulating blast waves and shock waves to evaluate the response of structures under blast load.

A new shocktube test facility has been installed at Indian Institute of Technology, Delhi, India consisting of both horizontal and vertical configurations for evaluating the response of structures and geological media respectively under blast load. The vertical shock tube (VST) is 4 m in length with 200 mm internal diameter and horizontal shock tube (HST) is 10 m in length with 300 mm internal diameter. The shocktube mainly consists of two sections, namely driver section and driven section separated by a diaphragm. The variation in shock wave profile is introduced by using different driver section length. The strength of the shock wave is varied by incorporating the diaphragms made of different materials such as Lexan and Aluminum with different thicknesses and groove depths. The diaphragm of the shock tube is either ruptured by increasing the pressure difference between the driver and driven sections or by puncturing it with a mechanical device. It is necessary to study the variation in shock waves' profiles prior to the testing of samples in shocktube by incorporating different diaphragms for both vertical and horizontal configurations. In the present study, the effect of diaphragms on the reflected pressure is demonstrated for both HST and VST configurations. The burst pressures in driver section and corresponding reflected pressures obtained at the end of driven section are tabulated for HST and VST in Table 1 for fully opened conditions of diaphragms after bursting using Nitrogen gas in the driver section. The driver section length is kept 0.5 m for both HST and VST configurations in these tests.

Table 1: Burst pressure and reflected pressure for HST and VST configurations for different diaphragms

Configuration	Diaphragm	Thickness (mm)	No. of sheets	Groove depth (mm)	Burst Pressure (Bar)	Reflected Pressure (Bar)
HST	Lexan	1.5	1	-	7.9	4.82
HST	Lexan	1.5	2	-	11.9	7.16
HST	Lexan	1.5	3	-	15.4	8.54
VST	Aluminum	3	-	1.5	7.0	7.85
VST	Aluminum	4	-	1.5	12.2	7.91
VST	Aluminum	4	-	0.75	22.8	11.2

* Corresponding author. Email ID: lekhani.gaur@sire.iitd.ac.in

Figure 1 depicts the reflected pressure profile generated at the end of driven section of shocktube for VST and HST configurations. It can be observed that shock wave is generated in the VST configuration and blast wave is generated in the HST configuration due to the different ratio of driver section length to the total length of the shocktubes. The decay time of shock wave is more in HST as compared to VST. Further, the FE simulation is performed to validate the shock wave generated in HST when the burst pressure is 15.4 Bar using eulerian elements in Abaqus. The tube and diaphragm are not modelled in this preliminary study. It can be observed that FE simulation represents the ideal conditions of shock wave propagation and hence peak reflected pressure is higher (9.62 Bar) than that obtained from experiments (8.54 Bar).

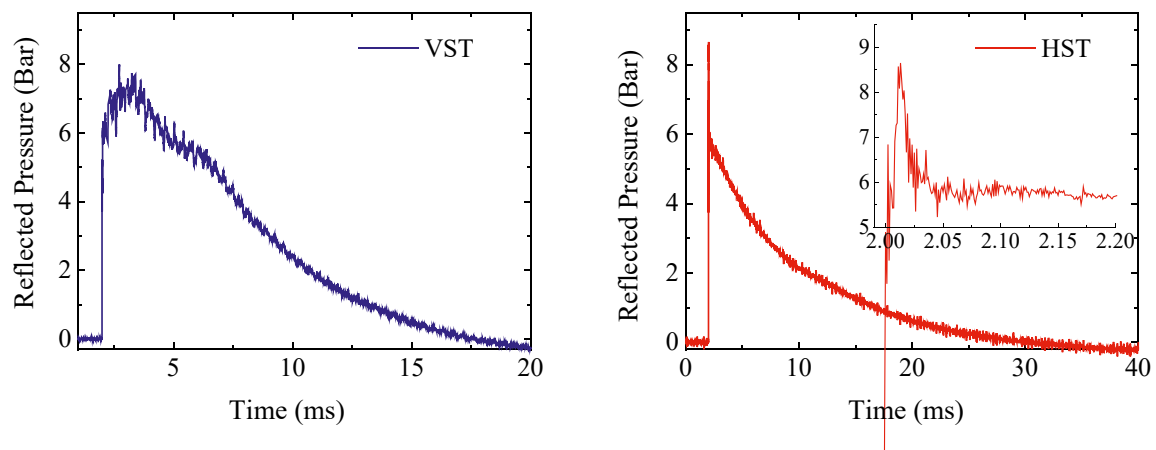


Figure 1: Reflected pressure profiles generated in VST using Aluminum diaphragm (3 mm thick with 1.5 mm deep groove) and HST configurations using Lexan diaphragm (3 no. of 1.5 mm thick sheets)

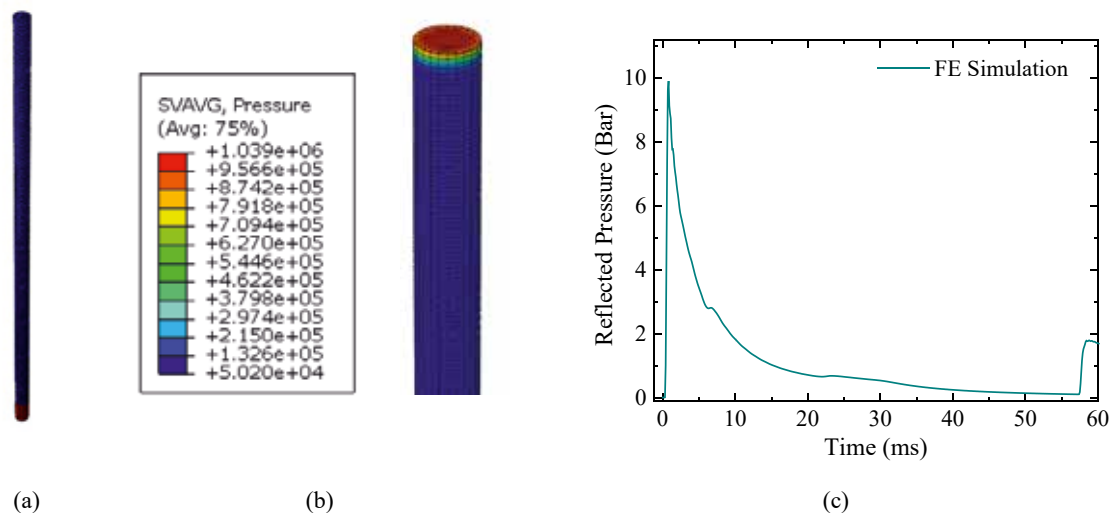


Figure 2: FE validation of the reflected pressure profile for HST configuration for burst pressure of 15.4 Bar generated using Lexan diaphragm (3 no. of 1.5 mm thick sheets). (a) FE model of 10 m long shocktube, (b) contours of reflected pressure at the end of driven section, (c) reflected pressure time history at the end of driven section obtained from Abaqus

3rd International Conference on Impact Loading of Structures and Materials
ICILSM 2022

Theoretical predictions of dynamic necking formability of ductile metallic sheets with evolving plastic anisotropy and tension-compression asymmetry

M. Anil Kumar^{1*}, K. E. N'souglo¹, N. Hosseini¹, N. Jacques², J.A. Rodriguez Martinez¹

¹*Department of Continuum Mechanics and Structural Analysis, University Carlos III of Madrid, Avda. de la Universidad, 30. 28911 Leganés, Madrid, Spain; E-mail address: amurlidh@pa.uc3m.es, knsouglo@ing.uc3m.es, nhossein@pa.uc3m.es, jarmarti@ing.uc3m.es; URL: <https://www.nonsolmecgroup.com>*

²*ENSTA Bretagne, CNRS UMR 6027, IRDL, 2 rue François Verny, F-29806 Brest Cedex 9, France*

Abstract

In this paper, we have investigated necking formability of anisotropic and tension-compression asymmetric metallic sheets subjected to in-plane loading paths ranging from plane strain tension to equibiaxial tension. For that purpose, we have used a three-pronged approach which includes a linear stability analysis, a nonlinear two zone model and unit-cell finite element calculations. We have considered three materials --AZ31-Mg alloy, high purity α -titanium and OFHC copper-- whose mechanical behavior is described with an elastic-plastic constitutive model with yielding defined by the CPB06 criterion which includes specific features to account for the evolution of plastic orthotropy and strength differential effect with accumulated plastic deformation. From a methodological standpoint, the main novelty of this paper with respect to the recent work of N'souglo et al.[1] --which investigated materials with yielding described by the orthotropic criterion of Hill-- is the extension of both stability analysis and nonlinear two-zone model to consider anisotropic and tension-compression asymmetric materials with distortional hardening. The results obtained with the stability analysis and the nonlinear two-zone model show reasonable qualitative and quantitative agreement with forming limit diagrams calculated with the finite element simulations, for the three materials considered, and for a wide range of loading rates varying from quasi-static loading up to 40000s⁻¹, which makes apparent the capacity of the theoretical models to capture the mechanisms which control necking formability of metallic materials with complex plastic behavior.

Keyword:- Dynamic formability, Linear stability analysis, Two-zone model, Finite elements

ACKNOWLEDGEMENT

The research leading to these results has received funding from the European Research Council (ERC) under the European Union's Horizon 2020 research and innovation program. Project PURPOSE, grant agreement 758056.

REFERENCE

- [1] N'souglo, K.E., Jacques, N., Rodriguez-Martinez, J.A. A three-pronged approach to predict the effect of plastic orthotropy on the formability of thin sheets subjected to dynamic biaxial stretching. *Journal of the Mechanics and Physics of Solids*. (2021) **146**.

* Corresponding author. Tel.: +34-685570067.
E-mail address: amurlidh@pa.uc3m.es

3rd International Conference on Impact Loading of Structures and Materials
ICILSM 2022

A simple and computationally efficient stress integration scheme based on numerical approximation of the yield function gradients: Application to advanced yield criteria

Navab Hosseini^{a,*}, José A. Rodríguez-Martínez^a

^a*Department of Continuum Mechanics and Structural Analysis, University Carlos III of Madrid, Avda. de la Universidad, 30, Leganés 28911, Madrid, Spain*

Abstract

In this work, we have developed a stress integration scheme based on the numerical approximation of the yield function gradients, to implement in the finite element code ABAQUS three elastic isotropic, plastic anisotropic constitutive models with yielding described by Yld2004-18p [1], CPB06ex2 [2] and Yld2011-27p [3] criteria, respectively. Moreover, we have developed both VUMAT and UMAT subroutines for the three constitutive models, and cylindrical cup deep drawing test simulations and calculations of dynamic necking localization under plane strain tension have been carried out, using explicit and implicit analyses. An original feature of this work is that these finite element simulations are systematically compared with additional calculations performed using (i) the numerical approximation scheme developed by Choi and Yoon [4]; and (ii) the analytical computation of the first and second order yield functions gradients. This comparison has shown that the numerical approximation of the yield function gradients proposed in this work simplifies the implementation of the constitutive models, and in the case of the implicit analyses, it leads to a significant decrease of the computational time without impairing the accuracy of the finite element results. In addition, we have indicated that there is a critical loading rate below which the dynamic implicit analyses are computationally more efficient than the explicit calculations.

References

- [1] F. Barlat, H. Aretz, J.W. Yoon, M.E. Karabin, J.C. Brem, R.E. Dick, Linear transformation-based anisotropic yield functions, *Int. J. Plast.* 21 (5) (2005)1009–1039.
- [2] B. Plunkett, O. Cazacu, F. Barlat, Orthotropic yield criteria for description of the anisotropy in tension and compression of sheet metals, *Int. J. Plast.* 24 (5) (2008)847–866.
- [3] H. Aretz, F. Barlat, New convex yield functions for orthotropic metal plasticity, *Int.J. Non Lin. Mech.* 51 (2013) 97–111.
- [4] H. Choi, J.W. Yoon, Stress integration-based on finite difference method and its application for anisotropic plasticity and distortional hardening under associated and non-associated flow rules, *Comput. Methods Appl. Mech. Eng.* 345 (2019)123–160

Acknowledgements

The research leading to these results has received funding from the European Research Council (ERC) under the European Union's Horizon 2020 research and innovation programme. Project PURPOSE, grant agreement 758056.

* Corresponding author. Tel.: +34-91-624-9588; fax: +34-91-624-9430.
E-mail address: nhosseini@pa.uc3m.es

3rd International Conference on Impact Loading of Structures and Materials
ICILSM 2022

Impact of Power Transmission Lines by Powder Avalanches

Olga Gorynina¹ and Perry Bartelt

WSL Institute for Snow and Avalanche Research SLF, Flüeleralstrasse 11, CH-7265, Davos, GR, Switzerland

Abstract

Unlike many avalanche mitigation problems which can be solved by placing structures outside the reach of the avalanche, power transmission lines and cableways must traverse dangerous avalanche paths by necessity. For this reason, the hanging cables and tall, cable-supporting structures represent an important category of man-made constructions that are exposed to snow avalanches. In general, both the cables and the cable-supporting structure are hit by the avalanche. However, in this presentation we focus only on the response of hanging cables to avalanche impact, assuming that cable-supporting structures remain untouched by the avalanche. Moreover, as the avalanche core typically flows below power line transmission cables, we also assume that the cable impact implies loading by the avalanche powder cloud only.

Avalanche impact with the transmission lines and cableways induces large elastic deformations in the cable. The cable tension, therefore, increases because of the large transverse displacements which cause an additional, dynamic longitudinal strain in the cable. This may lead to large loads on cable-supporting structures or destruction of the cable. Therefore, it is important to determine the cable displacements in order to predict the tension in the cable and the pull and collapse forces acting on the supporting towers.

The system of partial differential equations for the cable displacements reads as follows. The cable displacements in the avalanche flow direction and the vertical blow-out direction are given by two one-dimensional wave equations with appropriate boundary conditions. In both equations, the wave speed is a function of the initial tension in the cable. The right-hand side terms are varying both in time and position along the cable and are determined by the powder cloud loading. The longitudinal displacements of the cable are also described by the one-dimensional wave equation. The right-hand side term contains a nonlinear function from the cable displacements in the transverse directions. However, the equation remains linear for the longitudinal displacements.

All three one-dimensional wave equations can be easily solved numerically with the weighted finite differences method. In our numerical examples, we are using explicit and unconditionally stable implicit variants of the second-order scheme in time and space. Both approaches give similar numerical results, but the explicit scheme requires an accurate spatial and temporal discretization for the transverse displacements problems since it is only conditionally stable and the stability depends on the values of the wave speed.

To conclude and to illustrate that the avalanche impact can induce large collapse forces acting on the supporting masts, we shall present numerical examples for different types of powder avalanche loading obtained from the numerical RAMMS simulations.

¹* Corresponding author. Tel.: +41 1 739 2470 .
E-mail address: olga.gorynina@slf.ch

3rd International Conference on Impact Loading of Structures and Materials
ICILSM 2022

Identification of armour technological solutions following experiment-simulation correlation

Yohan Cosquer^{a1}, Patrice Longère^a, Olivier Pantalé^b and Claude Gailhac^c

^aICA, Université de Toulouse, ISAE-SUPAERO, MINES ALBI, UPS, INSA, CNRS, 31000 Toulouse, France, yohan.cosquer@isae-supaero.fr, patrice.longere@isae-supaero.fr

^bLGP, ENI de Tarbes, Avenue d'Azereix - BP 1629, 65016 Tarbes cedex, France, olivier.pantale@enit.fr

^cCNIM Systèmes Industriels, Zone portuaire de Brégaillon - CS 60208, 83507 La Seyne-sur-Mer Cedex, France, claude.gailhac@cnim.com

Abstract

In the context of numerical simulation-aided design of armour technological solutions for ground vehicles regarding terminal ballistics, the work presented in this communication is focused on the validation of a numerical model applied to a three-layer armour solution, consisting of two metal alloy plates as front and rear layers, and air as an intermediate layer.

A ballistic test campaign was conducted using ICA STIMPACT impact platform, notably by varying the projectile geometry, the impact velocity, the plates and air layer thickness, and the boundary conditions. Impact velocity-residual velocity curves are obtained and protection limit velocities (VPL) are estimated. Depending on the configuration, two failure modes are observed: plugging and petalling.

At the same time, numerical simulations were carried out using the commercial finite element computation code Abaqus/Explicit. The deviatoric part of the metal alloy behaviour is described by the engineering-oriented rate- and temperature-dependent Johnson-Cook model [1], and its hydrostatic part by a Mie-Grüneisen equation of state (see for example [2]). The failure is tentatively driven by a critical strain which depends on strain rate and stress triaxiality.

Knowing that material data available in literature are often incomplete or/and not adapted to the materials under consideration, the objective is here to calibrate a set of constants by coupling Abaqus/Explicit computation code and ISIGHT optimization module from a series of impact tests on mono-layer armours. The set of constants is then applied to impact configurations involving three-layer armours in order to validate the numerical model.

From the comparison between experimental and numerical results for the three-layer armour configuration under consideration, one can conclude to a qualitatively fair experiment-simulation agreement. In addition, the method makes it possible to find a good approximation of the impact velocity-residual velocity curves, and to assess the effectiveness of the tested technological armour solutions.

Works in progress consist in enriching the experimental database and in improving the description of the failure mechanisms (plugging vs petalling).

[1] Johnson, G. R., & Cook, W. H. (1983). A constitutive model and data for metals subjected to large strains, high strain rates and high temperatures. Proc. 7th Int. Sympo. Ballistics. Proc. 7th Int. Sympo. Ballistics.

[2] Anderson, C. E., Cox, P. A., Johnson, G. R., & Maudlin, P. J. (1994). A constitutive formulation for anisotropic materials suitable for wave propagation computer programs—II. Computational Mechanics, 15(3), 201-223.

* Corresponding author. Tel.: +33-561-171-195.
E-mail address: yohan.cosquer@isae-supaero.fr

3rd International Conference on Impact Loading of Structures and Materials
ICILSM 2022

On the Mechanical Properties of Tungsten Heavy Alloy at Low, Intermediate and High Strain Rates

Christian C. Roth^{a*}, Teresa Fras^{a,b} and Dirk Mohr^a

^a*Department of Mechanical and Process Engineering, ETH Zurich, 8092, Zurich, Switzerland*

^b*French-German Research Institute of Saint-Louis (ISL), 68301 Saint-Louis, France*

Abstract

Due to their superior material properties, tungsten alloys find wide application in tool making, machining as well as ballistic applications. More specifically, so called long rods made from tungsten heavy alloy (WHA) are used as kinetic energy penetrators travelling at speeds >1km/s. In the present study the material response of bars with a diameter of 5mm and a length of 80mm is assessed at various strain rates ranging from 0.001/s to more than 10000/s. Uniaxial compression experiments are carried out at low (0.001/s), intermediate (1/s) and high (1000/s) strain rates on a universal testing machine and a Split-Hopkinson Pressure bar (SHPB). Very high strain rates (>>1000/s) are obtained in Taylor impact experiments performed on a single stage gas gun. Besides optical (high speed) photography for digital image correlation purposes, high speed infrared imaging is used to measure the temperature rise due to plastic work at intermediate strain rates of 1/s.

A recently developed micro-testing system is employed to test sub-sized tensile specimens extracted from the tungsten bars. Overall, six different geometries comprising shear (SH), central hole (CH) and notched tension with two different cut-out radii (NT6, NT20) are used to investigate the effect of the stress state on the plastic and fracture response. In addition, uniaxial tensile (UT) experiments are performed along and transverse to the cylinder axis to assess any strength differential effect or anisotropy.

Based on the experimental results, a constitutive modeling framework is developed and calibrated for Finite Element simulations. It comprises a yield surface accounting for the strength differential effect in conjunction with a strain rate and temperature dependent hardening law. To represent the strain hardening, a mixed Swift-Voce law is used. A stress state and strain rate dependent fracture initiation model is calibrated based on the results of the hybrid-numerical experimental analysis.

* Corresponding author. Tel.: +41(0)44 633 9250
E-mail address: ccroth@ethz.ch

3rd International Conference on Impact Loading of Structures and Materials
ICILSM 2020

Experimental study on the response of sandwich claddings

Ludovic Blanc*, Dominique Eckenfels, Jean-François Legendre

French German Research Institute of Saint-Louis, 5 rue du General Cassagnou, BP 70034, F-68301 Saint-Louis, France

Abstract

The French German Research Institute of Saint-Louis (ISL) has been working on blast mitigation for more than 15 years. Targets with different characteristic dimensions, ranging from the unprotected soldier to the steel-reinforced concrete bunker, can be exposed to blast waves generated by high explosive detonation. This study focuses on the concept of sandwich cladding, a very last resort against undetected threat. The sandwich cladding is a blast mitigation technique which focuses on lowering the load generated by an explosion on a target by increasing its duration of application. It is based on three components: an absorber, named crushable core, sandwiched between two thin plates (front and rear plate). The applied blast load accelerates the front plate which compresses the crushable core. Through this process, the core stores the energy of the blast and transmits it to the rear plate at a lower level over a longer time span, thus mitigating the load [1, 2]. Depending on the cladding parameters, it is also possible to decrease the momentum transmitted to the target by exploiting Fluid-Structure Interaction (FSI).

In our study, experimental test were performed using an Explosive-Driven Shock Tube (EDST). First, the incident and reflected blast parameters were measured for different charges. These parameters are necessary to compute the analytical models taken from the literature [3] and compute the necessary conditions for FSI to occur [4]. Then, a full cladding is placed at the end of the tube. The rear plate is considered rigid and a load sensor is placed behind it (Fig.1). A high speed camera records the test, and the front plate displacement during the crushing process (Fig.2).

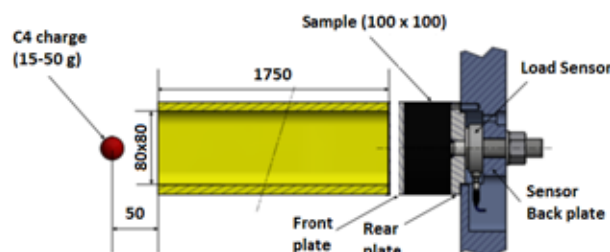


Fig.1 EDST schematic



Fig.2 Pictures of a 20 mm thick galvanized (Cu) foam during the crushing process, taken every 0.33 ms

* Corresponding author.

E-mail address: ludovic.blanc@isl.eu

This experimental set-up allows the dynamic characterisation of cellular material, at a macroscopic scale, under compression [5]. The stress-strain curve of the sample can be plotted by cross-referencing the video recording and the load measurement. Then, the parameters of importance (knowingly the plateau stress, the onset of densification and the toughness) can be computed using the methodology chosen by Li [6].

Based on preliminary results, fluid-structure interaction with a sandwich cladding has been indirectly observed on some claddings, through a diminution of the transmitted impulse to the target (Fig.3). Fortunately, FSI effects do not prevent material characterisation with this set-up and material parameters are necessary to compute the front plate velocity of the cladding [2] and estimate the transmitted impulse beforehand.

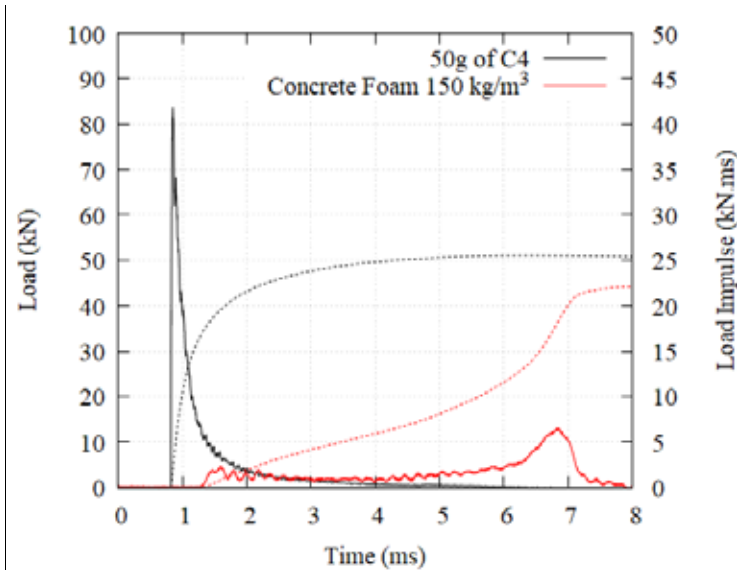


Fig.3 Load and load impulse transmission of a cladding filled with concrete foam

Consequently, many materials were tested at ISL in order to create a database of absorber, including cellular material of all kind, bio-sourced materials, granular material and auxetic material [7].

References

- [1] Gibson L. J., Ashby M., *Cellular Solids, Structure and properties*. Cambridge University Press, 1997
- [2] Hanssen A. G., Enstock L., Langseth M., *Close-range blast loading of aluminium foam panels*, International Journal of Impact Engineering 27, pp. 593-618, 2002
- [3] Kambouchev N., Noels L., *Non linear compressibility effects in fluid-structure interaction and their implications on the air-blast loading of structures*, Journal Of Applied Physics 100, 063519, 2006.
- [4] Blanc L., Lebaillif D., Buffalo A., Sturtzer M.-O., *Experimental and numerical investigation on load impulse reduction with a sandwich add-on armor*, 18th International Symposium for the Interaction of the Effects of Munitions with Structures ISIEMS18, USA, 2019
- [5] Ousji H., Belkassam B., Louar M. A., Reymen B., Martino J., Lecompte D., Pyl L., Vantomme J., *Air-blast response of sacrificial cladding using low density foams: Experimental and analytical approach*, International Journal of Mechanical Sciences 128-129: 459-474, 2017
- [6] Li Q.M., Magkiriadis I., Harrigan J.J., *Compressive strain at the onset of densification of cellular solids*, Journal of Cellular Solid 42 (5): 371-392, 2006
- [7] Blanc L., Schunck T., Eckenfels D., Legendre J.-F., *Screening of absorbing materials for blast mitigation technology based on sandwich claddings*, LWAG, 2019

3rd International Conference on Impact Loading of Structures and Materials
ICILSM 2022

The Treatment of Contact/Impact Problems in Rockfall Dynamics

Andrin Caviezel^{a,b,*}, Joël Borner^{a,b}, Andreas Lanter^c and Perry Bartelt^{a,b}

^aWSL Institute for Snow and Avalanche Research SLF, 7206 Davos Dorf, Switzerland

^bClimate Change, Extremes and Natural Hazards in Alpine Regions Research Centre CERC, 7206 Davos Dorf, Switzerland

^cGeobrugg AG, 8590 Romanshorn, Switzerland

Abstract

Falling rocks endanger many mountain communities throughout the world. Rocks, both small ($< 1 \text{ m}^3$) and large ($> 5 \text{ m}^3$) can destroy buildings and disrupt transportation lines. Engineers charged with the task of mitigating rockfall hazard employ a variety of methods to ensure the safety of the population. These methods include hazard mapping, the construction of rockfall barriers, typically rockfall dams or flexible nets, and managing the protective forest to provide optimal stopping capacity against falling rocks. Transportation engineers often construct rockfall sheds to protect dangerous road or railway segments.

Rockfall hazard engineering is essentially synonymous with the science of impact. All mitigation measures share, to large degree, the problem of calculating the forces involved in a two-body impact problem. For example, the preparation of hazard maps relies on rockfall trajectory models to predict the reach and lateral spread of possible rockfall runout distances. The core problem here is describing the energy dissipation when rocks, treated as rigid bodies with irregular geometry, impact and scar the ground. In natural terrain, ground materials will vary strongly, ranging from soft soils to hard scree surfaces. The interaction with the ground defines not only the post-impact velocity and rotation rates, but also the rockfall jump heights, a quantity of great interest to rockfall engineers charged with the task of designing reliable dam and barrier heights. Impact methods are sought which reliably predict frictional forces with little computational expense. When rockfall dams and barriers are impacted by falling rocks they dissipate both translational and rotational energies in fractions of a second, leading to large internal stress and possible structural failure. Flexible rockfall barriers attempt to reduce internal forces caused by rock impact, by stopping falling rocks over longer distances, thereby reducing the forces in the structural components. Rockfall dams employ an alternative approach: by increasing the stopping capacity of the dam by increasing the internal strength of the structure, either using natural materials, or geotextiles. An especially important problem is rock interaction with trees, both vertical tree trunks, or fallen deadwood. In many mountainous countries, the primary protection against rockfall arises from the energy dissipation during discrete rock-tree interaction events in mountain forests.

In this presentation, we discuss the experimental and numerical methods involved in rockfall dynamics. We first present the design of a special-purpose impact sensor – a so-called StoneNode - that can be installed in falling rocks to measure impact forces and pre- and post-impact rotations. Coupled with videogrammetric analysis, this method allows us to quantify the physics of ground impact. We find that it is impossible to describe impact dynamics without considering rock shape. We then show how these sensors were applied in full-scale dynamic tests of rockfall barriers. Finally, we present a hard-contact, rigid-body numerical method where we model energy dissipation during ground scarring via work-energy type analytical methods. The combination of hard-contact approaches, with soft-energy methods provides reliable estimates of rockfall runout distances in general three-dimensional terrain.

* Corresponding author. Tel.: +41 81 4170 361, E-mail address: caviezel@slf.ch

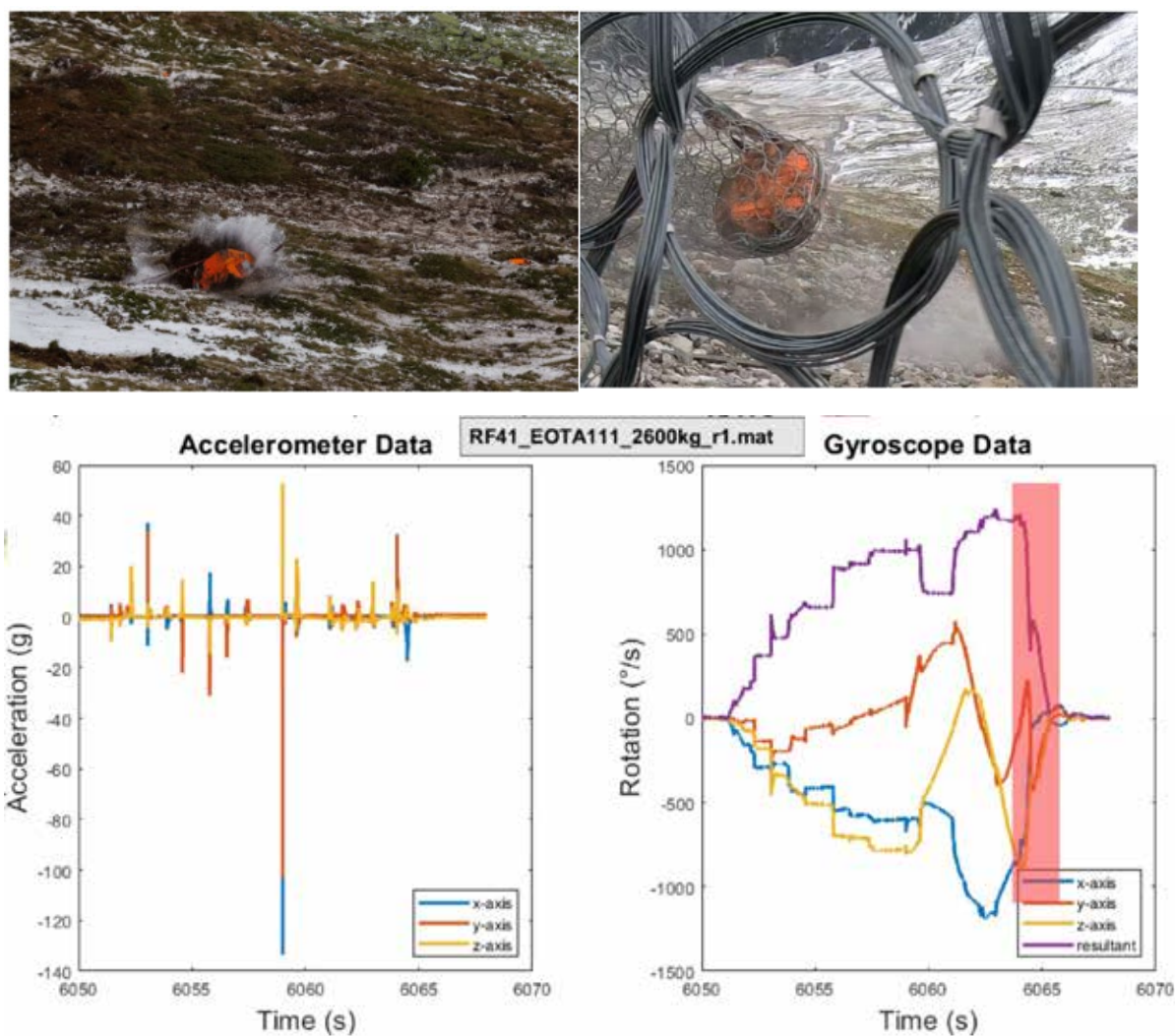


Figure 1: a) Soil impact of a 2.6 ton test block in soft, compactable alpine meadow soil. b) Impact of the same test rock into a flexible rockfall net. c) StoneNode data output: acceleration and angular momentum readings upon soil and net impact. Deceleration phase during net impact is clearly visible.

3rd International Conference on Impact Loading of Structures and Materials
ICILSM 2022

Numerical simulation of a climber fall: comparison of different models

Massimiliano Avalor^{a,b,*}, Alessandro Scattina^c

^aDipartimento di Ingegneria Meccanica, Energetica, Gestionale e dei Trasporti,
Università di Genova, Via all'Opera Pia 15/A, 16145 Genova, Italy

^bClub Alpino Italiano-Centro Studi Materiali e Tecniche,
Via Petrella 19, 20124 Milano, Italia

^cAlessandro Scattina, Dipartimento di Ingegneria Meccanica ed Aerospaziale,
Politecnico di Torino, Corso Duca degli Abruzzi 24, 10129 Torino, Italy

Abstract

Climbing, that is the ascent on rock or ice or in other situations such as in climbing gyms, is an inherently dangerous activity due to the unavoidable possibility of a fall. Except a few rare cases where no safety measures are adopted, in the large majority of cases a series of countermeasures are used to minimize the consequences of a fall (in the modern climbing ethics the possibility of a fall is accepted but the safety measures are not used to reduce it, but only to mitigate the consequences). The consequences of a fall, ranging from impacting the climbing wall to falling on the ground, are almost always reduced by means of the so-called *safety chain* made of a series of safety devices primarily connected by the main component which is the *climbing rope*: those devices are carabiners, slings, brakes, etc. and the harness [1]. The harness connects the rope to the body of the climber whereas the rope is dynamically connected to the climbing wall by means of the carabiners that are joined to anchors fixed to the wall: this connection avoids or limits the possibility of a fall to the ground or to other obstacles. Similar principles can also be used in the practice of work at height on ropes, which is expanding in constructions or tree management. In Italy the *Centro Studi Materiali e Tecniche* (CSMT, Center for Studies on Materials and Techniques) of the *Club Alpino Italiano* (CAI, Italian Alpine Club) since decades is actively studying the mechanics of climbing falls with the aim of reducing the risks and consequences both in laboratory and field experiments.

During a test campaign at the testing facility (tower) of the Padova laboratory of CSMT, a series of simulated falls were conducted. The tests consisted of leaving a free mass from different heights and in different conditions and measuring accelerations and forces exerted during the fall (Fig. 1). The falling mass is typically a rigid body made of a steel cylinder (Fig. 1a): during those tests, an anthropomorphic dummy was also used (Fig. 1b), to understand whether different results were obtained. The falling height was 1, 2 and 4 m and two values of the *fall factor* (the ratio between the theoretical falling height and the length of rope between the belayer and the climber; the fall factor is considered essential to evaluate the severity of a fall) were considered.

Aim of the present work was to develop numerical models able to reproduce the falling phenomena. The problem is quite complex due to the several non-linearity of the involved systems (first of all the behavior of the rope [2]) and the uncertainties involved in the event. By the way, most published works [3, 4] restricts to the case where the falling climber is considered a point mass, equivalent to the rigid mass.

* Corresponding author. Tel.: +39-010-3532241; fax: +39-010-3532241.

E-mail address: massimiliano.avallo@unige.it

A considerable effort was devoted to model the rope which is non-linear visco-elastic [2] and to implement the rope model into the simulation code (Altair Radioss 2020). A detailed model of the dummy and of the harness worn by the climber was then introduced. The experimental falls were then reproduced numerically (Fig. 2a) with a satisfactory level of correlation between the results, both in terms of the load-time curves (Fig. 2b) and the maximum loads but also in terms of the influence of the various examined affecting factors (Fig. 2c). Therefore, the model is a promising starting point to improve current models developed by the CSMT to study the complexity of real falls that happen in climbing and to further ameliorate the safety of climbers.

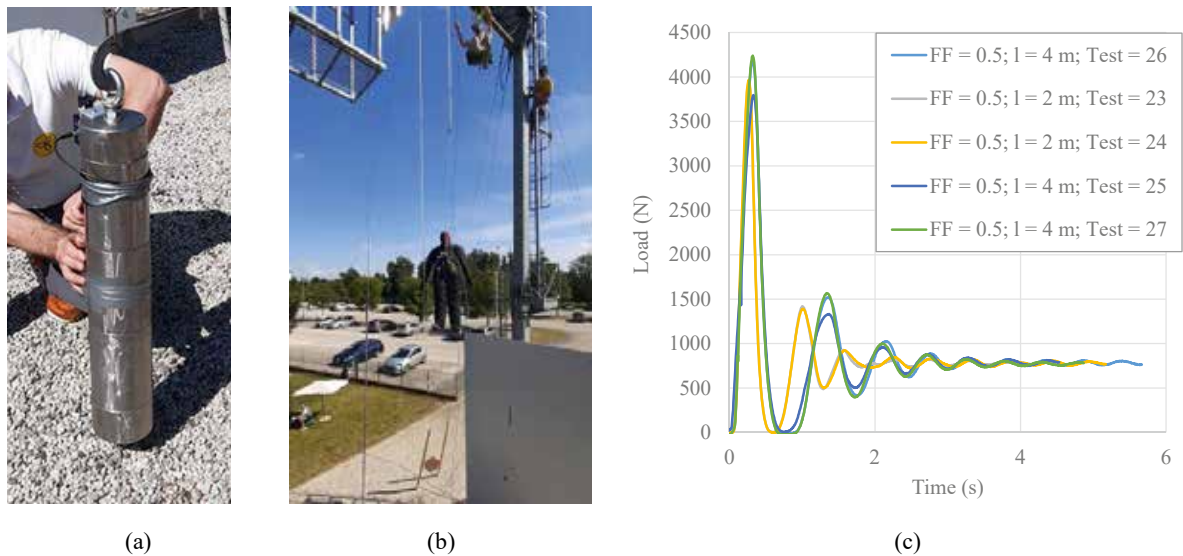


Fig.1 (a) the 80 kg rigid falling mass; (b) the anthropomorphic dummy during a simulated fall; (c) some typical records of the load on the belay vs. time during the fall of the dummy for different fall factors (FF) and length of the rope

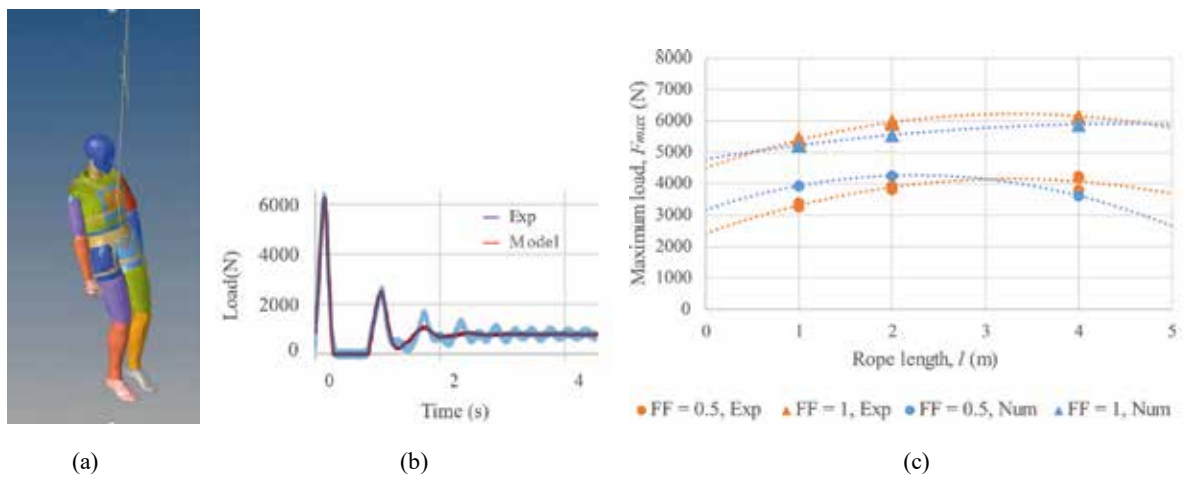


Fig.2 (a) numerical model of the dummy during a simulated fall; (b) comparison in terms of numerical/experimental results; (c) influence of the fall factor and rope length on the maximum force, numerical/experimental comparison

References

- [1] Various authors, Alpinismo su roccia, CAI Handbook No. 16, 2008
- [2] A. Manes, V. Bedogni, Procedia Engineering, 10 (2011) 3353-3358
- [3] M. Pavier, Sports Engineering, 1 (1998) 79-91
- [4] M. Spörri, Sports Engineering, 17 (2014) 61-72

3rd International Conference on Impact Loading of Structures and Materials
ICILSM 2022

High strain-rate behavior of 316L architected materials manufactured by LMD-P and SLM

C.Buros^a, P.Viot^b, J.Lartigau^{c*}

^aUniv. Bordeaux, ESTIA INSTITUTE OF TECHNOLOGY, F-64210 Bidart, France

^bArts et Métiers, I2M, F-33405 Talence, France

^cUniv. Bordeaux, ESTIA INSTITUTE OF TECHNOLOGY, F-64210 Bidart, France

Abstract

Due to its high-energy absorption and low density properties, architected materials are widely used for various applications. One of its particular application is the protection of goods and persons. An effective protection is guaranteed when the energy absorbed is maximized for a minimized impact force. Architected materials can undergo large strains for moderate stress, making them excellent candidates for impact energy absorption applications. The emergence of additive manufacturing (AM) technologies has made it possible to design and produce new architected geometries for these type of materials, with the goal of optimizing the structure depending on the final application. The arrangement of the cells constituting the architected material can be modified and controlled to achieve a targeted mechanical behavior. This study focuses on the mechanical behavior and the microstructure analysis of periodic architected structures obtained by metallic AM processes. We decided to highlight the behaviour of tri hexagonal structures under high strain rates because we would like to evaluate the mechanical response of 3D printed industrial parts - filled by this type of structures - under severe loadings (crash impact).

Two metallic additive manufacturing technologies are considered in this study: Laser Melting Deposition Powder (LMD-P) and Selective Laser Melting (SLM). The LMD-P technology consists of a local projection of metallic powders through a nozzle melted by a high-powered laser. SLM technology consists of a power bed fusion where layers of metallic powders are successively deposited. A part of this layer is fused by a laser according to the desired geometry. To study the influence of both processes and the mechanical behavior of these material, 316L stainless steel architected structures are designed and manufactured via LMD-P and SLM processes. For this first phase of study, structures with tri-hexagonal patterns and different geometries of samples are fabricated from both AM technologies. Cubic samples of dimensions 30x30x30 mm³ and cylinders of 25 mm diameter -of different heights- are fabricated to evaluate their behaviour under quasi static loadings and dynamic loadings with Hopkinson bars. Large parallelepiped samples of 100x100x30 mm³ are also printed to qualify the response of the generic industrial part under drop tower. Concerning the LMD-P fabrication of the tri-hexagonal cells, several tests of laser priming were necessary to pilot the manufacture of walls crossing.

After the pre-polishing, polishing and etching steps, the microstructure of the wall material is studied using an OLYMPUS PMG3 digital microscope. The 3D-printed structure is cut into the fabricated direction to observe the stacking of layers. Several overlapping melt pools with curved borders are highlighted. This microstructural characteristic is typical of additive manufacturing processes and is a consequence of the Gaussian distribution of laser energy. Different morphologies of grains are observed within the microstructure : columnar grains and equiaxed grains. Columnar grains are represented in an elongated shape growing in the direction on a maximum thermal gradient. In Figure 3, the growth direction of columnar dendrites are perpendicular to the curved melt pool borders and converge towards the center. On the contrary, in the central area of the melt pool, equiaxed dendrites are observed. This phenomenon is the consequence of a change of heat transfer mode. Higher solidification rates promote a transition from columnar grain to equiaxed ones. In the final microstructure negligible porosities, generally caused by unfused powder particles, are observed (Figure 3).

Uniaxial quasi-static compression tests are performed on a ZWICK Roel 250 machine equipped with a 250 kN load cell to analyze the compressive macroscopic behavior of these structures. Tests are conducted at 10 mm/min and 500 mm/min. Each test is then performed with engineering strain rates of $5.0 \times 10^{-3} \text{ s}^{-1}$ and 0.2 s^{-1} respectively (in considering an initial sample height of 28 mm). Given the large cells of the structure, a force-displacement diagram was preferred compared with a stress-strain one (Figure 4a). Images of the deformation process are captured via a CANON EOS 50D camera at an image capture frequency of 1 Hz at 10 mm/min and 20 Hz at 500 mm/min (Figure 4b). Thermal images are capture via a FLYR SC 7000 camera at a frequency of 150 Hz (Figure 4c). The obtained compressive curve of tri-hexagonal structure made by SLM starts with a linear elastic region followed by a plastic plateau characterized by a significant ondulation. This plateau region comes from the walls buckling of the structure, visible in Figure 4b. With the captured images at different time, we observe the structure deformation for different displacement imposed by the machine's crossbar. These deformations are typical of buckling phenomenon. The observed bucklings induce local plasticity but only few crackings. This testifies of the part quality presenting few porosities which could have initiate a cracking. This plasticity leads to an augmentation of local temperature quantified with the thermic camera. This phenomenon is particularly visible at high displacement speeds as no thermal diffusion happen.

* Corresponding author. Tel.: +33 5 59 43 84 58.

E-mail address: camille.buros@estia.fr

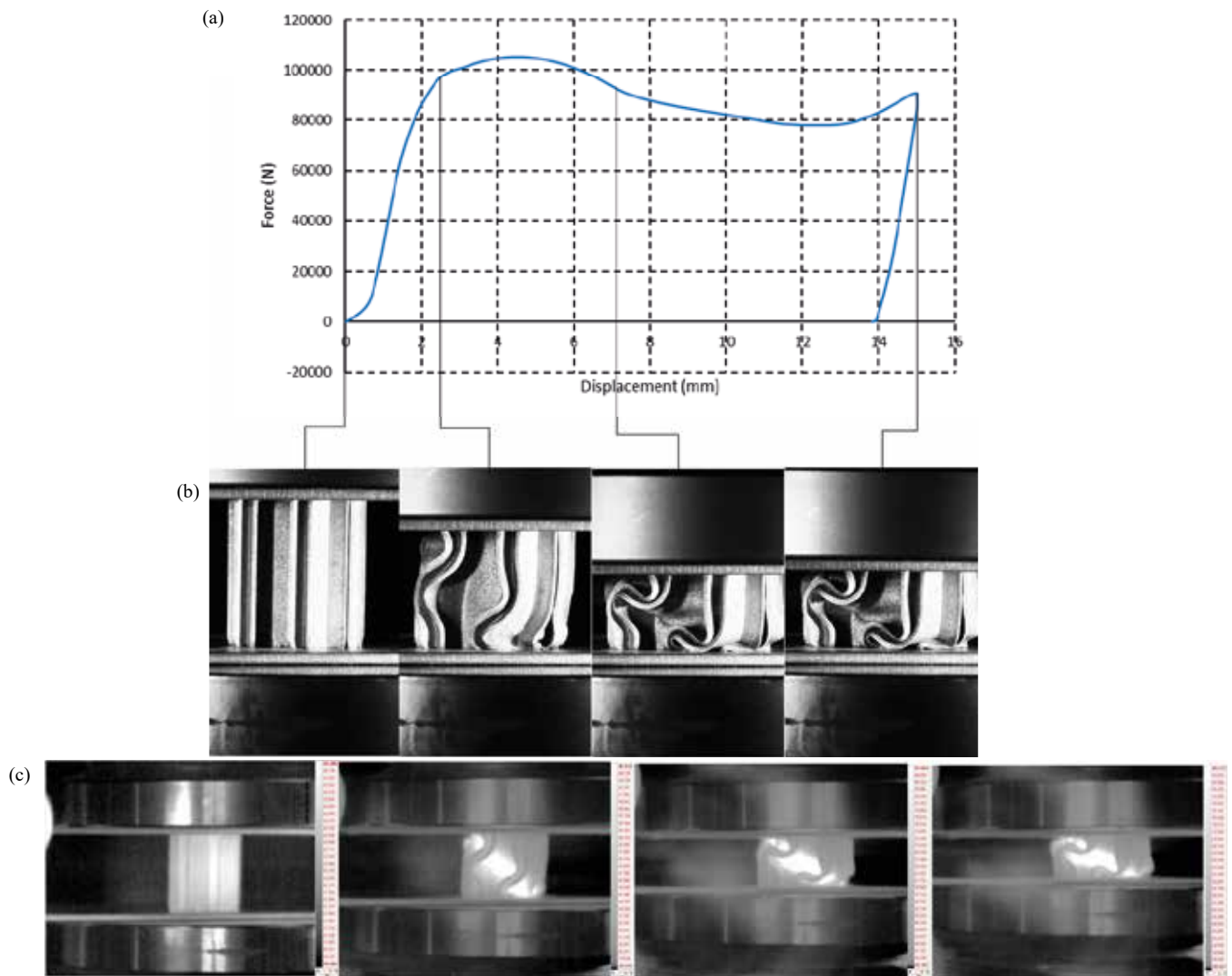
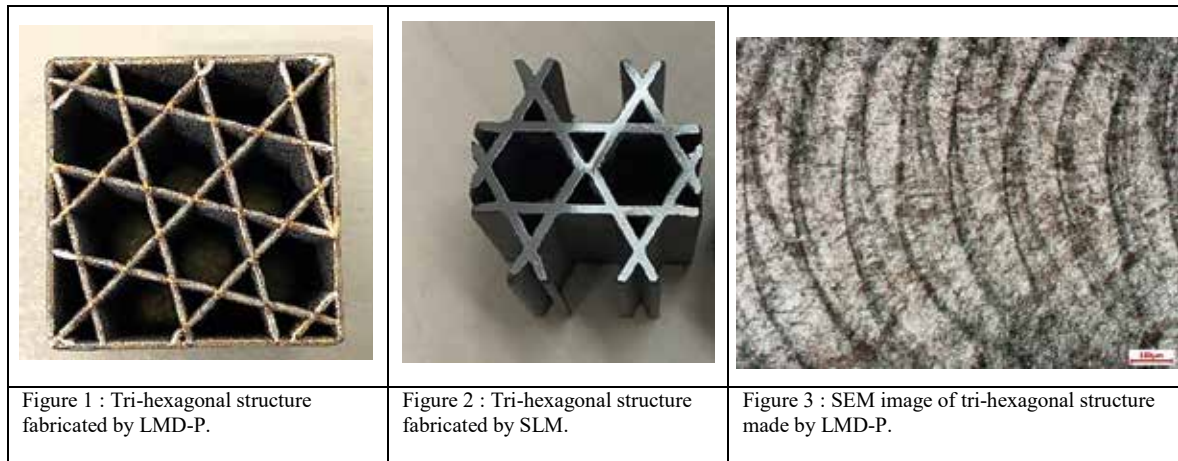


Figure 4 : Compressive behaviour of tri-hexagonal structure at 500 mm/min fabricated by SLM (a) : Force-displacement compressive curve; (b) : Images of the deformation process; (c) : Images of thermal change during compressive loading.

